



**Investigation of the physiological basis of the
rind disorder oleocellosis in Washington navel
orange (*Citrus sinensis* [L.] Osbeck)**

Toby George Knight
B.Ag.Sc. (Hort.Sc.)

Submitted in fulfilment of requirements for the degree of
Doctor of Philosophy

Department of Horticulture, Viticulture and Oenology
The University of Adelaide

June, 2002

Table of Contents

Abstract.....	i
Declaration.....	iii
Acknowledgments.....	iv
List of Abbreviations.....	vi
List of Figures.....	viii
List of Plates.....	ix
List of Tables.....	x

Chapter 1

General Introduction.....	1
---------------------------	---

Chapter 2

Literature Review.....	5
2.1. The fruit.....	5
2.1.1. Botanical classification.....	5
2.1.2. Rind anatomy.....	5
2.2. The oil gland.....	7
2.2.1. Gland development.....	7
2.2.2. Gland anatomy.....	8
2.3. The rind oils.....	9
2.3.1. Oil synthesis and accumulation.....	9
2.3.2. Oil composition.....	10
2.3.3. Oil properties.....	10
2.4. Oleocellosis.....	11
2.4.1. Terminology.....	11
2.4.2. Cause.....	11
2.4.3. Symptoms.....	11
2.4.4. Artificial induction.....	13
2.4.5. Oleocellosis physiology.....	14
2.4.6. Fruit susceptibility to oleocellosis.....	15
2.4.7. Oleocellosis control.....	16
2.4.8. Fruit treatments affecting oleocellosis.....	18
2.5. Summary.....	20
2.6. Aims.....	21

Chapter 3

Oil gland development: structure and quantification.....	22
3.1. Introduction.....	22
3.1.1. Background.....	22
3.1.2. Aims.....	23

3.2. Materials and Methods.....	23
3.2.1. Plant material	23
3.2.2. Gland counts	23
3.2.3. Microscopy	24
3.2.4. Gland age survey.....	26
3.2.5. Image analysis.....	26
3.2.6. Statistical analysis	26
3.3. Results.....	27
3.3.1. Anatomical gland development	27
3.3.2. Timing of gland development.....	30
3.3.3. The mature gland	33
3.4. Discussion.....	36
3.5. Conclusion	40

Chapter 4

Rind oil visualisation: method development	41
4.1. Introduction.....	41
4.1.1. Background.....	41
4.1.2. Aims.....	42
4.2. Materials and Methods.....	43
4.2.1. Light microscopy (LM).....	43
4.2.2. Scanning electron microscopy (SEM)	46
4.2.3. Fluorescence microscopy	47
4.3. Results.....	49
4.3.1. Light microscopy (LM).....	49
4.3.2. Scanning electron microscopy (SEM)	51
4.3.3. Fluorescence microcopy	53
4.4. Discussion.....	58
4.4.1. Method development	58
4.4.2. Rind oil observations	63
4.5. Conclusion	64

Chapter 5

Inducing oleocellosis in the laboratory	65
5.1. Introduction.....	65
5.1.1. Background	65
5.1.2. Aims.....	66
5.2. Materials and Methods.....	67
5.2.1. Preliminary induction methods test	67
5.2.2. Oil method refinement	71
5.2.3. Penetrometer method refinement	72
5.3. Results.....	73
5.3.1. Preliminary induction methods test	73
5.3.2. Oil method refinement	78
5.3.3. Penetrometer method refinement	83

5.4. Discussion.....	86
5.4.1. Mechanical induction.....	86
5.4.2. Oil induction.....	89
5.5. Conclusion.....	91

Chapter 6

Oleocellosis: macroscopic and microscopic development.....	92
6.1. Introduction.....	92
6.1.1. Background.....	92
6.1.2. Aims.....	93
6.2. Materials and Methods.....	94
6.2.1. Symptom time course.....	94
6.2.2. Microscopy.....	97
6.3. Results.....	101
6.3.1. Symptoms.....	101
6.3.2. Rind surface damage.....	105
6.3.3. Rind sub-surface damage.....	108
6.4. Discussion.....	124
6.4.1. Symptoms.....	124
6.4.2. Oleocellosis mechanism.....	125
6.4.3. Oil effects.....	128
6.4.4. The link between microscopic damage and symptoms.....	130
6.5. Conclusion.....	133

Chapter 7

General Discussion.....	134
7.1. Addressing limitations of current control practices.....	134
7.2. More factors influencing fruit susceptibility to oleocellosis.....	136
7.3. Developing new strategies for oleocellosis control.....	139
7.4. Oleocellosis diagnosis.....	141
7.5. Summary.....	142

Appendix 1: Video Pro programs.....	143
--	------------

Appendix 2: Publications.....	145
--------------------------------------	------------

Appendix 3: Conference presentations.....	146
--	------------

Appendix 4: Industry communication.....	151
--	------------

Bibliography.....	152
--------------------------	------------

Personal Communications.....	165
-------------------------------------	------------

Abstract

Oleocellosis is a rind disorder of citrus fruit, which produces an unattractive surface blemish, and causes significant economic losses to the Australian citrus industry. It is caused by phytotoxic oils released from oil glands located in the rind, as a result of mechanical damage. In this study, microscopy investigations into the oil glands, localisation of the rind oils and the development of oleocellosis have been carried out in Washington navel orange fruit (*Citrus sinensis* [L.] Osbeck).

Changes in the structure, size and the number of oil glands located in the rind were assessed in the developing fruit from pre-anthesis to fruit maturity. Gland initiation was restricted to early fruit development, but glands continued to develop and reached maturity by fruit size 30 to 50 mm diameter. Mature glands continued to enlarge with fruit growth, but their final size and form varied within each fruit. Mature fruit had between 8,000 and 12,000 oil glands. Glands were found to develop from a cluster of cells adjacent to the fruit epidermis, into a structure consisting of a central cavity surrounded by several layers of epithelial cells. All glands were joined to the fruit epidermis by a 'stalk'. Gland cavity formation appeared to involve schizogeny.

Methods of tissue preparation were investigated in an effort to retain the essential oil contained within the glands. The modification of chemical fixation methods for improved rind oil retention gave limited success based on light microscopy observations. However, the examination of cryofixed material with scanning electron microscopy and fresh tissue with multi-photon microscopy were promising techniques for oil visualisation in orange rind tissue.

Oleocellosis was artificially induced in mature fruit under controlled conditions. This was achieved by mechanically damaging the fruit or applying rind oils to the fruit surface. Based on a range of criteria, penetrometer damage and d-limonene treatment were chosen as the optimal methods for inducing oleocellosis. These

methods were considered to simulate the two forms of naturally occurring oleocellosis; namely gland rupture and oil transfer between fruit.

Following induction, oleocellosis development was examined using a detailed time course assessment of surface symptoms and microscopic rind damage. Based on these observations, the events leading to oleocellosis blemish formation were proposed. Mechanical damage resulted in rupture of the epidermis above the glands and release of oil to the fruit surface. Surface oil appeared to infiltrate the rind via the cuticle, and via the ruptured epidermis in injured fruit. Once in the rind, the phytotoxic oils caused rapid cell content degeneration and cell collapse, with early stages of ultrastructural damage detected within six hours of induction. The resulting blemish, which was characterised by rind collapse and darkening, developed substantially within three days and was attributed to the sub-surface rind damage.

Declaration

This thesis contains no material which has been accepted for the award of any other degree or diploma in any university or other tertiary institution and, to the best of my knowledge and belief, contains no material previously published or written by another person, except where due reference has been made in the text.

I give consent to this copy of my thesis, when deposited in the University library, being available for loan and photocopying.

Toby George Knight.

Date: 14.6.02

Acknowledgments

Thanks to my supervisors, Andreas Klieber and Margaret Sedgley, for their ongoing support and encouragement.

This study was funded by the Australian Research Council through the Strategic Partnership with Industry – Research and Training (SPIRT) Scheme. Thanks to our industry partner, the Citrus Board of South Australia, for their support and for enabling me to travel to the International Society for Citriculture 2000 Congress in Orlando, Florida. Special thanks to Andrew Green.

Thanks to Gueue Bros. Pty. Ltd., Mypolonga, for their contribution of fruit.

Thanks to all my Microscopy Lab mates over the years, especially Merran Matthews, Raelene Mibus and Leanne Pound, for their friendship and support, during the countless hours on the microtome and weekends in the darkroom. Also to all my other friends from HVO, who have made it such an enjoyable place to work.

Special thanks to Meredith Wallwork for her unwavering support on every level, and to Peter Kolesik for his advice and constant humour. Thanks also to Meredith, Chris Ford and Bob Barrett for their proof reading prowess.

Thanks to the staff of The Centre for Electron Microscopy and Microstructural Analysis (CEMMSA), especially Lyn Waterhouse, for their technical advice and instruction, and for making the dungeon always a fun place to be.

Thanks to the University of Adelaide, for enabling me to travel to the Sixth International Botanical Microscopy Meeting, St Andrews, Scotland, with a Research Abroad Scholarship. To Chris Hawes, Oxford Brookes University, for

allowing me to visit, and Rebecca Morden, Royal Microscopical Society, for her help and humour.

To all others who have helped with this project, including:

- Michelle Lorimer, Biometrics SA, for her support with statistics.
- Brian Loveys, Sue Maffei and Sue Johnson, CSIRO Plant Industry.
- Barry Tugwell and other staff of SARDI Postharvest Horticulture.
- Karen Churchill and Lynn Jarvis for technical support for Video Pro.
- Sharon Clapham and other staff of the Image and Copy Centre, Waite Campus.

Last but definitely not least. To my family, for seeing me through the many years of study. And to my friends, who have always provided a welcome distraction. Gold stars to Tony, Penny and Matt.

List of Abbreviations

α-pinene	alpha-pinene
β-myrcene	beta-myrcene
β-glucan	beta-glucan
$^{\circ}$C	degree(s) Celsius
CBSA	Citrus Board of South Australia
CEMMSA	Centre for Electron Microscopy and Microstructural Analysis
CLSM	confocal laser scanning microscope or microscopy
cm	centimetre(s)
CSIRO	Commonwealth Scientific and Industrial Research Organisation
CW	Calcofluor White
ER	endoplasmic reticulum
ESEM	environmental scanning electron microscope or microscopy
<i>et al.</i>	and others
FEGSEM	field emission gun scanning electron microscope or microscopy
Fig.	Figure
g	gram(s)
GA	gibberellic acid
GMA	glycol-methacrylate
h	hour(s)
HCl	hydrochloric acid
kg	kilogram(s)
kPa	kiloPascal(s)
kV	kilovolt(s)
LM	light microscope or microscopy
LSD	least significant difference
M	mole(s)
min	minute(s)
mm	millimetre(s)
ms⁻²	metres per second, per second

N	Newton(s)
nm	nanometre(s)
NR	Nile Red
P	probability
Pa	Pascal(s)
PA	Procure-Araldite
PAS	periodic acid-Schiff's
Pers. Comm.	Personal Communication
PIRSA	Primary Industries and Resources South Australia
PPO	polyphenol oxidase
RORP	rind oil release pressure
SARDI	South Australian Research and Development Institute
SBB	Sudan Black B
SEM	scanning electron microscope or microscopy
TBO	Toluidine Blue O
TEM	transmission electron microscope or microscopy
µm	micrometre(s)
µl	microlitre(s)
USA	United States of America
UV	ultraviolet
VPD	vapour pressure deficit

List of Figures

Figure 2.1. Cross-section of mature lemon rind.	6
Figure 2.2. Oleocellosis symptoms on mature navel orange fruit.....	12
Figure 3.1. Changes in oil gland density and total gland number per fruit with fruit growth.	31
Figure 3.2. Gland age survey in fruit stages A to E.	32
Figure 3.3. Mature gland volume in fruit stages A to E.....	34
Figure 5.1. Preliminary induction methods test. The effect of induction method and induction time on blemish severity at days 1 and 3.	74
Figure 5.2. Preliminary induction methods test. The effect of induction method and induction time on blemish area at days 1 and 3.....	77
Figure 5.3. Oil method refinement. The effect of d-limonene concentration on blemish severity at days 1 and 3.	79
Figure 5.4. Oil method refinement. The effect of citral concentration and 100% d-limonene on blemish severity at days 1 and 3.	79
Figure 5.5. Oil method refinement. The effect of d-limonene concentration on blemish area at days 1 and 3.....	82
Figure 5.6. Oil method refinement. The effect of citral concentration and 100% d-limonene on blemish area at days 1 and 3.....	82
Figure 5.7. Penetrometer method refinement. The effect of induction time on blemish severity at days 1 and 3.	84
Figure 5.8. Penetrometer method refinement. The effect of induction time on blemish area at days 1 and 3.....	84
Figure 6.1. The relationship between time and rind collapse.	102
Figure 6.2. The relationship between time and rind discolouration.	102
Figure 6.3. The relationship between time and blemish area.	103

List of Plates

Plate 3.1. Light micrographs of the gland developmental series.	28
Plate 3.2. Light micrographs depicting the gland stalk and gland form.	29
Plate 3.3. Micrographs depicting mature gland anatomy and cavity formation. ...	35
Plate 4.1. Rind oil visualisation using light microscopy.....	50
Plate 4.2. Rind oil visualisation using scanning electron microscopy.....	52
Plate 4.3. Rind oil visualisation using light fluorescence microscopy.	54
Plate 4.4. Rind oil visualisation using confocal laser scanning microscopy.	55
Plate 4.5. Rind oil visualisation using multi-photon microscopy.....	57
Plate 5.1. Blemish severity scoring system.....	70
Plate 5.2. Oleocellosis symptoms induced in the preliminary induction methods test.	75
Plate 5.3. Oleocellosis symptoms induced in the oil method refinement experiments.	80
Plate 5.4. Typical oleocellosis blemish resulting from penetrometer induction....	85
Plate 6.1. Modified blemish severity scoring system.	96
Plate 6.2. Rind profile image of healthy rind tissue.....	100
Plate 6.3. Dissecting microscope images of fruit surface damage and oleocellosis symptoms.	106
Plate 6.4. Scanning electron micrographs of the fruit surface following mechanical damage, with the penetrometer.	107
Plate 6.5. Light micrographs of the oleocellosis-damaged rind.....	109
Plate 6.6. Scanning electron micrograph of the oleocellosis-damaged rind, resulting from oil treatment.	110
Plate 6.7. Multi-photon microscope images of healthy and oleocellosis-damaged rind.	111
Plate 6.8. Rind profile images of healthy and oleocellosis-damaged rind.....	113
Plate 6.9. Transmission electron micrographs of rind ultrastructure in an untreated fruit sample.	114
Plate 6.10. Transmission electron micrographs of rind ultrastructure in an oil- treated fruit sample, after 30 minutes.	116
Plate 6.11. Transmission electron micrographs of rind ultrastructure in an oil- treated fruit sample, after six hours.....	118
Plate 6.12. Transmission electron micrographs of rind ultrastructure in an oil- treated fruit sample, after two days.....	119

Plate 6.13. Transmission electron micrographs of rind ultrastructure in an oil-treated fruit sample, after ten days.	121
Plate 6.14. Transmission electron micrographs of rind ultrastructure in a penetrometer-damaged fruit sample, after three days.....	123

List of Tables

Table 4.1. Summary of fixation, dehydration and embedding schedules for LM Methods 1 to 7.	43
Table 6.1. Variance strata for blemish collapse, colour and area at day 3, expressed as percentage of total variation. Experiment 1, fruit harvested from five trees and different fruit assessed at each time. Experiment 2, fruit harvested from one tree and same fruit assessed at each time. Sample refers to replicate treatments on the one fruit.	104

Chapter 1

General Introduction

For fresh fruit markets worldwide, the production of blemish free fruit is of primary importance to the consumer, and in most citrus growing regions of the world, fresh fruit grades are based on the extent of rind damage attributable to blemishes (Davies and Albrigo, 1994). Fruit blemishes are caused by a range of biotic and abiotic factors (Albrigo, 1978). Oleocellosis is one of a host of physiological rind disorders which result in blemishes; others include chilling injury, albedo breakdown, splitting, granulation, puffing and stem-end breakdown (Whiteside *et al.*, 1988).

Oleocellosis is distinct from other physiological disorders in that it arises from a combination of physical and physiological events (Albrigo, 1978). As a result of mechanical damage to the fruit, oil glands located in the rind are ruptured, releasing phytotoxic oils, which act upon the rind tissue (Fawcett, 1916). Oleocellosis can result from various types of damage to the fruit, including insect damage, hail damage or wind rub (Whiteside *et al.*, 1988), but arises most commonly from damage at or near harvest (Wardowski *et al.*, 1976). Undamaged fruit develop oleocellosis by coming into contact with oil on the surface of damaged fruit. It has also been suggested that, in rare cases, rind oil liberation can take place when turgid fruit are subjected to sudden cold (Grierson, 1981).

Oleocellosis produces a superficial blemish, characterised by sunken and discoloured areas on the fruit surface (Shomer and Emer, 1989). Symptoms vary with fruit age; in mature fruit, tissue darkening or browning occurs, whereas if immature, green fruit are damaged, oleocellosis-affected areas of the rind fail to colour normally, and remain a green/yellow colour (Fawcett, 1916). On the basis of surface symptoms, oleocellosis in mature fruit is also difficult to distinguish

from other rind disorders such as rind staining (Eaks, 1964) and pitting (du Plessis, 1978).

Oleocellosis is considered to be a major concern for the South Australian citrus industry, which accounts for 31% of Australia's production, as well as 46 % of exports valued at approximately A\$180 million (Barry Tugwell, Chief Scientist, SARDI; Pers. Comm., 2001). It has been estimated that oleocellosis can affect up to 10% of a crop (Andrew Green, Technical Officer, CBSA; Pers. Comm., 1998). Oleocellosis is often detected during grading and fruit can be discarded prior to packing, but delayed symptom detection can necessitate further fruit discard and repacking at destination markets (Green, Pers. Comm., 1998). In addition, rind damage associated with oleocellosis can predispose the fruit to pathogen infection during storage.

In recent years in Australia, the oversupply of domestic markets has placed an emphasis on the export of fresh fruit, to help maintain the industry's viability. In 1992, after many years of negotiations over quarantine issues, South Australian growers were granted access to fresh fruit markets in the USA. In trial shipments of navel oranges to the USA, it was estimated that A\$1 million was lost due to repacking costs incurred as a result of the presence of oleocellosis-like blemishes. Today, the industry's export drive continues to be led by navel orange exports to the USA. Two million cartons of oranges in total, particularly navels, are exported to the USA and Japan each year. Reports indicate that a high incidence of oleocellosis-like blemishes was again observed during the 2000 season (Green, Pers. Comm., 2001).

Oleocellosis control strategies currently employed by growers include careful fruit handling at all stages of production and the use of oleocellosis prediction tests prior to harvest. A range of practices have been implemented to minimise mechanical damage to the fruit; for example, the training of pickers to handle fruit with care, and the design of packing lines to remove all potential impact points. Oleocellosis prediction is based upon the premise that fruit with a high turgor are

more likely to develop oleocellosis (Eaks, 1955). For this reason, varieties that bear through winter, such as Washington navel orange, are more prone to oleocellosis. The two measurements used to predict oleocellosis are pressure gradient and 'rind oil release pressure' or RORP (Cahoon *et al.*, 1964). Pressure gradient is the difference between fruit and wet-bulb temperatures, and RORP is measured with a hand-held pressure tester, or penetrometer. Fruit are considered 'safe' to pick when the pressure gradient is above 2 °C and RORP is above 3 kg (Feutrill, 1997). A comparison between 1993 and 1994 USA navel orange exports shows the potential of adjusting harvesting practices to reduce oleocellosis. Oleocellosis incidence dropped from 15% to 6% as a result of harvesting fruit in the afternoon, when humidity and fruit turgor were low (Tugwell and Chvyl, 1995). However, delaying harvest to the afternoon is not practical from a commercial standpoint. A recent study in South Australian orchards showed that picking navel oranges would frequently be delayed and on some days not possible when adhering to pressure gradient guidelines (Loveys *et al.*, 1998). Studies have also questioned the effectiveness of RORP as a test for fruit susceptibility to oleocellosis (Gillespie and Tugwell, 1971; Erner, 1982; Loveys *et al.*, 1998), but investigation of new tests has shown no improvement on current methods (Loveys *et al.*, 1998).

Oleocellosis has been observed to vary greatly from season to season. Variability between orchards has also been reported (Edwards *et al.*, 1994; Tugwell and Chvyl, 1995), but studies have failed to produce a correlation between oleocellosis and specific management practices used in Australian orchards (Edwards *et al.*, 1994; Loveys *et al.*, 1998). Factors such as fruit age, variety and position in the tree canopy have been reported to influence fruit susceptibility to oleocellosis, but the reasons for these effects have not been explored. Similarly, it has been suggested recently that preharvest gibberellic acid (GA) application may reduce oleocellosis incidence (Loveys *et al.*, 1998), but such an effect has not been explained in terms of physiological changes to the fruit.

In simple terms, oleocellosis can be considered to comprise both physical and physiological elements. To date, control practices for oleocellosis have focussed upon minimising mechanical damage to the fruit. This has been achieved by the implementation of careful handling practices at all stages of production, and also by picking fruit which are considered less susceptible to damage, due to low turgor. Despite the current precautions implemented by the industry, oleocellosis is still occurring at unsatisfactory levels and compromising the quality of fresh citrus fruit for domestic and export markets. An improved understanding of the physiological basis of oleocellosis is required to overcome the limitations of current control practices.

Chapter 2

Literature Review

2.1. The fruit

2.1.1. Botanical classification

Citrus sinensis (L.) Osbeck or 'sweet orange', belongs to the subgenus *Citrus*, of the genus *Citrus*, of the subfamily Aurantoideae, of the family Rutaceae (Swingle, 1943). Within Aurantoideae, the genus *Citrus* belongs to the 'True Citrus Fruit' group, within which the subgenus *Citrus* is classified by its edible fruits (Swingle, 1943). Further subdivisions within subgenus *Citrus* have been made by Tanaka (1961). The sweet oranges have been divided into the common oranges, acidless oranges, pigmented oranges and navel oranges (Hodgson, 1967). The navel oranges are identified by the presence of "a small and rudimentary secondary fruit embedded in the apex of the primary fruit" (Hodgson, 1967). Some characteristics of the 'Washington' navel fruit include: deep orange colour, globose to ellipsoid shape, medium sized calyx, medium to large navel, medium rind thickness and conspicuous oil glands (Webber, 1943). With respect to flavour, sweetness, fruit size and appearance, and relative seedlessness, it is considered "the most important variety of the sweet orange" (Webber, 1943).

2.1.2. Rind anatomy

The rind or pericarp consists of three layers: the epicarp, hypoderm and mesocarp (Fig. 2.1) (Bartholomew and Reed, 1943). The epicarp is the cuticle-covered epidermal layer, composed of 'isodiametric' and 'polygonal' cells, and laterally flattened cells above the oil glands in mature fruit. The hypoderm, located beneath the epicarp comprises two or more layers of compacted collenchyma cells. The outer mesocarp is composed of thin-walled parenchyma cells, in which the oil glands are embedded.

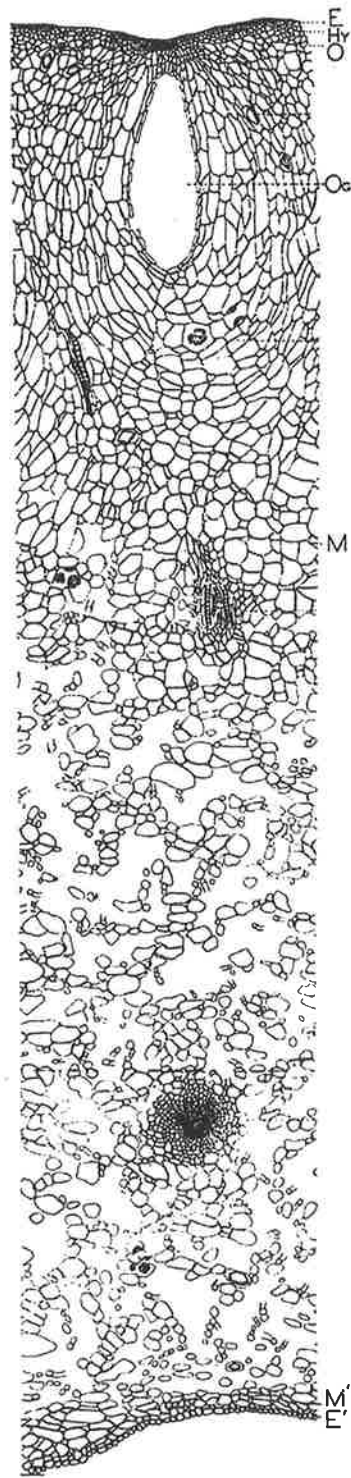


Figure 2.1. Cross-section of mature lemon rind. E, epicarp; Hy, hypodermis; O to M, outer mesocarp; Og, oil gland; M to M', inner mesocarp; E', endocarp.
(Adapted from: Bartholomew and Reed, 1943).

The epicarp, hypoderm and outer mesocarp constitute the coloured portion of the mature fruit, or the 'flavedo'. The inner mesocarp, comprising branching cells and large intercellular spaces is referred to as the colourless 'albedo'.

2.2. The oil gland

Secretory cavities occur naturally in all species of the family Rutaceae (Fahn, 1979). As pointed out by Schneider (1968), the structures are more complex than mere cavities, and are commonly referred to as 'oil glands'. In *Citrus* species, oil glands have been documented in various parts of the plant, including the stem (Webber and Fawcett, 1935; Schneider, 1955), leaves (Schneider, 1968; Thomson *et al.*, 1976; Turner *et al.*, 1998), all parts of the flower except the stamens (Bartholomew and Reed, 1943), and the fruit (Turrell and Klotz, 1940; Ford, 1942; Bartholomew and Reed, 1943; Scott and Baker, 1947; Bain, 1958; Schneider, 1968; Holtzhausen, 1969; Shomer, 1980; Bosabalidis and Tsekos, 1982a, 1982b). For the oil glands of the fruit, characteristics such as shape, size, arrangement and position of the glands, and kind, amount and aroma of the oils are thought to be highly variable among citrus fruit types (Hodgson, 1967).

2.2.1. Gland development

In the fruit, oil glands have been observed as early as the ovary stage, in Eureka lemon (Ford, 1942), Valencia orange (Schneider, 1968), Washington navel orange (Holtzhausen, 1969) and Mediterranean mandarin (Bosabalidis and Tsekos, 1982a). Gland formation in *Citrus* species has been reported by some to be confined to early stages of fruit development (Ford, 1942; Bain, 1958), whilst others have suggested continuous formation with fruit growth (Schneider, 1968). Glands have also been reported to enlarge with fruit growth (Bain, 1958; Holtzhausen, 1969).

2.2.2. Gland anatomy

2.2.2.1. Gland ontogeny

According to Bartholomew and Reed (1943), early studies by Sieck (1895) and Biermann (1896) suggested that citrus oil glands originated from the differentiation of four polyhedral cells from the surrounding tissue. Anatomical examination of the floral ovaries of *C. deliciosa*, has shown glands to differentiate from a pair of meristematic cells, one epidermal and one underlying (Bosabalidis and Tsekos, 1982a). The two initial cells were reported to be precursors to the two parts of the differentiated glandular complex; the globular/oval gland situated in the parenchyma, and the 'conical stalk' joining the gland to the epidermis. Ontogeny of secretory cavities in *Citrus* (Bosabalidis and Tsekos, 1982a) appears to show similarities to those in *Eucalyptus* (Carr and Carr, 1970).

2.2.2.2. The mature gland

Secretory cavities are considered to consist of "relatively large intercellular spaces (lumina or lacunae) lined by an epithelium of secretory cells" (Fahn, 1979). Observations of the mature oil glands of *Citrus* appear to be consistent with this description; glands are composed of a central cavity surrounded by several layers of radially flattened epithelial cells (Thomson *et al.*, 1976; Shomer, 1980; Bosabalidis and Tsekos, 1982a, 1982b; Turner *et al.*, 1998). Epithelial cells are thought to be gradually modified into a protective sheath of cells with thickened cell walls, referred to as 'boundary' or 'envelope' cells (Thomson *et al.*, 1976; Bosabalidis and Tsekos, 1982b).

2.2.2.3. Cavity formation

There is contradiction in the literature regarding the origin of the gland cavity; schizogenous vs. lysigenous. 'Schizogeny' refers to the separation of walls of neighbouring cells, and 'lysigeny' to the disintegration of cells, to form the intercellular space (Fahn, 1979). Using electron microscopy, Heinrich (1966; 1969) reported lysigeny in the glands of *C. medica* and *C. limon*, as did Bosabalidis and Tsekos (1982b) in *C. deliciosa*. Thomson *et al.* (1976), concluded that the cavities of the foliar glands of *C. sinensis* formed schizogenously, but did

not exclude the possibility of lysigeny occurring at later stages of development. In the most recent study, Turner *et al.* (1998) examined the effect of a range of fixatives on the foliar glands of *C. limon*, and demonstrated artefactual swelling and bursting of inner epithelial cells due to hypotonic fixatives. In a later review of cavity formation in *Citrus* and related species, Turner (1999) pointed out the difficulties in distinguishing between fixation artefact and a true lysigenous process, suggesting that schizogeny be favoured in cases where there is dispute.

2.3. The rind oils

2.3.1. Oil synthesis and accumulation

The inner epithelial cells of citrus oil glands appear to be secretory in nature (Thomson *et al.*, 1976; Bosabalidis and Tsekos, 1982b). The majority of transmission electron microscopy (TEM) studies have reported the major site of essential oil synthesis to be the plastids (Heinrich, 1966; Shomer, 1980; Bosabalidis and Tsekos, 1982b), however various mechanisms of oil secretion have been proposed. Heinrich (1966) suggested that lipids in the plastids were released into the cavity following cell lysis; however, more recent studies have suggested that an active secretion takes place (Shomer, 1980; Bosabalidis and Tsekos, 1982b). Shomer (1980) suggested that oil transfer from the cytoplasm into the wall takes place via ectoplast invagination. Bosabalidis and Tsekos (1982b) added to these observations by suggesting that oil movement from the plastids is facilitated by ER elements which fuse to the plasmalemma, depositing the oil into the apoplast, through which it is driven into the cavity.

For the microscopic examination of rind oils, it is important to take the methods of tissue preparation into consideration. This issue was addressed by Turner *et al.* (1998) in their study of *C. limon* foliar glands. On the basis of light microscopy (LM) and TEM observations, better lipid retention was achieved in osmium vapour fixed or cryofixed samples compared to those prepared with conventional chemical fixation procedures.

2.3.2. Oil composition

Essential oils largely consist of volatile, low molecular weight terpenes (Fahn, 1990). In *C. sinensis*, 116 oil components have been identified (Shaw, 1979). The monoterpene d-limonene constitutes more than 90% of total oil by weight, followed by β -myrcene and α -pinene, also terpenes. Other major components are aldehydes including neral and geranial, alcohols including linalool and terpineol, esters, ketones and non-volatiles (Shaw, 1979). d-limonene is the most abundant oil component of most *Citrus* species (Kesterson and Hendrickson, 1962; Attaway *et al.*, 1967; Sawamura *et al.*, 1984; Daito and Morinaga, 1984; Ruberto *et al.*, 1997; Loveys *et al.*, 1998; Sun and Petracek, 1999).

The effect of fruit maturation on the essential oils of citrus fruit has been well documented (Kesterson and Hendrickson, 1962; Attaway *et al.*, 1967; Scora *et al.*, 1968; Chandler *et al.*, 1976; Casas and Rodrigo, 1981; Daito and Morinaga, 1984). In Washington navel orange, an increase in total rind oil has been shown late in the season (Scora *et al.*, 1968). In the study by Scora *et al.* (1968), the levels of 18 major oil components were measured from eight months post-anthesis; showing a general increase in α -pinene, decrease in β -myrcene and linalool, and negligible changes in d-limonene levels. A biosynthetic relationship between d-limonene and linalool has been suggested (Attaway *et al.*, 1967).

2.3.3. Oil properties

Monoterpenes are important agents of insect toxicity (Taiz and Zeiger, 1998). Citrus oil components possess pesticidal (Don-Pedro, 1996) and antifungal properties (Ben-Yehoshua *et al.*, 1992). Essential oils also supply raw materials for various industries, such as resin for paper and textiles, pharmaceutical products, perfumes and spices (Fahn, 1979).

2.4. Oleocellosis

2.4.1. Terminology

In the literature, oleocellosis has been referred to by a range of names including 'oil spotting', 'oleo', 'bruising', 'green spot' and 'gas burn' (Grierson, 1986). However, discrepancies in the use of some names are obvious. The term 'rind oil spot' has been used to describe oleocellosis (Sawamura *et al.*, 1984; Sawamura *et al.*, 1987; Sawamura *et al.*, 1988), as well as blemishes induced by chilling (Kanlayanarat *et al.*, 1988b, 1988a) and high temperatures (Chikaizumi, 2000). The Japanese term 'Kohansho' has also been loosely used to describe oleocellosis (Tugwell, Pers. Comm., 1998), but a number of studies into Kohansho have shown characteristics that suggest the two disorders are not synonymous (Hasegawa and Iba, 1981; Manago, 1988; Hasegawa and Yano, 1992; Yano *et al.*, 1997). Hasegawa and Iba (1981) reported that Kohansho is not a result of fruit injury, but is largely dependent on storage temperature.

2.4.2. Cause

Terpenes and sesquiterpenes are highly phytotoxic (Soule and Grierson, 1986). Oleocellosis is caused by phytotoxic rind oils, which are released from oil glands following mechanical damage and act upon the rind tissue (Fawcett, 1916). In the earliest documented study of oleocellosis, Fawcett (1916) induced oleocellosis symptoms or 'green spotting' in lemon fruit, by either applying pressure to the fruit surface or by applying oils to the surface of uninjured fruit. In subsequent studies, oleocellosis has been induced by various mechanical and oil methods, see Section 2.4.4.

2.4.3. Symptoms

Oleocellosis produces a superficial blemish, characterised by collapse and discolouration of the rind tissue (Shomer and Erner, 1989). Oleocellosis symptoms are depicted in Figure 2.2. Tissue collapse between glands causes glands to appear more prominent on the fruit surface (Fawcett, 1916; Mustard, 1954). Oleocellosis is a particular problem in immature green fruit, as oleocellosis-damaged areas fail to colour normally (Fawcett, 1916; Miller and Winston, 1943; Cahoon *et al.*, 1964;

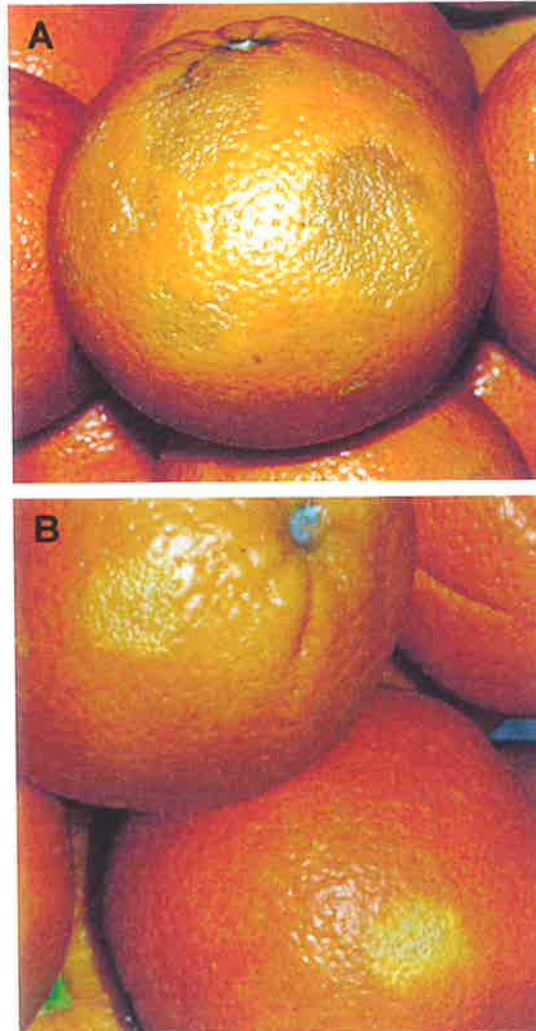


Figure 2.2. Oleocellosis symptoms on mature navel orange fruit. Oleocellosis damage to mature fruit, causes rind darkening (A). Oleocellosis damage to immature fruit; damaged areas fail to colour normally (B).
(Photos: Barry Tugwell)

Wardowski *et al.*, 1976; Shomer and Erner, 1989). Slight symptoms have been observed to develop as early as 20 minutes after oil application in lemon fruit (Fawcett, 1916). In mandarin fruit, symptoms have been monitored over four days, with rind undulation detected by 18 hours and 'necrotic spots' by 36 hours, forming lesions by 48 hours (Williams and Wild, 1996). In navel oranges, symptoms have been observed to develop within two to three days of oil application (Wild, 1998).

2.4.4. Artificial induction

2.4.4.1. Mechanical induction

Normal picking and packing procedures have been used to induce oleocellosis in Washington navel oranges (Levy *et al.*, 1979). Normal handling practices have also been simulated, by dropping fruit from a standard height onto a hard surface such as the back of a flat-bed truck (Cahoon *et al.*, 1964) or a picking trailer (Loveys *et al.*, 1998). The penetrometer has been used to induce oleocellosis in Shamouti orange fruit (Erner, 1982; Shomer and Erner, 1989). Pin-pricking glands has also been shown to produce severe rind injury in citrus fruit (Sawamura *et al.*, 1984).

2.4.4.2. Oil induction

Rind oils have been applied to fruit by bending excised rind segments (Sawamura *et al.*, 1984; Sawamura *et al.*, 1987; Sawamura *et al.*, 1988; Williams and Wild, 1996), applying single drops (Brodrick, 1970; Chikaizumi, 2000) or by smearing aqueous emulsions (Shomer and Erner, 1989). In the most recent study, oil was applied by attaching oil-treated cardboard discs to the fruit surface with adhesive tape (Wild and Williams, 1992). In navel orange fruit, typical symptoms have also been induced by injecting oils into the rind (Loveys *et al.*, 1998). Previous observations of oil-induced oleocellosis suggest that linalool is highly phytotoxic, moreso than d-limonene (Wild and Williams, 1992), but that both components are more damaging than α -pinene, n-nonanol, n-nonanal and carvone (Sawamura *et al.*, 1984).

2.4.5. Oleocellosis physiology

2.4.5.1. Rind anatomy and ultrastructure

The earliest documented microscopy studies of oleocellosis used LM to examine mature fruit oleocellosis (Labuschagne *et al.*, 1977; du Plessis, 1978). In oleocellosis-damaged tissue, the epidermis was observed to be ruptured above glands, suggesting surface oil release (Labuschagne *et al.*, 1977). A band of flattened cells, located six to eight cells deep from the surface and between oil glands, was also reported in damaged tissue (du Plessis, 1978). Both LM and TEM have been used to examine oleocellosis in artificially coloured or 'degreened' Shamouti orange fruit (Shomer and Erner, 1989) and mature Valencia orange and mandarin fruit (Williams and Wild, 1996). The study by Shomer and Erner (1989) reported oil-damaged cells localised either sub-epidermally or in all cell layers. Oil-damaged cells were observed to contain "dense contents trapped between collapsed cell walls without free vacuolar or plasmolyzed spaces". Protoplast concentration was observed as early as three hours following damage, and by three days, damaged cells were reported to contain a "giant chloroplast" and collapsed cell walls. Based on their observations, Shomer and Erner (1989) suggested that both external and internal oil release may occur. In the study by Williams and Wild (1996), the rind was observed to contain heavily stained upper rind layers, representing flattened cells. On the basis of TEM observations, flattened cell layers were suggested to result from tangential cell division rather than cell collapse.

2.4.5.2. Rind biochemistry

Ascorbic acid has been observed to concentrate around the oil glands located in the flavedo of Satsuma mandarin fruit (Kurosaki and Kawakami, 1974). In oil-damaged rind tissue, Sawamura *et al.* (1987) observed an elevated ratio of dehydroascorbic acid: total ascorbic acid compared to healthy tissue, suggesting a link between oleocellosis and the anti-oxidative action of ascorbic acid. In a following study, a similar link could not be made with tocopherols, which are another type of anti-oxidative substance in the citrus rind (Sawamura *et al.*, 1988).

Oleocellosis, along with desiccation and pathogen infection, has also been shown to alter the terpene content of oil glands (Scora and Adams, 1973).

2.4.6. Fruit susceptibility to oleocellosis

2.4.6.1. Fruit turgor

Fruit susceptibility to oleocellosis has been linked to fruit turgor; turgid fruit are more likely to develop oleocellosis (Eaks, 1955). Prior to this finding, oleocellosis incidence was related to orchard conditions (Fawcett, 1916; Miller and Winston, 1943; Mustard, 1954). Fawcett (1916) reported that oleocellosis occurred predominantly on lemon fruit that were wet, in a moist atmosphere, or just picked. Similarly, Mustard (1954) reported increased oleocellosis in Persian lime fruit that were wet from rain or dew. The conclusions of Eaks (1955) were based on observations of wet vs. dry fruit, snapped vs. clipped fruit, storage temperature and duration. In a later study in lemons, a quantitative relationship was established between oleocellosis and factors affecting fruit turgor, such as soil moisture and vapour pressure deficit (VPD) of the atmosphere (Cahoon *et al.*, 1964). A relationship was also established with rind oil release pressure (RORP), which was measured with a fruit pressure tester, and considered to integrate both soil and climatic conditions. In following studies, a similar relationship was established in Florida lemons (Oberbacher, 1965), Californian oranges and lemons (Eaks, 1968) and Florida limes (Pantastico *et al.*, 1966). The fruit pressure tester or 'penetrometer' used for RORP assessment was originally developed for fruit maturity assessment (Magness and Taylor, 1925). Christ (1967) described modifications of the pressure tester for use on citrus fruit, and recommended methods for detecting oil release. Fruit turgor estimation is the basis for current prediction tests for oleocellosis, see Section 2.4.7.1.

2.4.6.2. Fruit age and size

Wardowski *et al.* (1976) made the general statement that small-sized fruit tended to be more susceptible to oleocellosis than larger sizes. In lime fruit, lower RORP values (higher turgor) have been obtained in smaller fruit (Pantastico *et al.*, 1966). In lemon fruit, immature fruit have been suggested to be more susceptible

to gland rupture due to the 'fragility' of the rind (Cahoon *et al.*, 1964), or the rough surface and exposed glands (Oberbacher, 1965).

2.4.6.3. Fruit variety and species

The rind of lemons, limes and navel oranges are considered to be especially susceptible to oleocellosis (Whiteside *et al.*, 1988). The susceptibility of navel oranges has been confirmed by surveys of oleocellosis incidence (du Plessis, 1978). Wardowski *et al.* (1976) suggested that varieties with "numerous, prominent oil cells" were vulnerable to damage. Differences in rind sensitivity to applied oil have been reported between mandarin and Valencia orange fruit (Williams and Wild, 1996) and between various other citrus species (Sawamura *et al.*, 1984).

2.4.6.4. Fruit position and orientation

Gilfillan (1996) reported fruit position and orientation to influence RORP readings on navel oranges. In his study, the outside face of north aspect fruit showed greater RORP values (lower turgor) than the inside face of the same fruit and both orientations of south aspect fruit. Loveys *et al.* (1998) reported east aspect fruit to have lower RORP values (higher turgor) than those on the west aspect of the tree. The sun exposed face of citrus fruit have also shown a greater sensitivity to applied oils than the protected or shaded face (Wild, 1998; Loveys *et al.*, 1998; Chikaizumi, 2000).

2.4.7. Oleocellosis control

2.4.7.1. Prediction tests

Oleocellosis prediction tests used in Australia have been adapted largely from practices used in South Africa, developed by Dr Ian Gilfillan (1996). Australian growers are recommended to carry out a combination of two tests: (1) pressure gradient and (2) RORP (Feutrill, 1997).

(1) Pressure gradient measurement. Rind temperature is measured with a meat thermometer, and wet-bulb temperature using a sling hygrometer, on the shaded,

south aspect of the tree. This test is satisfied when fruit temperature exceeds wet-bulb temperature by 3°C for green fruit (or 2°C for coloured fruit).

(2) RORP measurement. This measurement is carried out assuming the required pressure gradient has been met. RORP is measured using a penetrometer with an 8 mm diameter tip, on at least 20 fruit not exposed to the sun that day (inside fruit or south aspect fruit preferred). It is said to be safe to pick when RORP is greater than 3 kg.

A recent study focussed on developing improved susceptibility tests (Loveys *et al.*, 1998). In this study, a transparent, acrylic penetrometer tip was shown to give more accurate RORP readings than the conventional brass tip. An electronic penetrometer was also shown to produce rind firmness readings with lower associated errors than RORP readings. However, RORP was judged to be a poor indicator of fruit susceptibility to oleocellosis. Previous studies support this finding (Gillespie and Tugwell, 1971; Erner, 1982). Pressure gradient and VPD were considered to be 'reasonable' indicators of oleocellosis susceptibility, but major delays in harvesting navel oranges in a South Australian orchard occurred when adhering to pressure gradient guidelines. Another test for oleocellosis susceptibility was also tested by Loveys *et al.* (1998), in which fruit were dropped from a height of 500 mm onto a filter paper on a flat surface, and the amount of oil released onto the paper was measured. At low temperatures, larger amounts of oil were released from the fruit, however amount of oil released did not correlate with resulting oleocellosis.

2.4.7.2. Careful fruit handling

Studies have shown that oleocellosis can be avoided, even in turgid fruit, if the fruit is handled with care. Eaks (1955) reported that oleocellosis could be avoided in wet lime fruit if they were clipped and handled carefully rather than snapped at harvesting. Other studies have also suggested that oleocellosis can be avoided if handled carefully, even early in the morning, when fruit turgor is high (Pantastico *et al.*, 1966; Loveys *et al.*, 1998).

Industry recommendations aim to minimise mechanical damage to fruit at all stages of handling (Feutrill, 1997). For example, pickers should be trained and picking bags clean and free of sand or dirt, and fruit should be transported by a good carrier, over graded roads, with reduced tyre pressure. Indicator papers have been used to detect oil release from fruit (Grierson, 1958). More recently, the 'instrumented sphere' has been adopted in Australian packing sheds; this device measures impact mass whilst travelling along the packing line (Jim Hill, Consultant, PIRSA Rural Solutions; Pers. Comm., 1998). Fruit injury along the packing line is reduced by removing potential impact points; in the USA the maximum acceptable limit is 150 g, whilst in South Australia, a limit of 70 g is used (Hill, Pers. Comm., 1998).

2.4.8. Fruit treatments affecting oleocellosis

2.4.8.1. Plant growth hormones

a. Ethylene

Ethylene is a plant growth regulator that is termed the 'ripening hormone' for many plants (Abeles, 1973). In citrus, preharvest ethylene has been shown to reduce oleocellosis in postharvest fruit, possibly by enhancing rind colouration (Levy *et al.*, 1979; Erner, 1982). However, Levy *et al.* (1979) also reported a corresponding decrease in RORP (increase in turgor), possibly related to reduced stomatal conductance. Preharvest ethylene may also facilitate reduced fruit damage by loosening fruit (El-Zeftawi, 1977). Postharvest ethylene is used to degreen citrus fruit, but can accentuate oleocellosis, as damaged areas remain green (Levy *et al.*, 1979).

b. Gibberellins

In citrus, gibberellins are thought to play an important role in the control of flowering and fruit development (Monselise, 1979). In Australia, preharvest GA (in the form of GA₃) is widely applied to delay fruit senescence and reduce the severity of albedo breakdown, another rind disorder (Monselise *et al.*, 1976). In

navel oranges, it has been suggested that preharvest GA treatment may also be effective in reducing oleocellosis (Loveys *et al.*, 1998).

2.4.8.2. Storage conditions

a. Storage temperature

In mature fruit, temperatures of 10°C and below have been shown to inhibit blemish development in navel oranges (Wild, 1998), as has cold disinfestation at 1°C prior to 10°C storage (Edwards *et al.*, 1994). However, curing fruit at ambient temperature prior to cold disinfestation has been reported to increase the levels of oleocellosis in lemons (Predebon and Edwards, 1992).

b. Storage atmosphere

Low oxygen storage has been shown to reduce darkening of the oleocellosis-damaged rind of navel oranges, but darkening recommenced once fruit were returned to a normal atmosphere (Wild, 1998). Low oxygen (5-12%) combined with very low carbon dioxide levels (0-2%) have been shown to minimise oleocellosis in lemons (Calero *et al.*, 1981). High carbon dioxide levels have also been reported to prevent the development of oleocellosis, rind pitting and membranosis in 'Primofiori' lemons (Artés *et al.*, 1993).

2.4.8.3. Miscellaneous treatments

Other methods reported to reduce rind sensitivity to applied oils include: mixing rind oil with potassium hydroxide (KOH) and ethanol (Wild, 1998), applying commercial citrus waxes Briteseal and Zidvar or sodium and potassium silicates to the fruit (Wild, 1998), and exposing fruit to ultraviolet light for five minutes or more (Loveys *et al.*, 1998).

2.5. Summary

This review highlights the need for further investigation of oleocellosis from a physiological perspective, and points to a number of avenues of investigation.

Oleocellosis results from damage to the oil glands and the effect of released oils on the rind tissue. An understanding of the anatomy of the glands, as well as the timing of gland development and oil accumulation in the fruit is required. Anatomical examinations of the glands have been carried out for a range of *Citrus* species and in different plant parts, but not in navel orange fruit. In addition, some contention currently exists regarding the timing of gland development in citrus fruit.

Seasonal fluctuations in the rind oils have been examined by quantitative methods, but the use of microscopy techniques to examine oil accumulation has in the past been limited. This may be explained by the inability of conventional tissue fixation methods to reliably retain oil within the glands. To enable rind oil visualisation, additional method development is still required.

Our understanding of oleocellosis physiology is limited and largely based upon a small number of microscopy studies. Previous studies have shown significant discrepancies in their findings, which have been based on LM and TEM observations. A detailed examination of oleocellosis, facilitated by the use of varied microscopy techniques is required.

This research will help to explain the limitations of current oleocellosis control practices and reveal possible alternatives. An improved understanding of factors influencing oleocellosis will also help to explain previous reports of oleocellosis variability and the effect of different fruit treatments on the expression of the disorder.

2.6. Aims

The aim of this research is to develop an improved understanding of the physiological basis of the rind disorder oleocellosis in Washington navel orange fruit.

To achieve this, the following strategies are proposed:

1. Examination of oil gland structure and quantification of gland developmental changes throughout fruit development.
2. Development of methods for oil visualisation in orange rind tissue.
3. Development of reliable methods for oleocellosis induction in the laboratory.
4. Detailed examination of oleocellosis development, using a range of microscopy techniques.

Chapter 3

Oil gland development: structure and quantification

3.1. Introduction

3.1.1. Background

Oil glands have been observed in the fruit as early as the ovary stage, in Eureka lemon (Ford, 1942), Valencia orange (Schneider, 1968), Washington navel orange (Holtzhausen, 1969) and Mediterranean mandarin (Bosabalidis and Tsekos, 1982a). However, there is some uncertainty surrounding the timing of gland development in the citrus fruit. Gland formation has been reported by some to be confined to early stages of fruit development (Ford, 1942; Bain, 1958), whilst others have suggested continuous formation with fruit maturation (Schneider, 1968). Glands have also been reported to enlarge with fruit growth (Bain, 1958; Holtzhausen, 1969).

Structural aspects of gland development have been reported in the floral ovaries of *Citrus deliciosa* (Bosabalidis and Tsekos, 1982a, 1982b), and the leaves of *C. limon* (Turner *et al.*, 1998) and *C. sinensis* (Thomson *et al.*, 1976), but not in the fruit of *C. sinensis* or more specifically, navel orange. The most detailed anatomical outline of gland development is confined to a single fruit stage, the floral ovary (Bosabalidis and Tsekos, 1982a). The process by which the central cavity forms, lysigeny or schizogeny, is also a contentious issue. A review of cavity formation in *Citrus* and related species has been put forward by Turner (1999). He points out the difficulties in distinguishing between fixation artefact and a true lysigenous process, and suggests that schizogeny be favoured over lysigeny in cases where there is dispute.

3.1.2. Aims

The aim of this study was to examine oil gland anatomy and quantify gland developmental changes in the fruit of Washington navel orange, from pre-anthesis to maturity. By establishing an anatomical outline of gland development, the timing of gland initiation, development and enlargement in relation to fruit growth was investigated, and mature gland anatomy was examined at different fruit ages.

3.2. Materials and Methods

3.2.1. Plant material

Fruit were collected from two 23 year old Washington navel orange trees on *Poncirus trifoliata* rootstock, located in the University of Adelaide, Waite Campus Alverstoke orchard (34°97'S, 138°63'E). The trees were positioned three metres apart, in a north-south facing row. Fruit were harvested at monthly intervals from pre-anthesis to fruit maturity (eight months). At each harvest, six fruit were picked from each tree, representing three sizes x two replicates. Each harvest was carried out at the same time of day to avoid possible discrepancies due to diurnal changes.

The equatorial and polar diameters of each fruit were measured. An average of the two diameters is used when referring to fruit diameter. Fruit surface area was extrapolated according to Turrell (1946). By this method, the fruit is considered a spheroid, and the difference between polar and equatorial diameters is incorporated into an equation to calculate surface area.

3.2.2. Gland counts

Gland density was measured on 9 mm to 88 mm diameter fruit. Within a sector of 180 mm² along the fruit equator (or an adjusted area for fruit smaller than this dimension), glands visible from the surface using a dissecting microscope were counted. Glands with deeper-seated cavities, difficult to detect from surface examination, were counted by dissection of the tissue along the flavedo/albedo boundary. The addition of these two counts gave total number of glands within the sector. For all fruit, gland density was expressed as number of glands per 180 mm².

Total number of glands per fruit was estimated using gland density and fruit surface area values:

$$\text{Total gland number} = \text{gland density} \times (\text{fruit surface area}/180 \text{ mm}^2).$$

3.2.3. Microscopy

3.2.3.1. Tissue sampling

Samples for microscopy were collected from each fruit. A minimum of six rind tissue samples was collected from the equatorial region of each fruit (three for each tissue preparation method).

3.2.3.2. Light microscopy (LM)

a. Tissue preparation

Two tissue processing methods were employed: aldehyde fixation and aldehyde fixation plus osmium tetroxide postfixation.

The first method was similar to that described by Feder and O'Brien (1968). Rind samples of approximately 5 x 5 mm were fixed in 3% glutaraldehyde (25% solution, Unilab, Auburn, Australia) in 0.025M phosphate buffer, pH 7.0, overnight at 0-4°C. Samples were rinsed in phosphate buffer and dehydrated through an alcohol series: methoxy-ethanol, ethanol, propanol and butanol. Samples were infiltrated overnight in a 1:1 mixture of butanol:glycol-methacrylate (GMA) (Sigma, St. Louis, USA) (prepared by mixing 93 ml 2-hydroxyethyl methacrylate, 7 ml polyethylene glycol 400 and 0.6g benzoyl peroxide), followed by three changes of 100% GMA over one week. Samples were embedded in gelatin capsules (size '00', Parke Davis Capsugel Division, Caringbah, Australia) and polymerisation achieved at 60°C. Sections (4 µm thickness) were cut with a Reichert-Jung 2050 Supercut Microtome using glass knives, placed on glass slides and stained with periodic acid-Schiff's (PAS) (Schiff's reagent, BDH, Poole, England) for carbohydrates and counterstained with Toluidine Blue O (TBO) (Aldrich, Milwaukee, USA) to provide detail of cell structure (O'Brien and McCully, 1981).

In the second method, rind samples of approximately 1 x 1 mm were fixed in a solution of 4% formaldehyde (paraformaldehyde powder, ProSciTech, Thuringowa, Australia), 1.25% glutaraldehyde (EM grade, 25% solution, ProSciTech) and 4% sucrose, in phosphate buffered saline (PBS), pH 7.2, overnight at 0-4°C. After two short rinses in PBS, samples were postfixed in phosphate buffered 1% osmium tetroxide (ProSciTech) for one hour. Samples were dehydrated through an acetone series: 70, 90, 95, 100%, and infiltrated overnight in a 1:1 mixture of acetone:Procure-Araldite (PA) resin (Procure-Araldite Embedding Kit, ProSciTech), followed by three eight hour changes of 100% PA resin. PA resin was prepared according to Mollenhauer (1964). Samples were flat embedded and polymerisation achieved at 70°C. Sections (1 µm thickness) were cut with a Reichert-Jung Ultracut E Microtome using glass knives, placed on glass slides and stained with TBO to provide detail of cell structure (O'Brien and McCully, 1981).

Histochemical staining for lignin using Phloroglucinol-HCl (May and Baker, Dagenham, England) (Jensen, 1962) and suberin using Sudan Black B (SBB) (Sigma) (O'Brien and McCully, 1981) was also employed. All material was observed with a Zeiss Axiophot Photomicroscope, using transmitted light.

b. Sample selection

Five fruit stages were chosen on the basis of size, to represent complete fruit development. The five fruit stages selected were: (A) floral ovary (at full bloom), (B) immature green coloured fruit 10 mm diameter, (C) immature green fruit 32 mm, (D) immature green fruit 52 mm, (E) mature orange coloured fruit 88 mm. For each fruit stage, samples were serial sectioned and used in a survey of gland age and image analysis of gland volume. In addition, 15 'in between' fruit sizes were sectioned for general anatomical observation.

3.2.3.3. Transmission electron microscopy (TEM)

Ultra-thin sections (70 nm in thickness) of aldehyde plus osmium tetroxide postfixed tissue were collected on a diamond knife, using a Reichert-Jung Ultracut

E Microtome. Sections were transferred to collodion coated copper grids, 200 mesh thin bar. Sections were stained with uranyl acetate and lead citrate (O'Brien and McCully, 1981), and observed under an accelerating voltage of 80 kV with a Philips CM 100 TEM.

3.2.4. Gland age survey

From each of the five fruit stages, a sample of 12 to 40 glands was selected, and glands were classed according to their stage of development. Using LM, the complete set of sections comprising each gland was examined to avoid discrepancies in gland classification.

3.2.5. Image analysis

From each of the five fruit stages, the volume of five mature glands was measured using the image analysis program Video Pro 32 version 3.42 (Leading Edge Pty. Ltd., Adelaide, Australia). For Video Pro programs see Appendix 1. The gland perimeter was defined by the outermost epithelial cells of the gland and included the gland stalk. Gland volumes were calculated from an equation incorporating area and distance between serial sections. For example, the volume between two sections 1 and 2 was:

$$\text{Volume 1 } (\mu\text{m}^3) = \text{Area 1 } (\mu\text{m}^2) \times \text{Distance between sections 1 and 2 } (\mu\text{m}).$$

3.2.6. Statistical analysis

Gland volume data were analysed using the statistical package Genstat for Windows version 4.1 (Lawes Agricultural Trust, IACR Rothamsted). A completely randomised design was applied to the data and Analysis of Variance (ANOVA) tables, and tables of means were generated. Statistical difference due to fruit age was tested at the 95% confidence level.

3.3. Results

3.3.1. Anatomical gland development

From LM observations of aldehyde fixed tissue samples, a series of six stages was chosen to outline anatomical gland development in Washington navel orange fruit. These were as follows: Stage 1, a cluster of up to ten cells adjacent to the epidermis. These gland initials were distinguished from surrounding parenchyma cells as slightly radially elongated and lacking starch (Plate 3.1A). Stage 2, a larger cell cluster of ten to 30 cells (Plate 3.1B). Stage 3, a larger cluster showing the start of differentiation into boundary and inner cells (Plate 3.1C). Stage 4, a differentiated gland with flattened boundary cells enclosing polyhedral shaped inner cells. Nuclei of the inner cells appear enlarged (Plate 3.1D). Stage 5, a differentiated gland with flattened boundary cells enclosing polyhedral shaped inner cells whose walls appear to form the cavity (Plate 3.1E). Stage 6, a mature gland with an expanded central cavity (Plate 3.1F). Differences in the appearance of surrounding parenchyma cells can be attributed to the differences in fruit age. This outline was used to quantify gland development in relation to fruit development. The anatomy of mature, cavity-containing glands (stages 5 and 6) was examined more closely in aldehyde plus osmium tetroxide postfixed tissue (Plates 3.3A and 3.3B).

At each stage of gland development, glands were joined to the fruit epidermis by a stalk-like structure. The stalk was often conical in shape (Plate 3.2A). The structure was solid rather than funnel-like, as revealed by tangential sectioning of the rind tissue (Plate 3.2B). The stalk appeared to be an extension of the inner gland cells, uninterrupted by boundary cells, which met the epidermis at its apex. Stalk cells were round to oblong shaped, and were smaller and different in form to other cells of the gland complex and surrounding parenchyma cells of the rind.

Plate 3.1

Light micrographs of the gland developmental series, stages 1 to 6 (A to F). Aldehyde fixed, medial, longitudinal, PAS/TBO stained sections. Bars = 10 μm .

A. Gland cells (arrow) are slightly elongated, and lacking starch which is visible as dense grains in surrounding cells.

B. Gland cells (arrows) form a larger cluster.

C. Boundary cells (b) form around inner gland cells (i).

D. Flattened layers of boundary cells (b) encapsulate the inner gland cells (i). Innermost cells show enlarged nuclei (arrow).

E. Inner cells give rise to central cavity (arrow).

F. Central cavity enlarges (c).

Gland stages 1 and 5 depicted are from fruit stage A, stage 2 from fruit stage B, stages 3 and 4 from fruit stage C and stage 6 from fruit stage D.

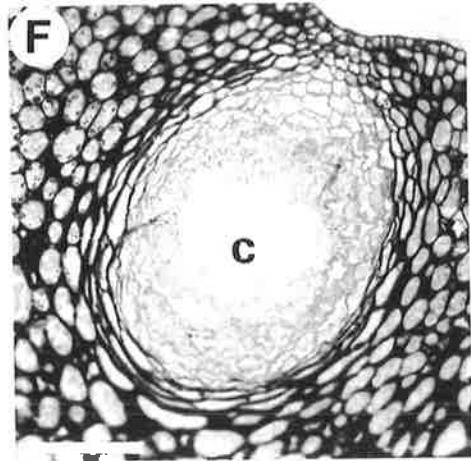
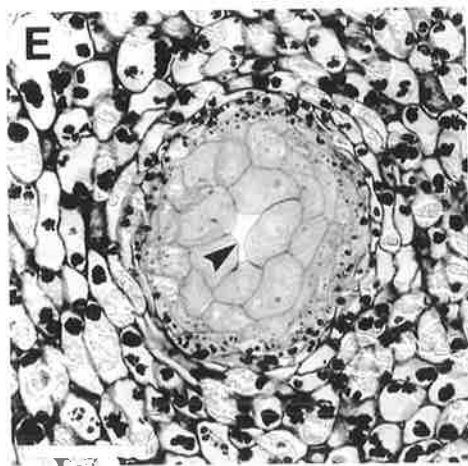
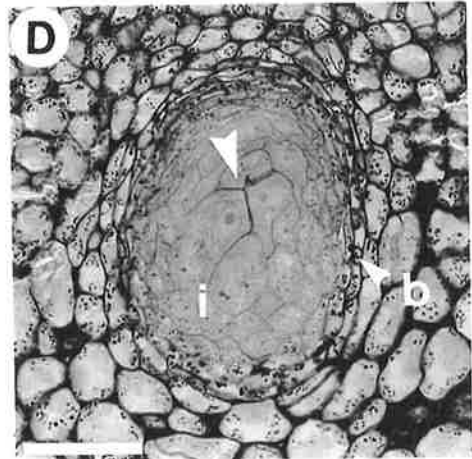
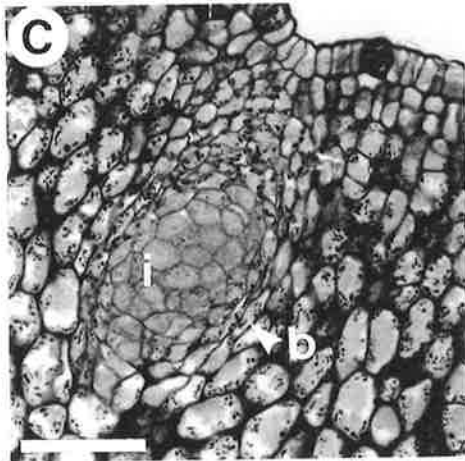
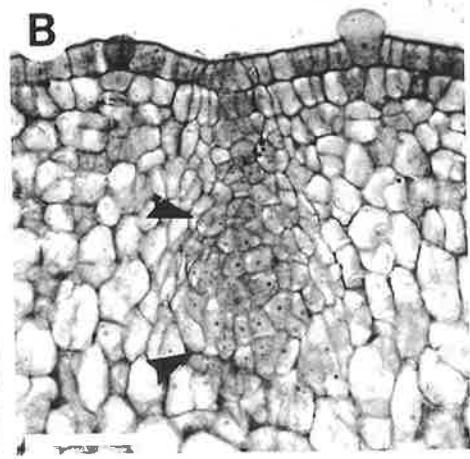
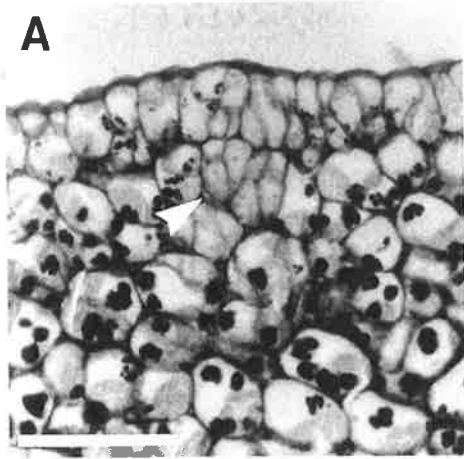


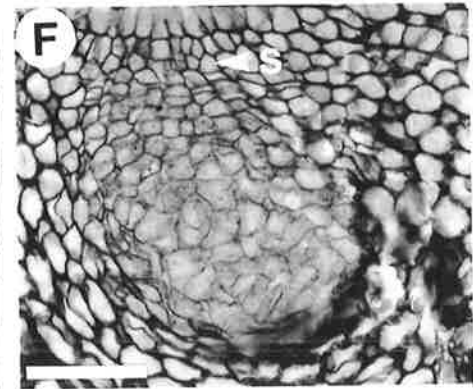
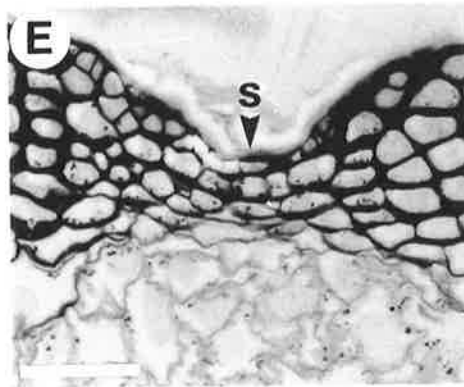
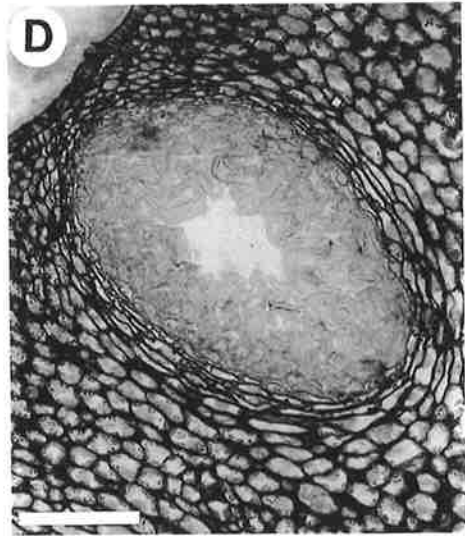
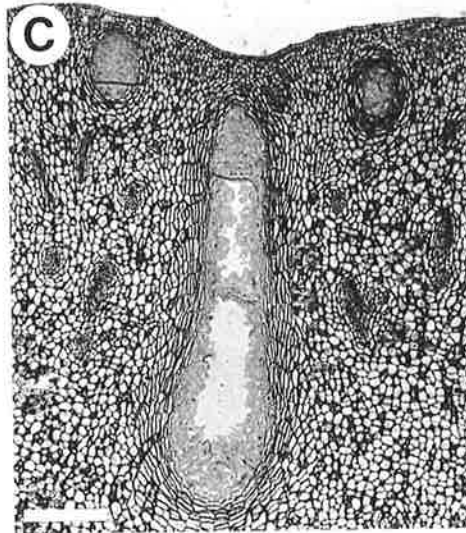
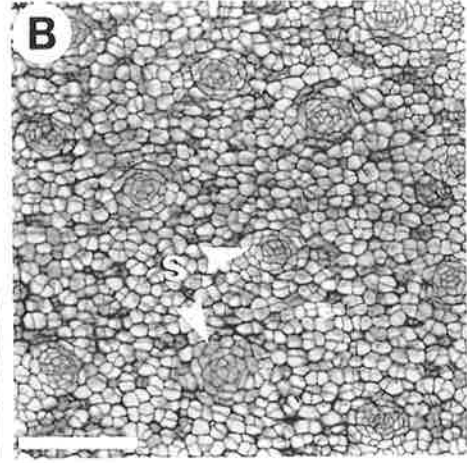
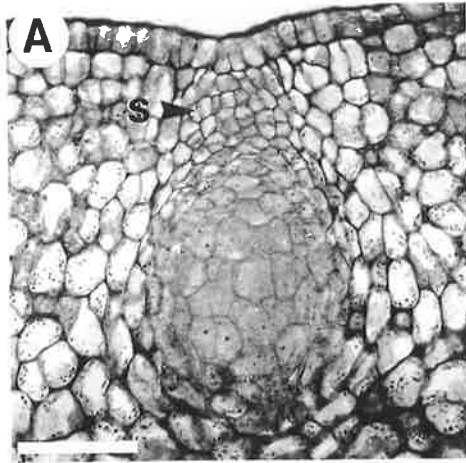
Plate 3.2

Light micrographs depicting the gland stalk and gland form. Aldehyde fixed, PAS/TBO stained sections.

A and B. Longitudinal (A) and transverse (B) sections through the gland stalk. A, A conical-shaped stalk (s) joins the gland to the fruit epidermis. B, A transverse section 16 μm from the fruit surface shows gland stalks are solid structures, appearing as round clusters of cells (s). Bars = 10 μm .

C and D. Medial, longitudinal sections through mature (stage 6) glands of different forms. C, Elongated gland. Bar = 50 μm . D, Oval-shaped gland. Bar = 20 μm .

E and F. Medial, longitudinal sections through the stalks of mature glands (s). E, In a mature fruit, stage E. F, In an immature fruit, stage B. Bars = 10 μm .



3.3.2. Timing of gland development

Glands were present in the pre-anthesis floral ovary. Glands at various stages of development were observed in the youngest sample collected, a flower bud of 8 mm length from the base of the calyx to petal tip, with an ovary of approximately 2.6 mm in diameter. The most advanced stage of gland development observed in this sample was stage 4.

Gland initiation was found to be restricted to early stages of fruit development. Gland counts under the dissecting microscope showed an exponential decline in gland density up until a fruit size of approximately 20 cm² surface area (25 mm diameter). From this time onwards, a more gradual decline was evident (Fig. 3.1A). Considering the possible effects of fruit growth on gland density values, total gland number per fruit was assessed. Total gland number per fruit appeared to show a slight initial increase, but remained fairly constant with increasing fruit size, concentrated around 8000 to 12000 glands per fruit (Fig. 3.1B). The approximate total gland number of a mature, 88 mm diameter fruit (247 cm² surface area) was similar to that evident in an immature, 20 mm diameter fruit (13 cm² surface area). This confirms that gland initiation was confined to early stages of fruit development, until a fruit size of approximately 20 mm diameter. Results of the gland age survey supported this finding, with gland initials (stage 1) comprising 27% of the gland population in the floral ovary at full bloom (stage A), declining to 11% in a 10 mm fruit (stage B) and disappearing thereafter (Fig. 3.2).

In the floral ovary, a high proportion of glands contained newly formed cavities (20%) and some showed a more advanced stage of cavity opening (3%) (Fig. 3.2). The proportion of mature glands increased from 23% in the floral ovary (A), to 64% in a 10 mm fruit (B), 87% in a 32 mm fruit (C) and to 100% in a 52 mm fruit (D) (Fig. 3.2). Hence, all glands reached maturity in an immature, green fruit, 32 to 52 mm in diameter.

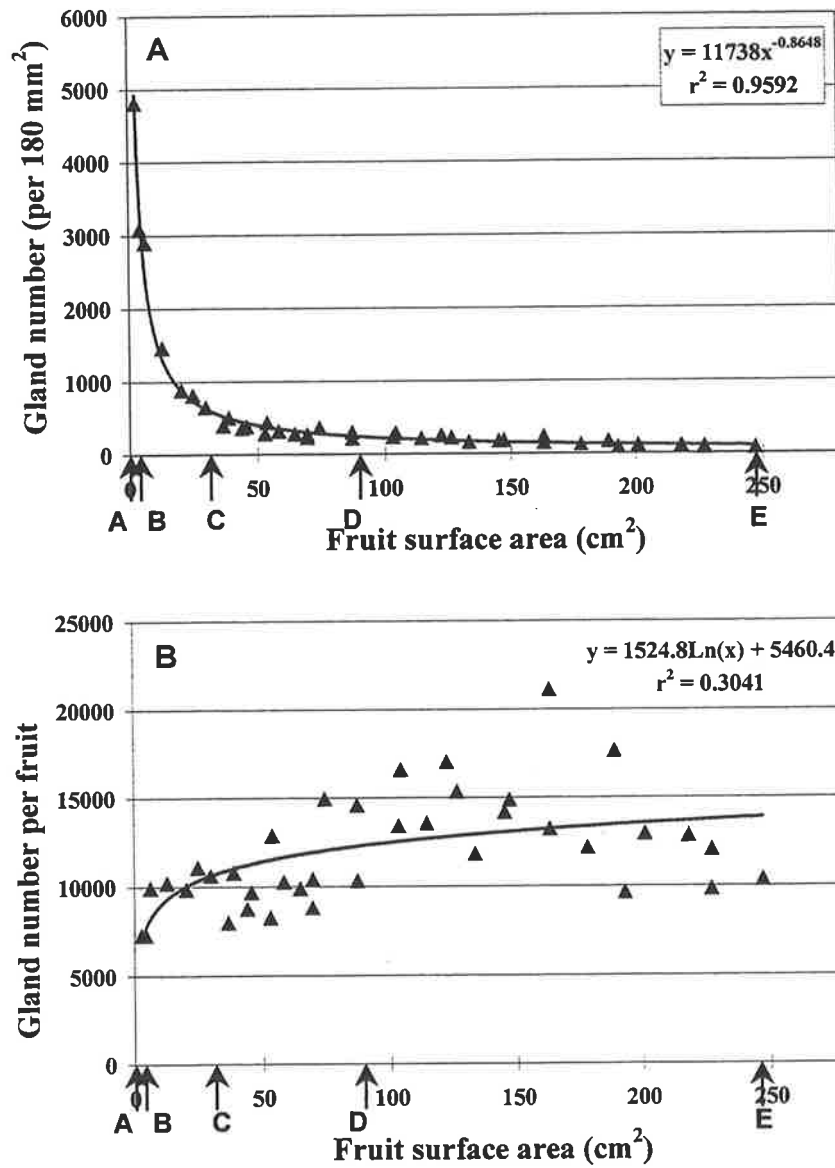


Figure 3.1. Changes in oil gland density (A) and total gland number per fruit (B) with fruit growth (represented by fruit surface area). The five fruit stages A to E are labelled.

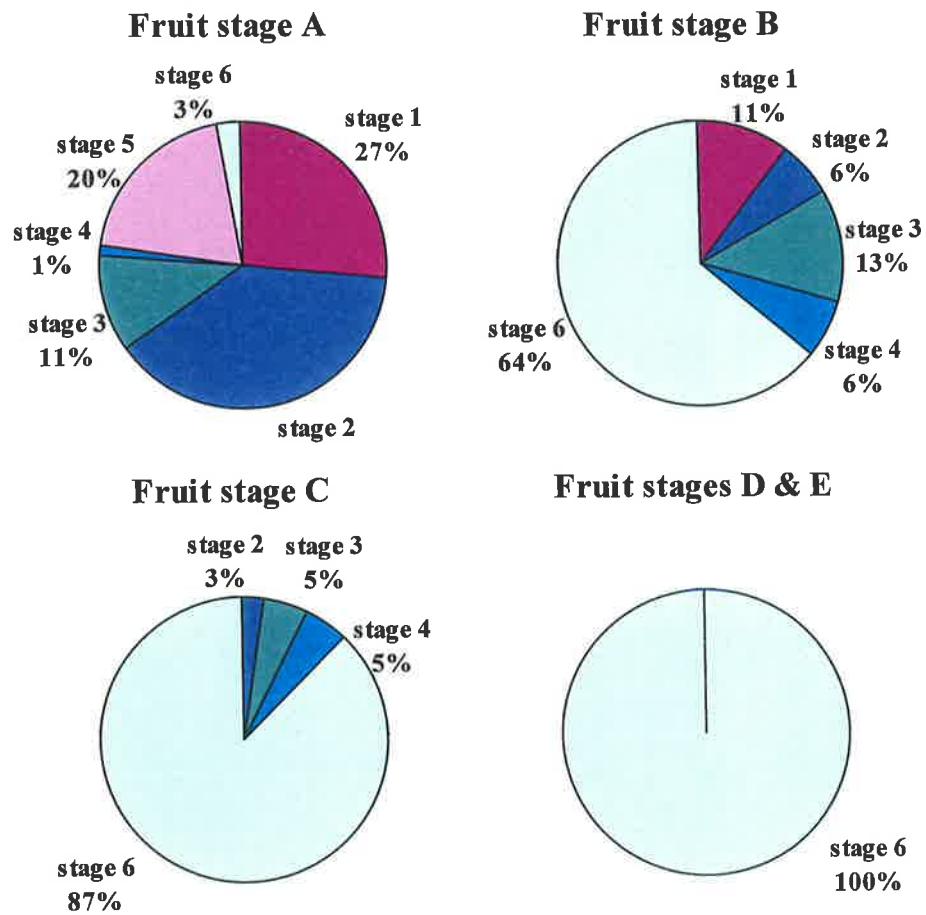


Figure 3.2. Gland age survey in fruit stages A to E. Frequency (%) of each gland developmental stage (1 to 6). Fruit stage A = full bloom sample, stage B = 10 mm diameter, stage C = 32 mm, stage D = 52 mm, stage E = 88 mm. Gland stage 1 = cell cluster up to ten cells, stage 2 = ten - 30 cells, stage 3 = differentiating gland, stage 4 = differentiated gland, stage 5 = newly formed cavity, stage 6 = expanded cavity.

3.3.3. The mature gland

The mature gland continued to enlarge with fruit growth (Fig. 3.3). Mean gland volume varied significantly between the five stages from full bloom to mature fruit ($P < 0.001$). Using the LSD test, a significant difference ($P < 0.05$) in mature gland volume was found between 52 mm (stage D) and 88 mm fruit (stage E), suggesting a period of rapid gland enlargement. Gland size also varied within each fruit sample as suggested by the high standard errors associated with gland volume (Fig. 3.3). Mature glands were not uniform in shape, as observed in LM tissue sections (Plates 3.2C and 3.2D).

The stalk of mature glands appeared to become less prominent as the fruit aged (Plates 3.2E and 3.2F). In mature fruit (stage E), the stalk is reduced to only a few cell layers in depth below the epidermis (Plate 3.2E). The orientation of the stalk in relation to the fruit surface also changed with fruit age. In young, rapidly growing fruit (stage B), gland stalks were positioned at an angle to the epidermal plane (Plate 3.2F), whereas in older fruit, the stalk was located in the medial section of the gland (Plate 3.2E).

At early stages of cavity formation, flattened boundary cells surrounded inner polyhedral shaped cells, whose walls appeared to form the cavity (Plate 3.3A). Inner gland cells showed large nuclei and many small vacuoles, and cells surrounding the cavity exhibited a densely stained cytoplasm. In mature glands, with an expanded cavity, inner cells appeared to be more flattened, but slightly swollen, with edges bulging into the cavity space (Plate 3.3B). Cell walls were also observed to increase in thickness towards the gland perimeter. The thickened walls of boundary cells have been demonstrated in an aldehyde fixed tissue section (Plate 3.3C). Histochemical staining was undertaken to show differences in cell wall composition, but failed to show the presence of lignin or suberin in the thickened cell walls. TEM examination of cells surrounding the newly formed gland cavity showed the presence of bulbous extracellular pockets (Plate 3.3D).

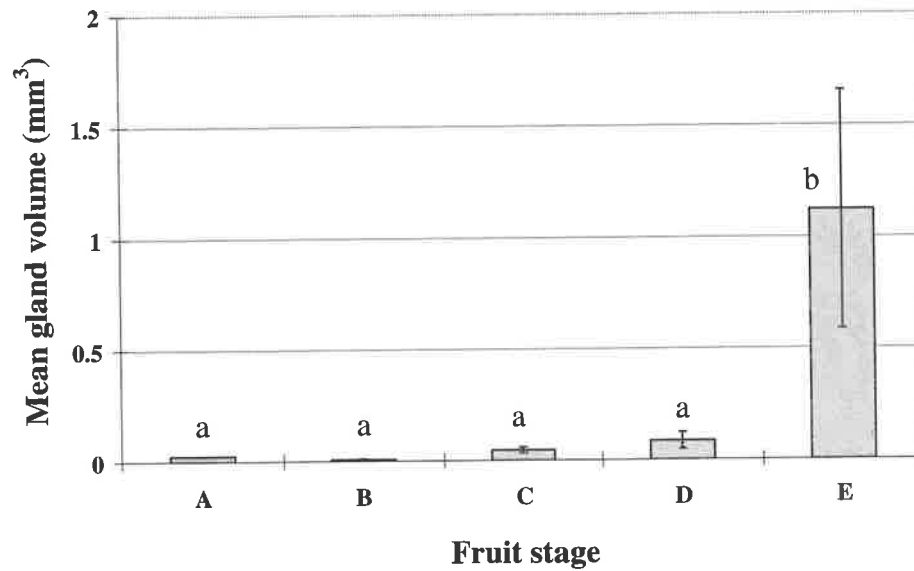


Figure 3.3. Mature gland volume in fruit stages A to E. Fruit stage A = full bloom sample, stage B = 10 mm diameter, stage C = 32 mm, stage D = 52 mm, stage E = 88 mm. Means and standard errors represented. Letters (a and b) represent significant differences ($P < 0.05$) between fruit stages.

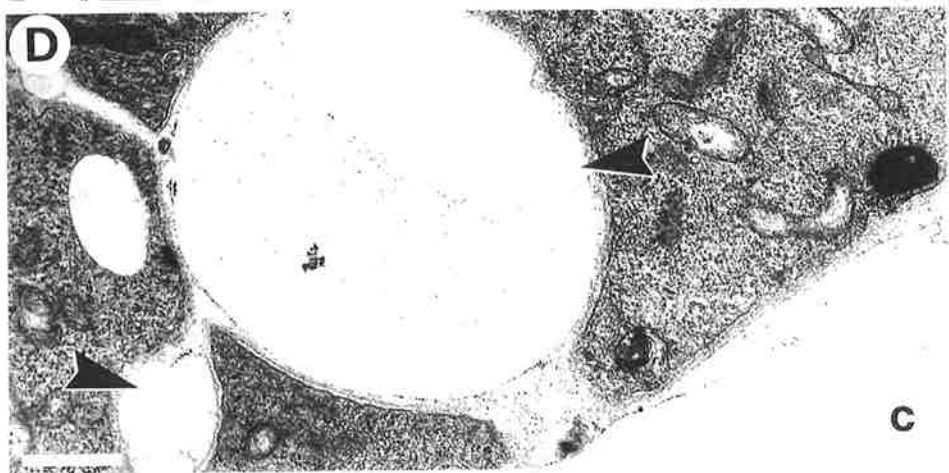
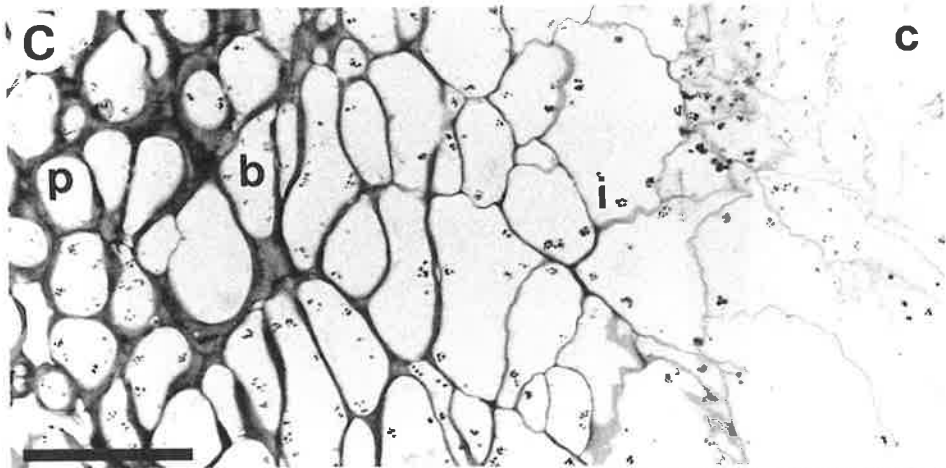
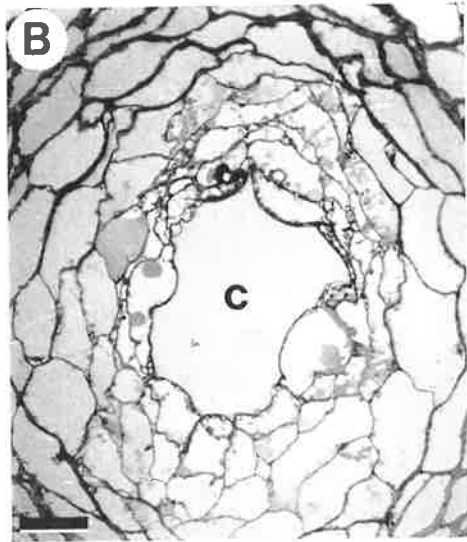
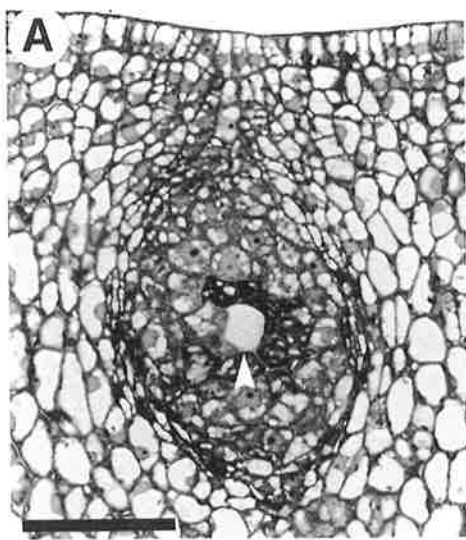
Plate 3.3

Micrographs depicting mature gland anatomy and cavity formation.

A and B. Light micrographs of aldehyde plus osmium tetroxide postfixed, medial, longitudinal, TBO stained sections through the gland cavity. A, Gland with a newly formed cavity (arrow), equivalent to stage 5. B, Gland with an expanded cavity (c), equivalent to stage 6. Bars = 10 μm .

C. Light micrograph of an aldehyde fixed, longitudinal, PAS/TBO stained section through a mature (stage 6) gland: gland cavity (c), inner gland cells (i), boundary cells (b) and surrounding parenchyma cells (p). Bar = 20 μm .

D. Transmission electron micrograph showing bulbous extracellular pockets (arrows) along the walls of cells surrounding the newly formed gland cavity (c). Bar = 1 μm .



3.4. Discussion

In this study, the effect of different tissue fixation methods used has been taken into consideration. Aldehyde fixed tissue facilitated the collection of large tissue samples and serial sectioning, which was required to establish the anatomical gland developmental series, and to carry out the gland age survey and gland volume measurements. Aldehyde fixation has been reported to cause artefactual swelling and rupture of inner epithelial cells in the foliar glands of *C. limon* (Turner *et al.*, 1998). For this reason, an improved fixation protocol was used to prepare tissue for the examination of mature gland anatomy and cavity formation. In addition, glands were not damaged during sample collection and have been captured in medial section.

Until this study, gland development had not been examined in fruit of the Washington navel orange. Gland development from the stage of cavity formation onwards has been examined in the foliar glands of Washington navel orange (Thomson *et al.*, 1976), but the most detailed anatomical outline of gland development has been achieved in the ovaries of *C. deliciosa* or Mediterranean mandarin (Bosabalidis and Tsekos, 1982a). LM observations in the present study were similar to those made in *C. deliciosa* ovaries (Bosabalidis and Tsekos, 1982a). In both studies, gland initiation and cavity formation clearly occurred as two separate events. The earliest detection of gland initiation as a small cluster of cells at the fruit surface supports Bosabalidis and Tsekos (1982a), who reported that glands differentiated from a pair of meristematic cells, one epidermal and one underlying. This also corroborates earlier descriptions of citrus gland differentiation by Bartholomew and Reed (1943) and Schneider (1968).

To date, the presence of a gland 'stalk' has been described only by Bosabalidis and Tsekos (1982a). In their study, they considered the two initial cells to be precursors to the two parts of the differentiated glandular complex; the globular/oval gland situated in the parenchyma, and the 'conical stalk' joining the gland to the epidermis. Epidermal cells referred to as 'oil-gland cover cells', have also been reported previously in the fruit (Scott and Baker, 1947; Safran, 1980)

and bark (Schneider, 1955) of *Citrus* species. Oil-gland cover cells were reported by Scott and Baker (1947) to have an area proportional to the underlying gland and appear somewhat flattened and polygonal in surface view. In the present study, the gland stalk was observed in all differentiation stages of Washington navel orange glands, as well as at different fruit ages. The stalk structure was less apparent in older fruit, which may be explained by a lateral flattening above oil glands (Bartholomew and Reed, 1943) or by the continual growth of cells in the epidermal and hypodermal layers (Bain, 1958), causing a bulging effect around the gland stalk. The inconspicuous nature of the stalk in mature fruit may explain why the majority of past studies have failed to describe an epidermal attachment of the oil glands in mature citrus fruit. In addition, if tissue sections are being examined, the stalk can go unnoticed if a longitudinal tissue section does not pass directly through it, as pointed out by Bosabalidis and Tsekos (1982a).

Gland initiation, development, and enlargement were all quantified with respect to fruit growth. Gland counts were localised to the equatorial region of the fruit, to correspond to microscopy samples. Gland initiation was found to be restricted to early fruit development, ceasing at a fruit size of approximately 20 mm diameter. This agrees with findings in Eureka lemon (Ford, 1942) and Valencia orange, where gland initiation was observed only in the 'cell division' stage of fruit development, which continued to a fruit size of approximately 16 mm (Bain, 1958). However, findings refute the statement of Schneider (1968) who suggested that oil glands continued to form as the citrus fruit matured. Similarly, it has been suggested that oil glands form in the very young stems of *C. sinensis* (Webber and Fawcett, 1935). Glands continued to develop, until all had reached maturity in an immature green fruit, 32 to 52 mm in size. This finding contradicts Holtzhausen (1969), who inferred that glands in Washington navel orange fruit continued to develop up until fruit ripeness.

Once mature, glands continued to enlarge with fruit growth, as has been reported previously in Washington navel orange (Holtzhausen, 1969), as well as Valencia orange (Bain, 1958). The period of rapid gland enlargement observed

between fruit sizes of 52 and 88 mm roughly coincides with the period of cell enlargement in the rind of Washington navel orange fruit described by Bouma (1959). Mature glands of different sizes were also found within each fruit examined, which may be explained by the non-uniform timing of both gland initiation and maturation in relation to fruit development. Gland shape was also non-uniform. Previously, the oil glands of *Citrus* have been described as varying from “oblate to spherical or ovoidal to pyriform” (Bartholomew and Reed, 1943). It has also been suggested that glands are located at different depths in the rind (Bartholomew and Reed, 1943; Ting and Attaway, 1971). In this study, although all glands were found to link to the epidermis by the gland stalk, gland cavities did occur at different depths due to size differences alone, often extending into the albedo layer.

Mature gland anatomy consisted of a central cavity surrounded by a multi-layered epithelium of radially flattened cells (Thomson *et al.*, 1976; Shomer, 1980; Bosabalidis and Tsekos, 1982a; Turner *et al.*, 1998). Observations suggest that inner gland cells are modified into boundary cells, as has been reported previously in the glands of *Citrus* (Thomson *et al.*, 1976; Bosabalidis and Tsekos, 1982b). The innermost gland cells appeared typical of what have been described as ‘secretory parenchyma’ cells, which usually possess thin and extremely permeable walls, allowing movement of secretion into and out of the cell (Mauseth, 1988). Boundary cells possessed thickened walls, but did not appear to contain lignin, a common component of plant secondary walls (Mauseth, 1988). Similarly, the foliar glands of *C. limon* have been observed not to contain lignin or suberin (Turner *et al.*, 1998).

An interesting feature of the mature gland is the mechanism by which the secreted material is isolated from the rest of the plant body. Fahn (1979) suggested that this may occur by deposition of waterproofing materials (usually lignin or suberin), viscosity of the secreted material, compactness of the wall, or by the absence of intercellular spaces. To our knowledge, previous microscopy studies of the oil glands of *Citrus* have not addressed this matter, except Thomson *et al.*

(1976), who described a “dense and diffuse” cavity wall, based on TEM observations. In the present study, histochemical staining showed neither suberin nor lignin to be present in the walls surrounding the cavity. However, suberin was difficult to detect with SBB, as oil bodies which are also sudanophilic, were localised in this region. Previously, suberin has been detected in the oil-containing cells of avocado (*Persea americana*) (Scott *et al.*, 1963), and lignin in the oil-containing cells of lemongrass (*Cymbopogon citratus* (DC.) Stapf.) (Lewinsohn *et al.*, 1998).

There is considerable contention in the literature regarding the mode of cavity formation in the oil glands of *Citrus* species; lysigeny or schizogeny. Lysigeny refers to a process of cell degeneration, and schizogeny a process of cell wall separation, to form a tissue cavity. This topic has been reviewed by Turner (1999). In an examination of the foliar oil glands of *C. limon* (Turner *et al.*, 1998), the lysigenous appearance of glands was concluded to be fixation artefact and a protocol for improved tissue preservation was recommended. Their method involved primary fixation with osmium tetroxide vapour, followed by fixation in an aldehyde plus osmium tetroxide solution, fixation in aldehyde alone and finally, an osmium tetroxide solution postfixation. Using osmium vapour as a primary fixative was reported to reduce vacuolar swelling and improve lipid preservation. In the present study however, the protocol resulted in extremely poor preservation of Washington navel orange rind samples (see Chapter 4 for more detail). Instead, aldehyde fixation plus osmium tetroxide postfixation was employed for the examination of gland cavity formation. At the LM level, both methods were reported by Turner *et al.* (1998) to give similar structural preservation of intact glands. Using this method, epithelial cells surrounding the gland cavity showed no signs of structural degeneration. At an earlier stage of cavity formation, cells surrounding the cavity appeared structurally intact, however a number of them exhibited a densely stained cytoplasm. TEM examination of these cells showed the presence of bulbous pockets along the cell walls. Similar observations were made in the foliar glands of *C. sinensis*, prepared by similar methods (Thomson *et al.*, 1976). In their study, the formation of

bulbous extracellular pockets was used as evidence of a schizogenous cavity formation.

3.5. Conclusion

Gland initiation was restricted to early stages of fruit development, and all glands matured in an immature fruit, but continued to enlarge throughout fruit growth. All glands were joined to the fruit epidermis by a stalk, irrespective of their stage of development or location of the cavity within the rind. LM and TEM observations suggest that glands of Washington navel orange fruit are anatomically similar to those of other *Citrus* species, and that early stages of cavity formation involve schizogeny.

Chapter 4

Rind oil visualisation: method development

4.1. Introduction

4.1.1. Background

Microscopic examination of oils in plant and animal tissues is limited due to difficulties in retaining lipids with conventional tissue fixation protocols. In a typical tissue fixation schedule for light or electron microscopy, tissues are fixed in a primary aldehyde fixative, rinsed in buffer, postfixed in osmium tetroxide, dehydrated, and infiltrated with a plastic resin, which is then polymerised using heat, catalysts or ultraviolet radiation (Dykstra, 1992). Primary aldehyde fixation (commonly glutaraldehyde or paraformaldehyde) assures the rapid stabilisation of proteins, but does not effectively preserve lipid (Dykstra, 1992). Postfixation with osmium tetroxide (OsO_4) stabilises both proteins and lipids, in particular cell membranes and other fatty components (Roland and Vian, 1991). Osmium oxidises the double bonds of unsaturated lipids, leading to the formation of monoesters, diesters and dimeric monoesters (Dykstra, 1992). Using osmium postfixation, oils have been preserved to some extent in the foliar oil glands of *Citrus sinensis* (Thomson *et al.*, 1976) and *C. limon* (Turner *et al.*, 1998), and in other plant secretory structures, such as the oil idioblasts of *Persea americana* (Platt and Thomson, 1992) and *Annona muricata* (Bakker and Gerritsen, 1990). However, osmium postfixation does not prevent lipid loss during dehydration (Hayat, 1989).

Modifications to conventional methods are required to improve oil retention. Such a method has been suggested by Turner *et al.* (1998) in their study of the foliar oil glands of *C. limon*. When compared with standard double fixation, they reported that using osmium vapour primary fixation achieved “enhanced lipid retention, both within the epithelial cells and in the central storage space” of

mature glands. In the same study, chemical fixation of the oil glands was compared to cryofixation. Tissue prepared by high pressure freezing was reported to show superior preservation to chemical methods, but inferior oil retention, due to oil extraction during freeze-substitution. Apart from freeze-substitution, cryofixed material can be prepared by a number of methods, including freeze-fracture, freeze-drying, immunolabelling and microanalytical approaches (Dykstra, 1992). Cryofixation and freeze-fracturing of oil glands has been shown to preserve oil droplets within the cavities, detected using a scanning electron microscope (SEM) (Shomer, 1980).

Some of the constraints associated with retaining oil by chemical or cryofixation can be overcome by visualising lipid in fresh tissue. This can be achieved with confocal microscopy. The essential oils contained within the glands of *Citrus* species contain highly fluorescent polymethoxylated flavones, making them autofluorescent under ultraviolet light (Loveys *et al.*, 1998). Oils can also be labelled with fluorescent dyes, as has been demonstrated in an examination of oil localisation in the rind of chilling injured Eureka lemon fruit (Obenland *et al.*, 1997).

4.1.2. Aims

The aim of this study was to develop a method to improve oil retention in the rind tissue of Washington navel orange, for visualisation with light microscopy (LM). Modifications were made to conventional chemical fixation procedures, and cryofixation was also tested. As an adjunct to LM, protocols were also developed for SEM and confocal microscopy. A secondary aim of the study was to use the improved method to examine the timing of rind oil accumulation, to complement the anatomical investigation of oil gland development (see Chapter 3). The success of each method was based on achieving the following criteria:

- good structural preservation of the rind tissue;
- good oil retention within the glands;
- the ability to visualise oil within the glands with minimal disruption to the tissue.

4.2. Materials and Methods

4.2.1. Light microscopy (LM)

Schedules for LM tissue preparation are summarised in Table 4.1.

Table 4.1. Summary of fixation, dehydration and embedding schedules for LM Methods 1 to 7.

Method	Primary fixation	Post-fixation	Dehydration	Embedding
1	Aldehyde	Aqueous osmium (1h)	Acetone (70-100%)	PA
2	Osmium vapour	Aldehyde/osmium solution, aldehyde, aqueous osmium	Ethanol (70-100%)	PA
3	Osmium vapour	Aldehyde/osmium solution, aldehyde, aqueous osmium	Ethanol (10-100%)	Spurr
4	Aldehyde	Aqueous osmium (4h)	Ethanol (50-100%)	PA
5	Aldehyde	Aqueous osmium (4h)	Ethanol (50-100%)	GMA
6	SBB staining	Aldehyde	Ethanol (30-100%)	GMA
7	Slam freezing		Methanol	Lowicryl

4.2.1.1. Method 1 - Osmium postfixation and Procure-Araldite embedding

Tissue preparation was carried out according to the second method outlined in Section 3.2.3.2. Rind samples of approximately 1 x 2 mm were fixed in a solution of 4% formaldehyde, 1.25% glutaraldehyde and 4% sucrose, in phosphate buffered saline (PBS), pH 7.2, overnight at 0-4°C. After two short rinses in PBS, samples were postfixed in phosphate buffered 1% osmium tetroxide for one hour. Samples were dehydrated through an acetone series (70, 90, 95, 100%), with each step consisting of three 20 minute changes, plus an additional one hour of 100% acetone. Samples were infiltrated overnight in a 1:1 mixture of acetone:Procure-Araldite (PA) resin, followed by three eight hour changes of 100% resin, all on rotator. Samples were flat embedded and polymerisation achieved at 70°C.

4.2.1.2. Method 2 - Osmium vapour fixation and Procure-Araldite embedding

Tissue fixation was similar to that of Turner *et al.* (1998). Rind samples of approximately 1 x 2 mm were placed on moistened filter paper in an enclosed petri dish and exposed to vapours from a pool of aqueous 2% osmium tetroxide, at room temperature for 30 minutes. They were then placed in a chilled solution of 2.5% glutaraldehyde, 2% formaldehyde and 0.1% aqueous osmium tetroxide in 0.05M Pipes buffer, pH 6.8, for one hour, and then transferred to the same

solution minus the osmium at 0-4°C overnight. The following morning, samples were postfixed in a solution of 1% osmium tetroxide in 0.05M Pipes buffer at 0-4°C for one hour. Dehydration was slightly modified from Method 1, with samples dehydrated at 0-4°C through an ethanol series (70, 90, 95, 100%), with each step consisting of three 20 minute changes, plus an additional one hour of 100% ethanol. Samples were infiltrated overnight in a 1:1 mixture of ethanol: PA resin, followed by three eight hour changes of 100% resin. Samples were embedded as in Method 1.

4.2.1.3. Method 3 - Osmium vapour fixation and Spurr embedding

Tissue fixation was conducted as described in Method 2. Dehydration, infiltration and embedding methods were adapted from those outlined by Spurr (1969). Samples were dehydrated at 0-4°C through a gradual ethanol series (10, 20, 30, 40, 50, 60, 70, 80, 90 and 100%), with each step consisting of two 10 minute changes, plus an additional one hour of 100% ethanol. Samples were infiltrated overnight in a 1:1 mixture of ethanol:Spurr resin, followed by three eight hour changes of 100% resin. Samples were flat embedded and polymerisation achieved at 70°C. A 'firm' resin was prepared according to the method of Spurr (1969). Osmium postfixed material was also processed.

Initially, blocks were found to be brittle and difficult to section. Softer blocks were not obtained by reducing polymerisation temperature or extending polymerisation time. Problems were rectified by changing the flexibiliser component of Spurr resin from DER 736 (Spurr kit, Sigma, St. Louis, USA) to DER 732 (Spurr's embedding kit, ProSciTech, Thuringowa, Australia).

4.2.1.4. Method 4 - Modified osmium fixation and Procure-Araldite embedding

Rind samples of approximately 1 x 2 mm were used. Samples were fixed in a solution of 2.5% glutaraldehyde and 2% formaldehyde in 0.05M Pipes buffer, pH 6.8, for 24 hours at 0-4°C. After two short rinses in Pipes buffer, samples were postfixed in 1% osmium tetroxide in 0.05M Pipes buffer at 0-4°C for four hours. After two further rinses in Pipes buffer, samples were dehydrated through an

ethanol series (50, 70, 90, 95, 100%), with each step consisting of three 20 minute changes, plus an additional one hour of 100% ethanol. Samples were infiltrated for 24 hours in a 1:1 mixture of ethanol:PA resin. Infiltration in 100% resin was carried out in several steps: overnight, eight hours, 24 hours, 24 hours and eight hours, all at 0-4°C. Samples were embedded according to previous methods.

4.2.1.5. Method 5 - Modified osmium fixation and glycol-methacrylate embedding

Rind samples of approximately 2 x 2 mm were used, and tissue was prepared according to Method 4, replacing PA resin with glycol-methacrylate (GMA). GMA preparation and embedding was carried out as outlined in Section 3.2.3.2.

4.2.1.6. Method 6 – Sudan Black B staining and glycol-methacrylate embedding

Rind tissue was injected with the lipid stain Sudan Black B (SBB) (Sigma) in 70% ethanol for ten minutes prior to sample collection. This method is similar to one previously observed to stain oil in the glands of navel orange rind tissue (Susan Johnson, Technical Officer, CSIRO Plant Industry; Pers. Comm., 2000). Samples of approximately 3 x 3 mm were rinsed briefly in 50 and 30% ethanol and fixed overnight in 3% glutaraldehyde in 0.025M phosphate buffer at 0-4°C (Feder and O'Brien, 1968). Samples were rinsed in phosphate buffer and dehydrated at 0-4°C through an ethanol series (30, 40, 50, 60, 70, 80, 90, 95, 100%), with each step lasting one hour. Samples were infiltrated in a 1:1 mixture of ethanol:GMA overnight, followed by two changes of 100% GMA for two days each. Samples were embedded in GMA, as in Method 5.

4.2.1.7. Method 7 – Cryofixation, freeze-substitution and low temperature embedding

Rind samples of 0.5 mm width and length were frozen by impact onto a liquid nitrogen cooled copper block using a MM 80 metal mirror cryofixation system attached to a Leica EM CPC cryopreparation unit. Frozen samples were transferred to the chamber of a Reichert AFS automatic freeze-substitution system at -80°C and substituted in methanol for 36 hours (Monaghan and Robertson, 1990). Samples were warmed 4°C per hour to -45°C, and infiltrated with Lowicryl

HM 20 (Chemische Werke Lowi, Waldkraiburg, Germany). The resin was polymerised by ultraviolet light for 48 hours at -45°C.

4.2.1.8. Microtomy and histochemistry

For each method, sections were collected from a minimum of four samples. For PA, Spurr and Lowicryl embedded material, sections (1 µm thickness) were cut on a glass knife with a Reichert-Jung Ultracut E Microtome, placed on glass slides and stained with Toluidine Blue O (TBO) (Sigma) (O'Brien and McCully, 1981) or SBB (Sigma) (Bronner, 1975). For GMA embedded material, sections (4 µm thickness) were cut on a glass knife with a Reichert-Jung 2050 Supercut Microtome, placed on glass slides, and stained with periodic acid-Schiff's (PAS) and TBO (O'Brien and McCully, 1981), or with SBB (O'Brien and McCully, 1981). All material was observed with a Zeiss Axiophot Photomicroscope, using transmitted light.

4.2.2. Scanning electron microscopy (SEM)

4.2.2.1. Environmental SEM (ESEM)

Rind samples of approximately 2 x 3 mm were examined using an ElectroScan ESEM.

4.2.2.2. Field emission gun SEM (FEGSEM)

a. Chemical fixation

Rind samples of 2 x 2 mm were fixed according to Section 4.2.1.1. Samples were dehydrated through an acetone series and critical-point dried with CO₂. Samples were mounted on aluminium stubs with sticky tabs (ProSciTech), carbon/gold coated and observed using a Philips XL 30 FEGSEM, at an accelerating voltage of 10 kV.

b. Freeze-fracture

Rind samples of approximately 2 x 3 mm were attached to a clamping holder, oriented to allow a longitudinal fracture through a selected gland. Samples were plunge frozen in a liquid nitrogen slush, and transferred under vacuum to the prechamber of an Oxford CT 1500 HF cryotransfer system, maintained at

approximately -130°C, where they were fractured with the end of a scalpel blade. After fracturing, the samples were sublimed for five minutes at -92°C and 5×10^{-5} Pa, recooled to -110°C, and coated with gold palladium. Samples were transferred to the cold stage mounted in the Philips XL 30 FEGSEM, and examined at approximately -190°C.

c. Cryofixation

Rind samples of approximately 2 x 3 mm were mounted onto aluminium stubs with carbon paint. Samples were cryofixed according to the above protocol, and sublimed for approximately three minutes at -92°C and 5×10^{-5} Pa, recooled to -110°C, and coated with gold palladium. Samples were examined as above.

4.2.3. Fluorescence microscopy

4.2.3.1. Light fluorescence microscopy

Rind sections approximately 1 mm thick and 10 mm long were stained with the fluorescent lipid dye Nile Red (NR) (0.01%) (Sigma) (Obenland *et al.*, 1997). The NR stain solution was prepared in either ethanol or in a mixture of polyethylene glycol (PEG) 400 and 90% glycerol (Brundrett *et al.*, 1991). Sections were mounted in 75% glycerol on glass slides, and observed with a Zeiss Axiophot Photomicroscope, using incident-light fluorescence, and a filter combination of excitation 450 - 490 nm and emission 520 nm long pass.

4.2.3.2. Confocal laser scanning microscopy (CLSM)

a. Method 1

Rind tissue was torn, rather than razor sectioned, to obtain intact glands, and then trimmed into sections approximately 2 mm thick and 15 mm long. Sections were mounted in 75% glycerol on glass cover slips and examined using a Bio-Rad MRC-1000 UV CLSM system, attached to a Nikon Diaphot 300 inverted microscope. A krypton/argon laser was used to excite specimens at 488/30 nm and images were collected using emission filter 522/35 nm.

b. Method 2

Rind sections approximately 2 mm thick and 15 mm long were collected. Sections were stained for two hours with aqueous Safranin O (Australian Biostain, Traralgon, Australia), to highlight cell walls. Sections were rinsed and counterstained for two hours with 0.01% NR (Sigma), prepared according to Brundrett *et al.* (1991). Sections were mounted as above. NR fluorescence was observed using the same settings as above, and Safranin O using excitation 568/10 nm and emission filter 605/32 nm.

4.2.3.3. Multi-photon microscopy

Rind sections approximately 2 mm thick and 15 mm long were collected. Sections were stained for 18 hours with 0.01% NR (Sigma) prepared as above, rinsed, and counterstained for five minutes in 0.01% Calcofluor White M2R (CW) (Sigma) prepared in distilled water (Hughes and McCully, 1975). Calcofluor stains mixed-linkage β -glucans (Wood *et al.*, 1983) and was used to highlight cell walls. Tissue sections were mounted as for CLSM, and examined using a Bio-Rad Radiance 2000 MP visualising system attached to a Nikon Eclipse TE300 inverted microscope. A Coherent Mira900-F titanium:sapphire ultrafast laser was used to excite the specimen at 800 nm (or 830 nm) and images were collected using emission filters 620/100 nm (for NR) and 450/80 nm (for CW).

4.3. Results

4.3.1. Light microscopy (LM)

4.3.1.1. Method 1 - Osmium postfixation and Procure-Araldite embedding

Rind tissue showed good preservation (Plate 4.1A). Some glands showed lightly stained oil within their cavity (Plate 4.1B), whilst others showed poorly preserved gland contents. Glands disrupted during tissue preparation showed empty oil cavities.

4.3.1.2. Method 2 - Osmium vapour fixation and Procure-Araldite embedding

The quality of tissue preservation was inferior to that obtained with Method 1 (Plate 4.1C), and sectioning damage due to fragility of the tissue occurred frequently. Oil was evident in all gland cavities and frequently stained darker than that observed in Method 1, but glands showed more signs of damage. The best preserved gland showed an oil-filled cavity with an intact lining, darkly stained inner gland cells, and slight damage to boundary cell layers (Plate 4.1D). Glands disrupted during tissue preparation showed empty oil cavities.

4.3.1.3. Method 3 - Osmium vapour fixation and Spurr embedding

The quality of tissue preservation was slightly improved from Method 2, appearing similar to that obtained with Method 1 (Plate 4.1E), however, sectioning damage due to fragility of the tissue occurred frequently. Darkly stained oil in the gland cavities was observed, but gland structure was poorly preserved (Plate 4.1F). Osmium postfixated samples showed better overall rind preservation than osmium vapour fixed samples, although glands showed similar artefactual damage (Plate 4.1G and 4.1H). The best preserved gland showed darkly stained oil in the gland cavity and inner gland cells (Plate 4.1H).

Plate 4.1

Rind oil visualisation using light microscopy. Longitudinal, TBO stained sections (A to H).

A. Aldehyde and osmium postfixed tissue, embedded in PA resin. Bar = 200 μm .

B. Higher magnification of the gland from A. Lightly stained oil in the cavity (c). Bar = 100 μm .

C. Osmium vapour fixed tissue, embedded in PA resin. Bar = 200 μm .

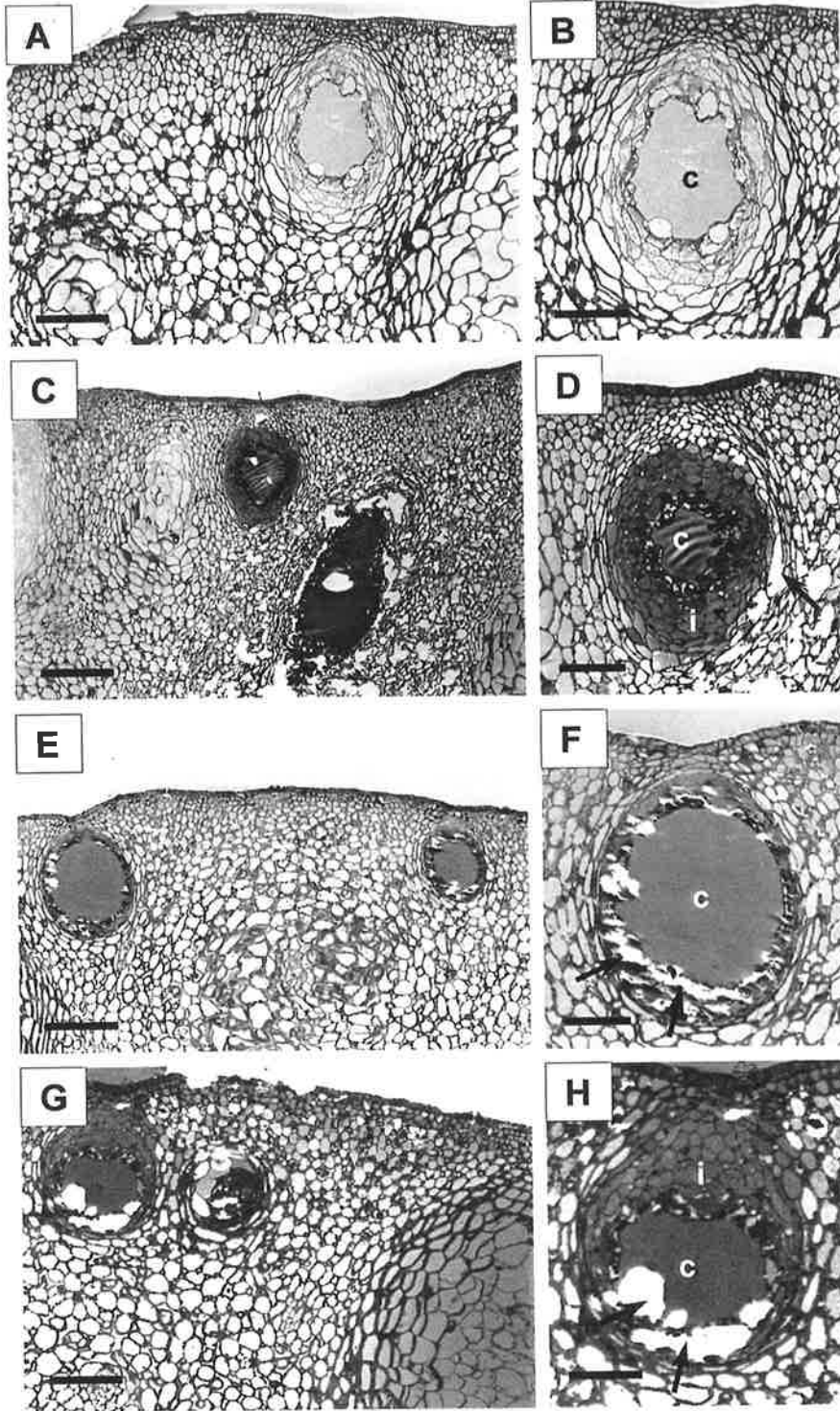
D. Higher magnification of the gland from C. Darkly stained oil in the cavity (c) and inner gland cells (i), and damage to boundary cells (arrow). Bar = 100 μm .

E. Osmium vapour fixed tissue, embedded in Spurr resin. Bar = 200 μm .

F. Higher magnification of the gland from E. Darkly stained oil in the cavity (c), and damage to gland cells (arrows). Bar = 100 μm .

G. Aldehyde and osmium postfixed tissue, embedded in Spurr resin. Bar = 200 μm .

H. Higher magnification of the gland from G. Darkly stained oil in the cavity (c) and inner gland cells (i), and damage to boundary cells (arrows). Bar = 100 μm .



4.3.1.4. Methods 4, 5 and 6

Sections from tissue prepared by these methods have not been presented due to poor preservation. Modified osmium fixation and PA embedding (Method 4) produced significant sectioning damage, and all glands were excessively damaged, or were completely absent, with oil retention difficult to assess. Embedding similarly fixed tissue in GMA (Method 5) improved rind preservation, but glands appeared distorted and oil was not present in the gland cavities. Staining tissue with SBB and embedding in GMA (Method 6) produced the worst preservation of all chemical fixation procedures.

4.3.1.5. Method 7 - Cryofixation, freeze-substitution and low temperature embedding

The small size of samples required for slam freezing resulted in glands either being not present in samples or damaged during tissue preparation.

4.3.1.6. Histochemistry

SBB frequently produced very strong staining of PA resin, hampering the visualisation of black stained lipid bodies. Another drawback of SBB for oil staining was its preparation in ethanol, which is a lipid solvent. TBO was preferred as it did not excessively stain the resin, provided a good contrast stain, and showed the oils.

4.3.2. Scanning electron microscopy (SEM)

4.3.2.1. Environmental SEM

Technical problems encountered with the ESEM examination of fresh tissue samples meant that images could not be obtained. Extreme 'flaring' of the on-screen image was thought to be a result of the sample contacting the detector or the effect of oil volatilisation from the rind tissue.

4.3.2.2. Field emission gun SEM

In chemically fixed tissue, the gland cavity was largely empty, however, small spherical oil bodies were associated with the inner surface of the gland cavity (Plate 4.2A). Oil bodies were also present inside inner gland cells, dissected

Plate 4.2

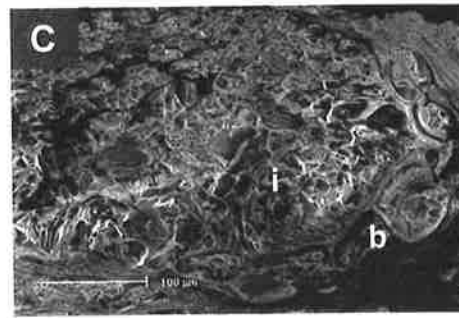
Rind oil visualisation using scanning electron microscopy. Longitudinal gland cross-sections.

A. Chemically fixed tissue, showing a largely empty gland cavity (c). Spherical oil bodies (arrow) associated with the inner surface of the cavity. Morphology of the epicuticular wax (ew) was also evident. Bar = 50 μm .

B. Higher magnification of the gland depicted in A. Spherical oil bodies (arrows) inside inner gland cells, dissected during tissue preparation. Bar = 50 μm .

C. Freeze-fractured tissue, showing an uneven fracture line. Boundary cells (b), and inner gland cells (i) were identifiable, but gland oil could not be detected. Bar = 100 μm .

D. Cryofixed tissue, showing an oil-filled cavity (c). Bar = 200 μm .



during tissue preparation (Plate 4.2B). In freeze-fractured tissue, oil could not be visualised due to the rough fractures achieved (Plate 4.2C), however, in tissue which was sectioned fresh and cryofixed, oil within the gland cavity was successfully preserved and visualised. The cavity of mature glands appeared to be full of oil (Plate 4.2D).

4.3.3. Fluorescence microscopy

4.3.3.1. Light fluorescence microscopy

In dissected glands, NR stained oil bodies were detected around the gland perimeter (Plates 4.3A and 4.3B). Oil bodies were also detected deeper in the gland cavity, and appeared to be associated with the cavity lining (Plate 4.3C). Closer inspection of glands suggested that oil was not present in the flattened boundary cells of the gland (Plate 4.3D). Oil bodies did not appear to be present outside the gland. Both NR preparations (ethanol and PEG 400 plus glycerol) resulted in intense oil fluorescence.

4.3.3.2. Confocal laser scanning microscopy (CLSM)

a. Method 1

Oil was autofluorescent under UV (excitation 351 nm/emission 460 nm), but was more clearly visualised when stained with NR, and examined at excitation 488 nm, with emission filter 522 nm. Rind tissue tearing resulted in a gland half-embedded in tissue and half exposed. Oil bodies were present over the exposed surface of the gland (Plate 4.4A), and were approximately 25 - 30 μm in width. Longitudinal optical sections were collected up to approximately 500 μm into the 1 mm wide gland. An optical section close to the gland centre showed oil bodies localised around the perimeter (Plate 4.4B). Faint fluorescent bodies were also visible deeper into the gland cavity, but could not be visualised. Oil was not present within the gland cavity. Oil bodies did not appear to be present outside the gland.

Plate 4.3

Rind oil visualisation using light fluorescence microscopy. Longitudinal gland cross-sections.

A. Fluorescing oil bodies localised around the gland perimeter at the cut surface. Gland cavity (c) out of focus. Gland attachment to the epidermis also evident (arrow). Bar = 100 μm .

B. Fluorescing oil bodies localised around the gland perimeter at the cut surface (arrows). Gland cavity (c) out of focus. Bar = 100 μm .

C. Same gland as depicted in B. Change of microscope focus shows fluorescing oil bodies deeper into the gland cavity (c). Cut edge is out of focus (arrows). Bar = 100 μm .

D. Basal region of a gland. Fluorescing oil bodies present in inner gland cells (i), but not in flattened boundary cells (b), or in the parenchyma cells (p) surrounding the gland. Bar = 100 μm .

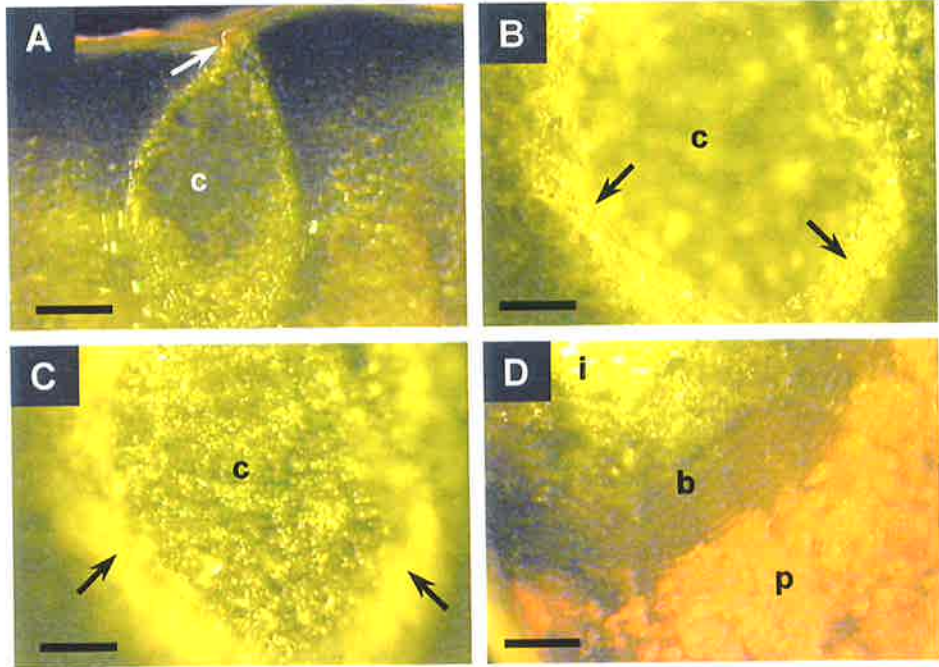


Plate 4.4

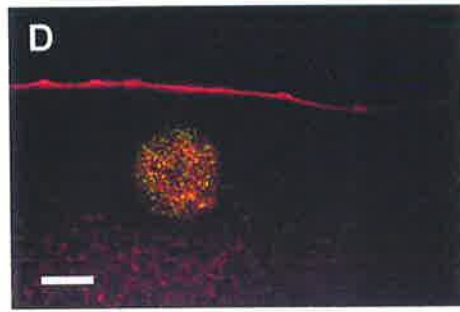
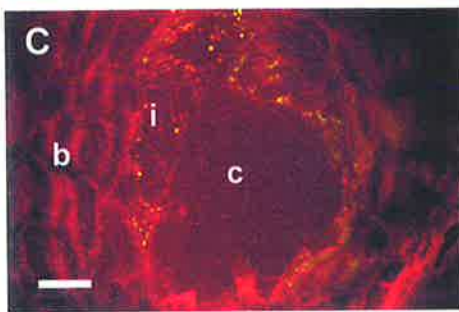
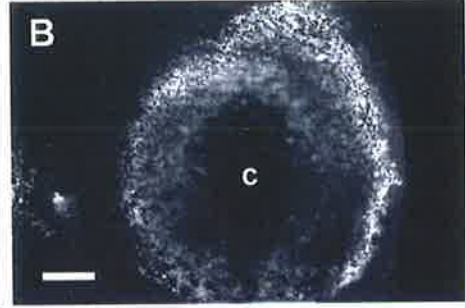
Rind oil visualisation using confocal laser scanning microscopy.

A. Extended focus image of an unstained, exposed gland. Autofluorescent oil bodies present over the exposed surface of the gland (arrows). Bar = 200 μm .

B. Single optical section, approximately 500 μm into the gland depicted in A. Autofluorescent oil bodies localised around the gland perimeter, surrounding the cavity (c). Bar = 200 μm .

C. Two-colour merged optical section (NR, green; Safranin O, red), approximately 26 μm into gland. Fluorescing oil bodies (green) present inside inner gland cells (i), but not in flattened boundary cells (b) or the gland cavity (c). Bar = 50 μm .

D. Two-colour merged optical section (NR, green; Safranin O, red), approximately 55 μm into gland. Fluorescing oil bodies (green) present inside inner gland cells, and central cavity not apparent. Bar = 100 μm .



b. Method 2

Glands were slightly damaged in razor sectioned tissue samples. In one gland, an optical section 26 μm from the cut surface showed oil bodies clearly associated with inner gland cells, but not present in boundary cells (Plate 4.4C). Oil was also not present in the gland cavity. In another gland, in which slightly deeper optical sections were obtained (55 μm from the cut surface), oil bodies were again associated with inner gland cells, and a cavity was not conspicuous (Plate 4.4D). Oil bodies did not appear to be present outside the gland.

4.3.3.3. Multi-photon microscopy

Oil bodies were detected to a depth beyond 180 μm from the cut surface, localised to inner gland cells but not present in boundary cells (Plate 4.5A). A higher magnification optical section through the inner gland cells showed a dense distribution of oil bodies (Plate 4.5B). The composite image of a z-series of optical sections through another gland showed boundary cells to be oil-free, and a dense distribution of oil bodies inside the gland cavity (Plate 4.5C). It appeared that the entire cavity space was filled with oil. A small number of NR labelled bodies were detected outside the gland. Calcofluor provided a more intense labelling of cell walls than Safranin O.

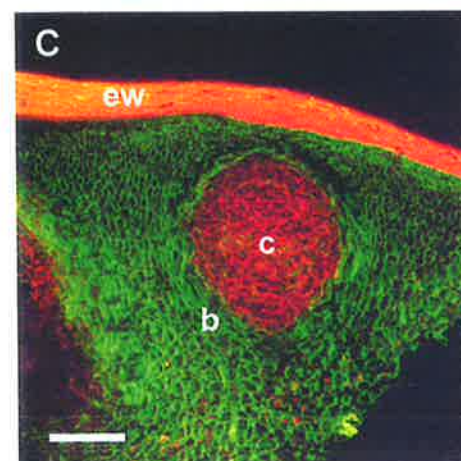
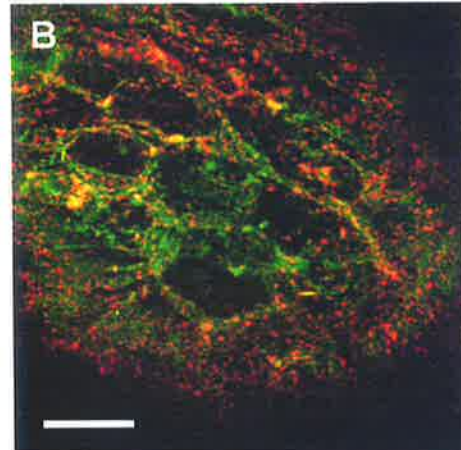
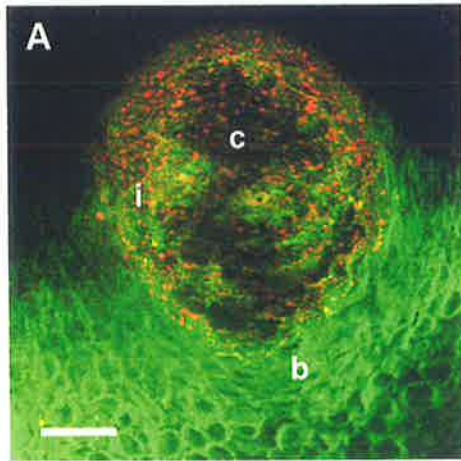
Plate 4.5

Rind oil visualisation using multi-photon microscopy.

A. Two-colour merged optical section (NR, red; CW, green), approximately 150 μm into damaged gland. Fluorescing oil bodies (red) present inside inner gland cells (i), but not in flattened boundary cells (b) or the gland cavity (c). Bar = 50 μm .

B. Two-colour merged optical section (NR, red; CW, green), approximately 180 μm into damaged gland. Fluorescing oil bodies (red) closely associated with the polyhedral shaped inner gland cells. Bar = 10 μm .

C. Two-colour merged composite image of a z-series of 16 optical sections, 1 μm apart, through a gland (NR, red; CW, green). Fluorescing oil bodies (red) filled the entire cavity space (c). Flattened boundary cells of the gland (b) appeared oil-free, and epicuticular wax (ew) stained strongly with the lipid stain NR. Bar = 250 μm .



4.4. Discussion

4.4.1. Method development

4.4.1.1. Light microscopy (LM)

Rind tissue fixed with aldehyde alone has been shown to result in empty gland cavities (see Chapter 3). In this study, aldehyde fixed and osmium postfixed tissue (Method 1) retained some oil, as in previous studies of citrus oil glands using similar fixation protocols (Thomson *et al.*, 1976; Turner *et al.*, 1998). Primary fixation with osmium vapour, shown to improve lipid preservation by Turner *et al.* (1998), was used as the starting point for method development in this study. In the majority of samples, osmium vapour fixation (Method 2) achieved enhanced lipid retention compared to osmium postfixation (Method 1), as reported in the foliar glands of *C. limon* (Turner *et al.*, 1998). However, this was accompanied by a major compromise in structural preservation, not previously observed in the leaf tissue of *C. limon* (Turner *et al.*, 1998). Poor structural preservation with osmium vapour primary fixation is explained by the fact that osmium tetroxide penetrates fresh tissue very slowly, and has very poor cross-linking capabilities compared to the aldehydes (Dykstra, 1992). Despite the fact that small (1 mm) rind samples were used, osmium vapour would have more easily diffused into the thin leaf tissue. In addition, some glands observed in this study were greater than 500 μm in width, compared to 200 μm foliar glands (Turner *et al.*, 1998). The mixture of osmium and aldehyde introduced after primary fixation may itself have contributed to fixation problems. Glutaraldehyde and osmium tetroxide were observed to react, and form a fine, dense precipitate of reduced osmium, which has been reported to ruin specimens (Hayat, 1989). The use of this fixative mixture has not been reported widely, and has been shown to produce inferior fixation of the petiolar hairs of *Lycopersicon esculentum* (Mersey and McCully, 1978). In poorly preserved rind tissue, artefactual damage was commonly localised to the glands. This observation suggested that the thickened walls of the gland boundary cells may have acted as a mechanical barrier to the penetration of fixatives. Similar fixation problems have been reported in plant tissues with a thick cuticle (O'Brien and McCully, 1981).

To improve tissue preservation, the embedding medium was changed from PA to Spurr resin (Method 3). Spurr resin was chosen as it was used in the original osmium vapour fix study by Turner *et al.* (1998), and has also been used in the other major anatomical studies of citrus oil glands (Bosabalidis and Tsekos, 1982a; Thomson *et al.*, 1976). Spurr also has a lower viscosity than Araldite resins (Spurr, 1969), and was expected to better infiltrate samples. However, this did not appear to be the case, with tissue preservation appearing to be slightly poorer. Intact tissue sections of both osmium vapour fixed and osmium postfixed material were found to be more difficult to obtain when embedded in Spurr resin.

Extending the duration of osmium postfixation (Method 4) did not improve lipid fixation as expected, but resulted in inferior tissue preservation. The use of another embedding medium, GMA (Method 5), slightly improved tissue preservation, but removed all traces of the oil. This is not surprising, considering GMA has been described as a 'lipid solvent' (Hayat, 1989). Polymerisation problems also occurred with osmium treated tissue, as GMA requires an oxygen free environment for polymerisation (Dykstra, 1992). A final test for an alternative to osmium vapour fixation involved staining tissue with SBB prior to aldehyde fixation. SBB is the most effective of the lipid colourants (Casselmann, 1959). This method was adapted from another study, which showed it to retain oil to some extent in the glands of the navel orange rind (Johnson, Pers. Comm., 2000). The ability of SBB to retain lipid may be explained by the fact that Sudan dyes partition into lipid, but are also capable of reacting chemically, by virtue of their two amino groups (Gurr, 1960). Unfortunately, past observations were not duplicated in this study, with poor tissue preservation hampering lipid visualisation. It is likely that tissue was damaged by the 70% ethanol in which the stain was prepared.

Changes were also made to dehydration steps to improve oil retention, and to staining techniques, to enhance oil visualisation. For all modified chemical fixation methods, ethanol was used instead of acetone, as it was considered a preferred dehydration agent for lipid retention (Wanner *et al.*, 1981). Dehydration

was modified to reduce the chance of lipid removal, by lowering the concentration of the first dehydration step and shortening the duration in each dehydrating solution. Dehydration was also carried out at 0-4°C to reduce lipid loss (Hayat, 1989), as was resin infiltration in some methods. However dehydration and infiltration for Spurr embedded samples was carried out at room temperature, to avoid condensation, which hampers polymerisation (Dykstra, 1992). Section staining with TBO was preferred over SBB as it showed a greater specificity for the tissue, rather than the epoxy resin. TBO also effectively showed the oil retained within the glands, as has been demonstrated previously in LM studies of the oil glands of *Citrus* (Turner *et al.*, 1998) and also *Eucalyptus* (Jocelyn Carpenter, Electron Microscopist, The University of Melbourne; Pers. Comm., 1999).

The ability to obtain intact glands with oil-filled cavities was limited by the small size of samples required for chemical fixation. Most chemical fixatives penetrate at least 0.5 mm into a sample within one hour, enabling the fixation of 1 mm thin samples (Dykstra, 1992), however, in the previous anatomical investigation of the oil glands of Washington navel orange (Chapter 3), glands of up to 1 mm in width were observed. Consequently, damaged glands with empty cavities were frequently observed in this study. Size limitations for samples also limited the success of cryofixation; samples of less than 0.2 mm were required for slam freezing effectiveness (Dykstra, 1992). As a result, no intact cryofixed glands were obtained. The use of slam freezing has been reported previously in apple tissue, although here, it was reported to produce inferior structural preservation to plunge freezing and conventional freezing (Golding *et al.*, 1995). High pressure freezing, on the other hand, has provided some success in oil gland fixation (Turner *et al.*, 1998). Unlike most cryotechniques, which freeze tissue to no more than 15 µm depth, high pressure freezing is an exception, enabling fixation to approximately 0.5 mm, analogous to chemical fixation (Dykstra, 1992). High pressure freezing is considered the only feasible method to fix large plant tissues without pretreatment (Kaeser *et al.*, 1989). Unfortunately, high pressure freezing equipment was not available for use in this study.

4.4.1.2. Scanning electron microscopy (SEM)

SEM is routinely used to examine tissue morphology. In the present study, SEM allowed the examination of fresh, chemically fixed and cryofixed material. Observations of fresh material using ESEM were hampered due to the nature of the material being examined. It is likely that volatilisation of the rind oils from the tissue contaminated the atmosphere of the ESEM specimen chamber, and affected the electron beam movement to the detector, preventing image collection.

Both chemical and cryofixation methods produced well preserved tissue for observation with FEGSEM, allowing a good comparison of oil retention, which was not possible with light microscopy. In glands which were dissected during fresh tissue preparation, oil was largely removed from the gland cavity by chemical fixation, as observed by light microscopy. However, in cryofixed tissue, oils were retained and appeared largely unaffected by fresh tissue sectioning. Based on these observations, freeze-fracture was expected to be the optimal method, as it involved fixation prior to gland dissection or fracture, minimising possible structural damage and oil removal. Unfortunately, the inability to produce a smooth fracture surface after several attempts prevented the visualisation of cavity oil using this method. Clean fractures, such as those previously achieved in the rind tissue of grapefruit (Petracek *et al.*, 1995) were not duplicated. Of the methods tested, sectioning of fresh tissue to expose gland cavities, followed by plunge freezing to fix the oils, was the optimal SEM method for oil visualisation.

4.4.1.3. Fluorescence microscopy

Confocal microscopy methods used were the most successful for oil visualisation in fresh rind tissue. To obtain real images of gland oils in fresh tissue, both good staining and optical penetration of the tissue were required. Prior to tissue examination with the confocal microscope, the ability of the fluorescent dye NR to stain lipids was tested using light fluorescence microscopy. Brightly fluorescent oil bodies were clearly distinguishable around the gland perimeter, but it was not clear whether this was real or could be attributed to dye localisation in cells at the cut surface. The ability to optically section into the tissue with the

confocal microscope removed the necessity for gland dissection. However, the ability to prepare intact glands close to the cut surface was extremely difficult, and most glands, when examined closely, appeared to be slightly damaged. Intact glands were obtained by tearing the rind tissue, but this method often caused excessive damage to the interconnecting tissue. Interestingly, intact glands were frequently observed to show poor staining of the oil in the gland cavity. Based on these observations, it appeared likely that slight disruption of the gland was beneficial, in that it provided improved stain penetration.

In razor sectioned tissue stained for lipid with NR and counterstained for cell walls (with Safranin O), optical penetration of up to 55 μm from the cut surface was achieved using CLSM. Using this method, the localisation of oil bodies to inner gland cells, as observed using epifluorescence, was confirmed. Boundary cells appeared oil-free and oil was also not detected inside the cavity. Given that gland damage occurred, and tissue was not fixed, it is likely that oil was removed from the gland cavity whilst tissue samples were immersed in the staining solutions. As a result, oil bodies observed were largely intracellular.

Using CLSM, the ability to capture images further from the cut surface was limited by sample opacity and inhomogeneity, and limitations of the working distance of the objective lens (Pawley, 1995). Clearing the tissue can overcome such obstacles, but this was not used because of its tendency to remove lipid. Instead, optical limitations were largely overcome by the use of the multi-photon microscope. Advantages of the two-photon system over single-photon system are that it utilises infra red light, which reduces photobleaching, cytotoxic effects and also light scattering, resulting in improved sensitivity and deeper optical sectioning (Pawley, 1995). Improved optical penetration of up to 180 μm into the gland was achieved using the multi-photon microscope. With thicker tissue slices and improved optical penetration, oils within the cavity were retained. In one gland, the large central cavity was filled with oil.

4.4.2. Rind oil observations

In previous light and transmission electron microscopy (TEM) studies of mature citrus oil glands, oil has been reported to be localised in the gland cavity and also the inner epithelial cells surrounding the cavity (Thomson *et al.*, 1976; Bosabalidis and Tsekos, 1982b; Turner *et al.*, 1998). The same observations were made in this study for glands of orange rind tissue prepared for LM. Cryofixed tissue examined using SEM, and fresh tissue examined using the multi-photon microscope also showed the oil-filled cavities of mature glands. However, for fresh material in which oil had been extracted from the cavity, the presence of oil bodies within the inner gland cells could be observed more clearly using confocal methods. Observations of fresh tissue in this study support previous reports in fixed tissue which suggest that the inner epithelial cells of the glands are secretory in nature (Thomson *et al.*, 1976; Bosabalidis and Tsekos, 1982b). Following oil synthesis, oils are believed to be actively secreted into the cavity space (Shomer, 1980; Bosabalidis and Tsekos, 1982b). In this study, SEM examination of chemically fixed tissue showed similar results to those of Shomer (1980), who observed numerous oil droplets associated with the inner surface of the cavity wall in freeze-fractured glands of Lisbon lemon.

Confocal microscopy (CLSM and multi-photon) observations in this study clearly contradict the findings from a previous confocal microscopy study of oil localisation in the rind of chilling injured Eureka lemon fruit (Obenland *et al.*, 1997). In their study, Obenland *et al.* (1997) prepared tissue using a similar protocol, but in healthy tissue, found large amounts of oil, in the form of discrete oil bodies, outside the glands. It seems likely that during the collection of 25 mm long and 2.5 mm thick rind samples for their examination, gland damage occurred without detection, resulting in oil spillage into surrounding tissues. The possibility of rind oil occurring naturally outside of the glands is unlikely due to its phytotoxicity (see Chapters 5 and 6). Indeed, the function of these glands, at least in part, is to isolate these substances from the rest of the plant (Fahn, 1979).

4.5. Conclusion

This study provides a detailed appraisal of methods for oil retention and visualisation in the oil glands of orange rind tissue, with the use of LM, SEM, CLSM and multi-photon microscopy. For LM, methods which appeared to improve oil retention compromised structural preservation of the rind tissue. Characteristics of the glands themselves, namely their size and the thickness of their outer walls, also limited the success of fixation. Based on our selection criteria, a reliable method for rind oil visualisation with LM was not achieved. A further study into oil accumulation in the developing fruit was not undertaken. As alternatives to LM, SEM showed the effectiveness of cryofixation of gland oils, whilst fluorescence microscopy showed the ability to preserve rind oils without tissue fixation. Although these techniques were revealed to be promising for oil visualisation, further work is required to develop optimal methods. In conclusion, rind oil localisation is best examined routinely in serial sections using LM or TEM, augmented by techniques such as cryoSEM and multi-photon microscopy.

Chapter 5

Inducing oleocellosis in the laboratory

5.1. Introduction

5.1.1. Background

Fawcett (1916) was the first author to attribute the oleocellosis blemish to the action of rind oils. In his study, oleocellosis was reported to develop as a result of surface oil release following fruit injury, as well as the transfer of oil from injured fruit to the surface of uninjured fruit. Since these early findings, oleocellosis has been artificially induced by both mechanical damage and oil application to the fruit.

To induce oleocellosis, some studies have mechanically damaged fruit in a non-uniform manner, by using or simulating normal handling practices (Cahoon *et al.*, 1964; Levy *et al.*, 1979; Loveys *et al.*, 1998). The penetrometer, used commercially to measure rind oil release pressure (RORP) prior to harvest, has also been used to induce oleocellosis (Erner, 1982; Shomer and Erner, 1989). The penetrometer is favoured over normal handling practices, in that it allows the user to control the applied pressure, enabling a more uniform and reliable induction. However, like other mechanical methods, the penetrometer has been reported to rely heavily on fruit turgor (Shomer and Erner, 1989). In their study on Shamouti oranges, Shomer and Erner (1989) reported that penetrometer pressure did not selectively rupture the oil glands in fruit which had lost a significant amount of moisture, but created excess tissue damage, particularly to the albedo layer. Like the penetrometer, pin pricking glands achieves localised damage, but does not rely on a high fruit turgor. In a study by Sawamura *et al.* (1984), pin pricking individual glands produced severe rind injury in all of the seven *Citrus* species examined, including *Citrus sinensis*. This method has also been successfully tested on South Australian Washington navel oranges (Loveys *et al.*, 1998).

In comparison to mechanical methods, inducing oleocellosis with rind oils overcomes the requirement of high fruit turgor and allows the observer to attribute rind damage entirely to oil effects. In previous studies, oil has been applied to the fruit surface by bending excised rind segments (Sawamura *et al.*, 1984; Sawamura *et al.*, 1987; Sawamura *et al.*, 1988; Williams and Wild, 1996), applying oil drops (Brodrick, 1970; Chikaizumi, 2000) and smearing aqueous oil solutions (Shomer and Erner, 1989). A more standardised method of oil application has been developed by Wild and Williams (1992), in which oil-treated discs are attached to the fruit surface with adhesive tape.

Oleocellosis symptoms have been assessed by such measures as number of spots (Cahoon *et al.*, 1964; Levy *et al.*, 1979; Erner, 1982; Loveys *et al.*, 1998) and spot size (Levy *et al.*, 1979; Erner, 1982; Sawamura *et al.*, 1984). In experiments using large volumes of fruit, percentage of fruit showing symptoms has also been used (Eaks, 1955). The measure of 'number of spots' is considered representative of severity in disorders where numerous spots develop naturally, and has been used to assess pitting (Petracek *et al.*, 1998). However, in oleocellosis, number of spots is a direct result of impacts to the fruit. Such a measure is considered misleading where oleocellosis has been induced by random mechanical damage, as appears to be the case in many previous studies (Cahoon *et al.*, 1964; Levy *et al.*, 1979; Loveys *et al.*, 1998). For the purposes of this study, blemish area or 'spot size' and blemish severity are considered to be informative measurements, where oleocellosis has been induced in a uniform manner. The term 'severity' is used to describe the extent of rind collapse and discolouration associated with the blemish. There is no indication that an equivalent measure of severity has been used in previous studies.

5.1.2. Aims

The aim of this study was to develop successful methods for oleocellosis induction by both mechanical means and oil application, in order to simulate the two forms of naturally occurring oleocellosis; namely gland rupture and oil

transfer between fruit. For mechanical induction, conditions for maximising fruit turgor were tested. For oil induction, various oil components and concentrations were assessed. The success of each method was based on fulfilment of the following criteria:

- must produce a localised blemish;
- must be reproducible;
- must produce an adequate blemish area to allow macroscopic assessment and the collection of rind samples for microscopy examination;
- must produce a blemish severity which increases at a rate which allows a detailed time sequence examination of changes;
- must be relatively easy to achieve.

In addition to these objectives, RORP values obtained from penetrometer induction were compared to the threshold value currently used by growers to predict oleocellosis.

5.2. Materials and Methods

5.2.1. Preliminary induction methods test

5.2.1.1. Plant material

Fruit were taken from 23 year old Valencia orange trees on Troyer citrange rootstock, located in the University of Adelaide, Waite Campus Alverstoke orchard (34°97'S, 138°63'E). Rows were N-S oriented, and the trees were spaced at approximately 5.3 x 5.9 metres. Fruit were harvested on October 6, 1997.

Fruit sampling was based on uniformity of fruit size, and to a lesser extent, fruit colour. Polar and equatorial diameter (mm) and fresh weight (g) values were recorded for each fruit. A uniform colour was considered important as colour has been reported to influence oleocellosis blemish perception (Levy *et al.*, 1979; Erner, 1982).

Fruit were picked from the east aspect of the tree, as these fruit normally show a higher turgor (Loveys *et al.*, 1998), indicating a higher susceptibility to mechanical oil gland rupture. Fruit were also picked at 9:00 am to avoid a decline in turgor due to increasing temperature and decreasing relative humidity (and increasing vapour pressure deficit) throughout the day (Cahoon *et al.*, 1964). The close proximity of the orchard to the laboratory allowed the rapid transfer of fruit, and minimal turgor loss between harvest and treatment. Mechanical damage to harvested fruit was reduced by the use of secateurs and careful handling.

5.2.1.2. Induction methods

a. Pin prick methods

A pin prick was used to rupture a single oil gland. Multiple pin pricks were used to rupture glands within an area of approximately 1 cm² on the rind surface.

b. Penetrometer

A penetrometer with an 11 mm diameter tip, and 0 to 13 kg pressure gauge was used (Effegi, Alfonsine, Italy). A similar tool was used in studies by Cahoon *et al.* (1964) and Eaks (1968), but a smaller tip was used by Shomer and Erner (1989). All RORP values were converted from kilograms into pressure units, a standard unit to allow correlation between studies which have used different sized penetrometer tips. For example, a mass reading of 3 kg is equivalent to a force of 29.4 N, when assuming acceleration (due to gravity) to be 9.8 ms⁻². With an 11 mm diameter penetrometer tip, this produces a pressure of approximately 309 kPa.

A standard pressure could not be guaranteed to cause gland rupture in all fruit, as RORP varied somewhat between trees and also between fruit on the same tree. Instead, standard damage was achieved by applying RORP to each fruit.

c. Oil methods

Cold-pressed orange oil (Tropico Fruits Pty. Ltd., South Australia), and two components of orange oil, d-limonene and linalool (Sigma, St. Louis, USA) were used. In a method similar to Wild (1998), 15 µl of 100% concentrations of each of the three oils was pipetted onto 6 mm cardboard discs (Antibiotic Assay discs,

Whatman International Ltd., Maidstone, England), which were attached to the fruit surface with adhesive tape. Non-phytotoxic sunflower oil was also included as a control oil treatment.

All of the methods were applied to each fruit around the equatorial region. Induction was carried out at 0, 6 and 21 hours after harvest. Time of induction after harvest was varied to assess the effect of fruit turgor on mechanical and oil induction methods. The times of induction were chosen on the basis of convenience with respect to the transport of fruit. Following induction, fruit were stored at ambient temperature (20°C).

5.2.1.3. Symptom assessment

Blemish severity and area were assessed on day 1 and 3 following induction. Adequate symptom development was expected by two to three days on the basis of past observations of Washington navel oranges (Wild, 1998).

Blemish area (in mm²) was measured using a grid sheet transparency. For mechanical methods, the area of oil spread outside of the damage site was assessed. For oil application, the area of oil spread outside of the oil disc application site was assessed.

Blemish severity was assessed using a scoring system, which took both rind collapse and discolouration into consideration. A single observer was used to score blemishes, and standard blemish images were used to improve consistency (Plate 5.1).

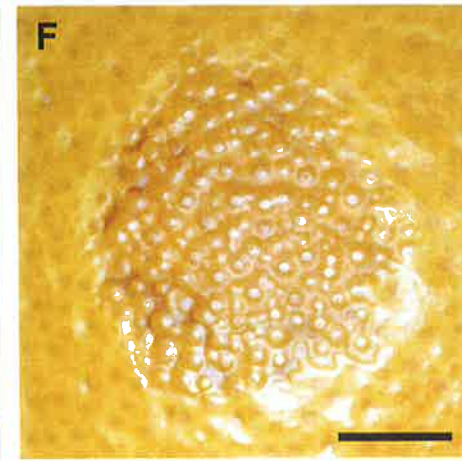
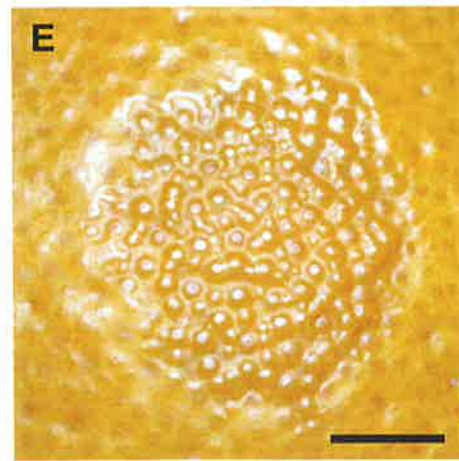
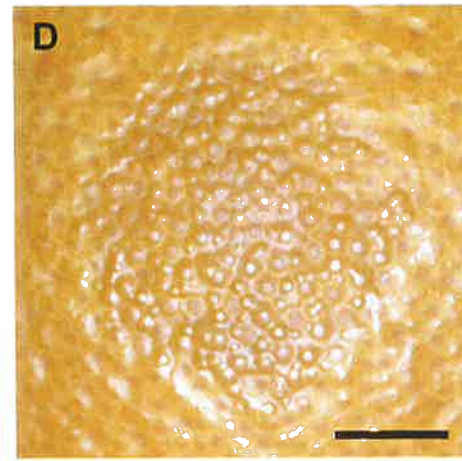
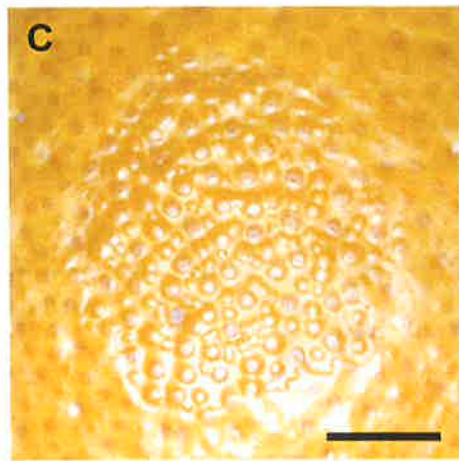
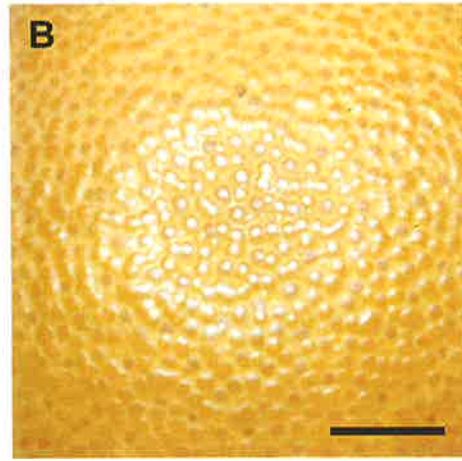
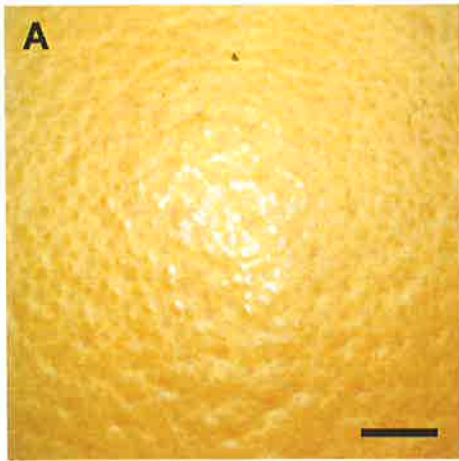
5.2.1.4. Experimental design

Sixty fruit were harvested in total, from five trees. Treatments were randomly allocated to the twelve fruit from each tree: three induction times x two assessment times x two replicates.

Plate 5.1

Blemish severity scoring system. Bars = 1 cm.

- A. 0 - nil.
- B. 1 - very slight.
- C. 2 - slight.
- D. 3 - medium.
- E. 4 - high.
- F. 5 - extreme.



5.2.1.5. Statistical analysis

Blemish severity and area data were analysed using the statistical package Genstat for Windows version 4.1 (Lawes Agricultural Trust, IACR Rothamsted). A split plot design was applied to the data and Analysis of Variance (ANOVA) tables used to test for statistical significance at the 95% confidence level. Data were also analysed using Restricted Maximum Likelihood analysis (REML), in cases where there was non-uniform replication between treatments. This was due to a small number of cases where oil discs did not adhere closely to the fruit.

5.2.2. Oil method refinement

5.2.2.1. Experimental plan

Fruit were harvested during the 1998 season from 23 year old Washington navel orange trees on *Poncirus trifoliata* rootstock located in the University of Adelaide, Waite Campus Alverstoke orchard (34°97'S, 138°63'E). Fruit sampling, oil induction and symptom assessment were carried out as in the preliminary experiment. Repeat assessments were made on individual fruit at days 1 and 3.

5.2.2.2. Oleocellosis induction methods

In experiment 1, ten fruit were harvested on May 6, 1998, and each fruit was treated with d-limonene concentrations of 25, 50 and 100%.

In experiment 2, six fruit were harvested on June 10, 1998, and each fruit was treated with d-limonene concentrations of 60, 70, 80 and 90%.

In experiment 3, six fruit were harvested on June 26, 1998, and each fruit was treated with 100% d-limonene and the oil component citral at concentrations of 20, 40, 60, 80 and 100%.

5.2.3. Penetrometer method refinement

5.2.3.1. Experimental plan

Fruit were harvested from the same trees used above. Fruit sampling, penetrometer induction and symptom assessment were carried out as in the preliminary experiment. In each experiment, RORP was measured on four fruit immediately after harvest and at each of the induction times, to give an indication of changes in fruit turgor. Repeat assessments were made on individual fruit at days 1 and 3.

5.2.3.2. Oleocellosis induction methods

In experiment 1, 12 fruit were harvested on May 26, 1998, at 8:30 am, and stored in plastic bags on ice, in a styrofoam box. Both plastic bags and low temperature storage were used to minimise moisture loss and maintain turgor.

In experiment 2, nine fruit were harvested on June 10 at 10:00 am. Trees were deep watered 24 hours prior to harvest, and following harvest each fruit was wrapped in moist paper towel and stored in a styrofoam box. The objective was to achieve a higher turgor at harvest and maintain turgor more effectively by keeping the fruit surface wet and cool. In the first two experiments, induction was carried out at 2, 4 and 8 hours after harvest.

In experiment 3, nine fruit were harvested on June 30 at 12:30 pm, slightly later in the day, due to rainy conditions. Experiment 3 was otherwise identical to the preceding experiment, except earlier induction times of 1, 3 and 5 hours were used, to test the effect of inducing damage closer to the time of harvest.

5.3. Results

5.3.1. Preliminary induction methods test

5.3.1.1. Blemish severity

The single pin prick treatment had a negligible effect and the penetrometer produced very low severity scores, whilst all other methods produced slight to medium severity blemishes (Fig. 5.1). These differences explain why the method effect was significant ($P < 0.001$). The pin prick produced no symptoms in 90% of samples by day 3. The multiple pin prick gave the highest severity scores of the mechanical methods, with a mean score of approximately 2.5, or slight to medium. d-limonene and orange oil produced a similar mean severity to the multiple pin prick treatment. Linalool gave the most severe blemishes, with a mean of approximately 3, or medium. At day 3, 80% of blemishes were classed as score 3 or 4 and 13% as score 5. Linalool typically produced a blemish with a darker coloured border (Plate 5.2A). By day 3, linalool also produced gland collapse, unlike the other oil treatments where collapse was localised between glands only. Sunflower oil, the non-phytotoxic oil used as the control, produced no signs of blemish.

Induction at 21 hours produced less severe blemishes than induction at 0 or 6 hours, for all oil methods and for the multiple pin prick treatment. Penetrometer showed the opposite trend, which may explain the significant interaction between method and induction time ($P < 0.001$). Assessment time had a negligible effect for mechanical methods, but for oil methods, mean severity increased from day 1 to 3 by a score of 1. The interaction between method and assessment time was also significant ($P < 0.001$).

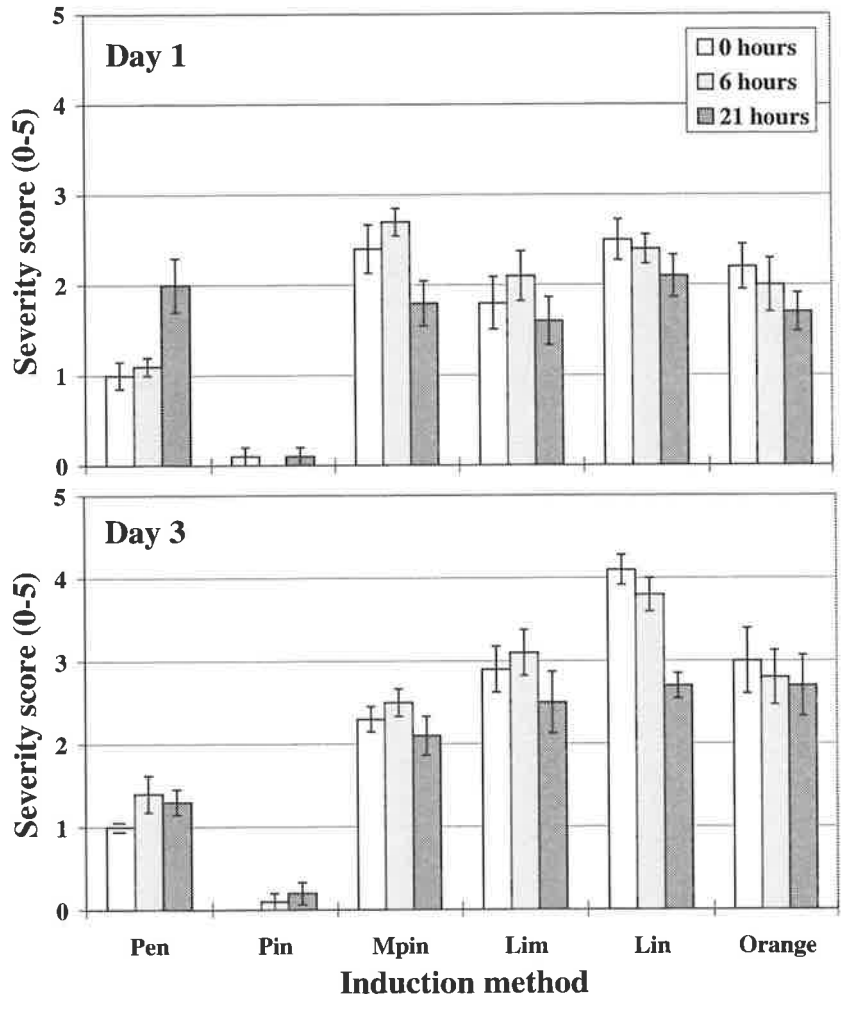


Figure 5.1. Preliminary induction methods test. The effect of induction method and induction time on blemish severity at days 1 and 3. Induction methods include penetrometer (pen), pin prick (pin), multiple pin prick (mpin), d-limonene (lim), linalool (lin) and orange oil (orange). Sixty fruit from five trees, treated with three induction times (0, 6 and 21 hours), two assessment times (days 1 and 3) and replicated twice. Means and standard errors represented.

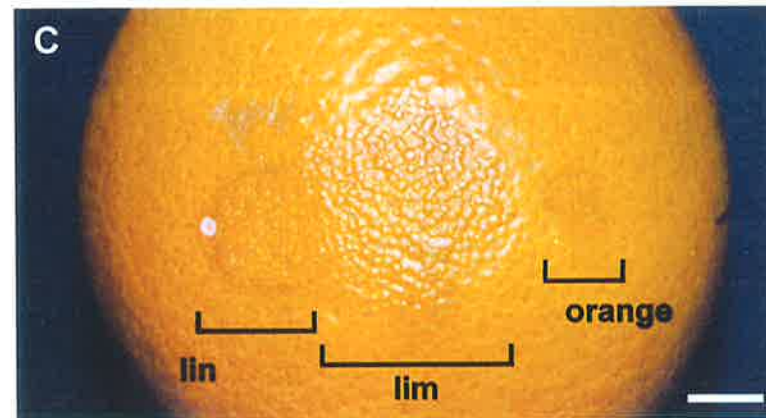
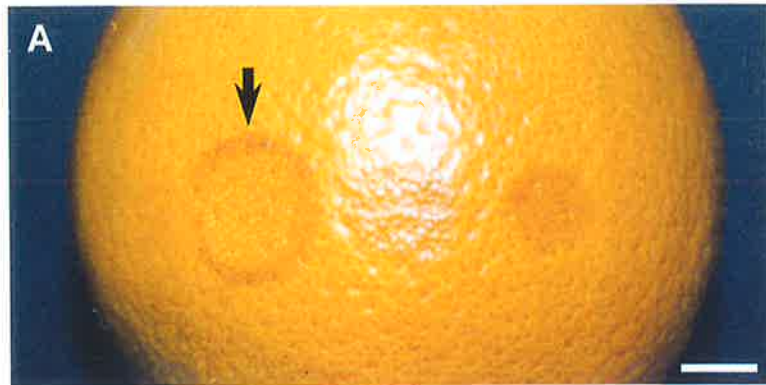
Plate 5.2

Oleocellosis symptoms induced in the preliminary induction methods test.

A. A fruit treated with linalool (left), d-limonene and orange oil (right). Linalool typically produced a blemish with a darker coloured border (arrow). Bar = 1 cm.

B. A fruit treated with multiple pin pricking. Area of rind damage due to oils is localised around the margins of the damage zone (dz). Bar = 1 cm.

C. The d-limonene blemish (lim) was typically larger than linalool (lin) and orange oil (orange) blemishes. Bar = 1 cm.



5.3.1.2. Blemish area

Blemishes produced by the penetrometer and pin prick methods were very small and poorly defined, and could not be measured accurately (Fig. 5.2). The multiple pin prick treatment also produced small blemishes, not exceeding 16 mm² by day 3 (Plate 5.2B). All three oil methods produced larger blemishes than mechanical methods (Fig. 5.2), explaining the significant method effect ($P < 0.001$). By day 3, orange oil blemishes were approximately 25 mm² and linalool blemishes were 60 mm². d-limonene produced larger blemishes than orange oil and linalool (Plate 5.2C). Induction time had a slight and inconsistent effect on blemish area. For d-limonene, induction time showed opposite trends for day 1 and 3. This unusual trend was the main difference observed between days 1 and 3, reflected in the significant interaction between method and assessment time ($P < 0.001$).

5.3.1.3. Rind oil release pressure (RORP)

Mean RORP at 0 hour induction was 546 kPa (5.3 kg). Mean RORP at 6 and 21 hour inductions was similar to that observed at 0 hours, varying from 484 to 577 kPa (4.7 to 5.6 kg). Negligible standard errors associated with RORP at each induction time suggested little variation due to tree or fruit effects (data not shown). RORP did not appear to influence the resulting blemish severity or area (data not shown).

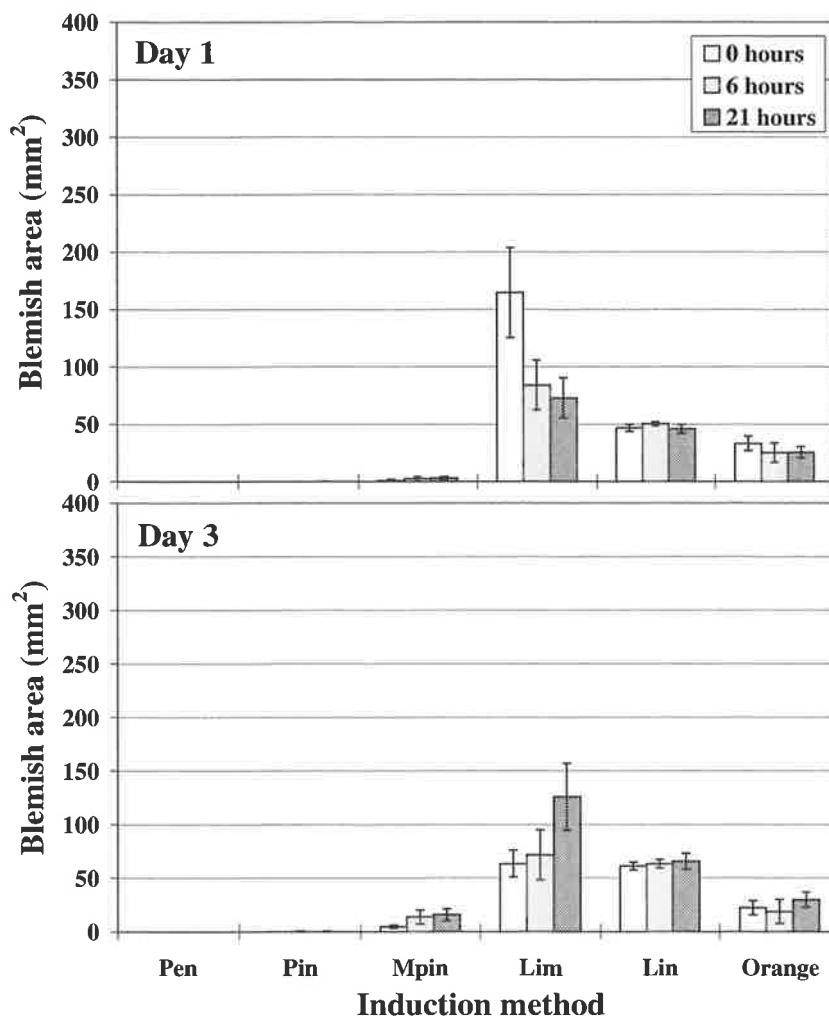


Figure 5.2. Preliminary induction methods test. The effect of induction method and induction time on blemish area at days 1 and 3. Induction methods include penetrometer (pen), pin prick (pin), multiple pin prick (mpin), d-limonene (lim), linalool (lin) and orange oil (orange). Sixty fruit from five trees, treated with three induction times (0, 6 and 21 hours), two assessment times (days 1 and 3) and replicated twice. Means and standard errors represented.

5.3.2. Oil method refinement

5.3.2.1. Blemish severity

In experiment 1, 100% d-limonene produced much more severe blemishes than 50% and 25% d-limonene (Fig. 5.3), explaining the significant concentration effect ($P < 0.001$). A d-limonene concentration of 25% produced no symptoms by day 3. A concentration of 50% gave a mean score of less than 1 by day 3, with 70% of fruit showing no symptoms. A concentration of 100% gave a mean score of 2.5 by day 3, or slight to medium. A very minor severity increase was observed between days 1 and 3.

In experiment 2, d-limonene concentrations of 90% and 80% produced more severe blemishes than 60% and 70% (Fig. 5.3), explaining the significant concentration effect ($P < 0.001$). Concentrations of 60% and 70% produced mean severity scores of less than 1, with the majority of fruit showing no symptoms by day 3 (83% and 67%, respectively). A concentration of 80% gave a low mean score of 1.5, whilst 90% d-limonene produced the most severe blemishes, with a mean score of 2.5 at day 3, the same as pure d-limonene in experiment 1. A consistent increase in severity from day 1 to 3 was also observed, explaining the significant assessment time effect ($P = 0.008$).

In experiment 3, all citral concentrations produced much higher severity scores than 100% d-limonene (Fig. 5.4), explaining the significant oil treatment effect ($P < 0.001$). d-limonene gave a mean score of only 1 at day 3, and a maximum score of 2, or slight. d-limonene produced less severe blemishes than in the preliminary experiment and experiment 1. d-limonene also showed a high standard error, which was attributable to fruit differences. Citral was very damaging to the rind; 20% citral gave a mean score of 2.5 by day 3, and blemish severity increased with citral concentration. A dramatic increase in severity from day 1 to 3 was observed, explaining the significant assessment time effect ($P < 0.001$). Citral also caused gland collapse, with the entire blemish area appearing to be depressed into the rind (Plate 5.3A).

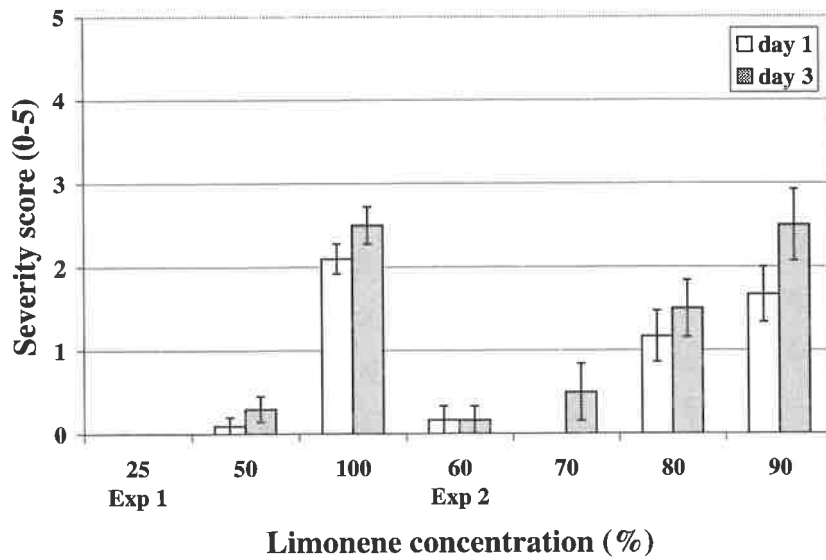


Figure 5.3. Oil method refinement. The effect of d-limonene concentration on blemish severity at days 1 and 3. Experiment 1, Ten fruit treated with three d-limonene concentrations (25, 50 and 100%). Experiment 2, Six fruit treated with four d-limonene concentrations (60, 70, 80 and 90%). Repeat assessments made at days 1 and 3. Means and standard errors represented.

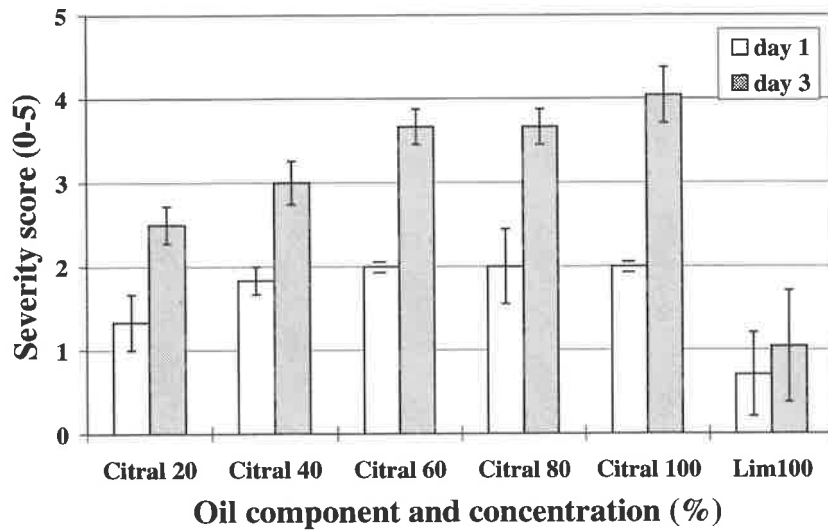


Figure 5.4. Oil method refinement. The effect of citral concentration and 100% d-limonene on blemish severity at days 1 and 3. Experiment 3, Six fruit treated with six oil treatments (citral 20, 40, 60, 80, 100% and d-limonene 100%). Repeat assessments made at days 1 and 3. Means and standard errors represented.

Plate 5.3

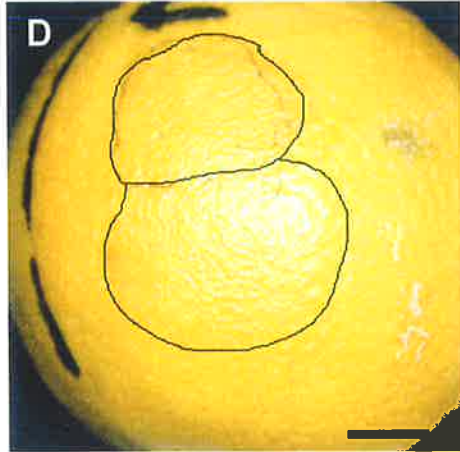
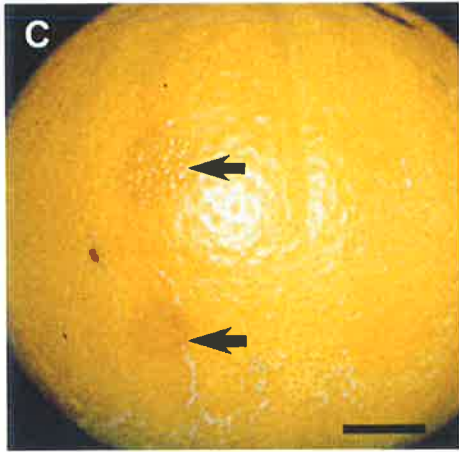
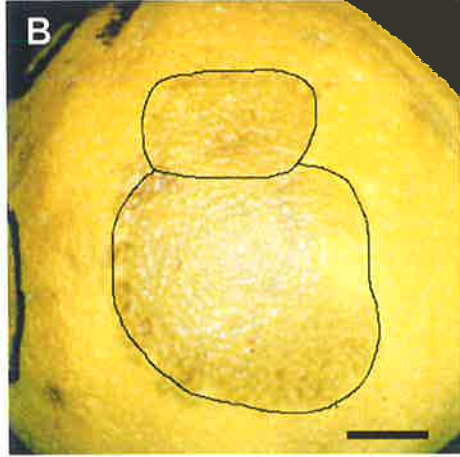
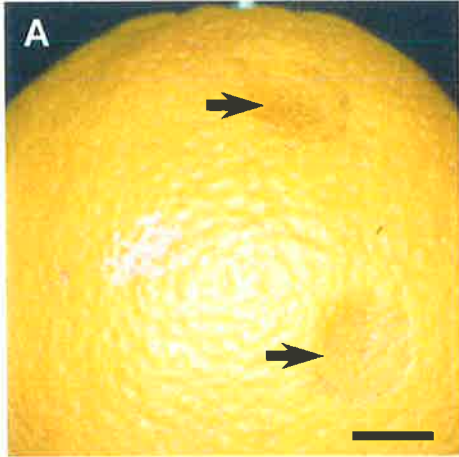
Oleocellosis symptoms induced in the oil method refinement experiments.

A. Citral produced severe rind collapse, including gland collapse. Two blemishes resulting from 100% citral (arrows). Bar = 1 cm.

B. A concentration of 100% produced the most advanced d-limonene blemish, with a severity score of 4 and an area of 476 mm² at day 3. Drawn lines delineate the blemish boundaries from two oil disc application sites. Bar = 1 cm.

C. d-limonene at 60% concentration produced small blemishes, with a mean area of 16 mm² (arrows). Bar = 1 cm.

D. d-limonene at 90% produced large blemishes, with a mean area of 166 mm² (outlines). Bar = 1 cm.



5.3.2.2. Blemish area

Blemish area showed a similar trend to blemish severity in all three oil experiments (Figs. 5.5 and 5.6). In experiment 1, 100% d-limonene produced much larger blemishes than 50% and 25% d-limonene (Fig. 5.5), explaining the significant concentration effect ($P < 0.001$). A concentration of 25% produced no symptoms, and 50% d-limonene produced small blemishes, with a mean area of 23 mm² at day 3. Pure d-limonene produced a mean blemish area exceeding 200 mm², but also showed high standard errors due to fruit variation. Differences between day 1 and 3 were negligible. The most advanced blemish observed was produced by 100% d-limonene and had a severity rating of 4, or high level, and was 476 mm² in area (Plate 5.3B).

In experiment 2, a gradual area increase was associated with increasing d-limonene concentration (Fig. 5.5), and the concentration effect was significant ($P = 0.002$). A concentration of 60% d-limonene gave the smallest mean area of 16 mm² (Plate 5.3C) whilst 90% d-limonene gave a mean area of 166 mm² (Plate 5.3D). A consistent increase in area between days 1 and 3 was also observed, explaining the significant assessment time effect ($P = 0.003$).

In experiment 3, all citral concentrations produced much larger blemishes than 100% d-limonene (Fig. 5.6), explaining the significant oil treatment effect ($P < 0.001$). Blemish area also appeared to increase consistently from day 1 to 3, explaining the significant assessment time effect ($P = 0.03$).

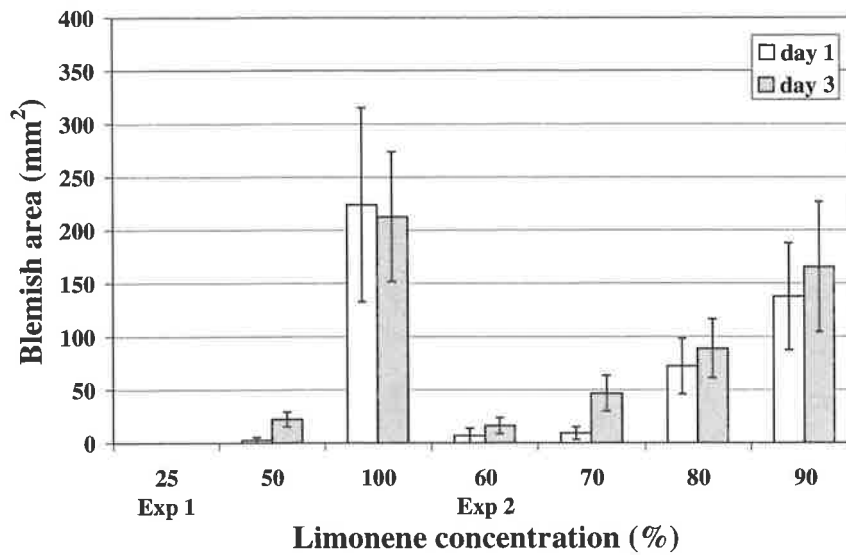


Figure 5.5. Oil method refinement. The effect of d-limonene concentration on blemish area at days 1 and 3. Experiment 1, Ten fruit treated with three d-limonene concentrations (25, 50 and 100%). Experiment 2, Six fruit treated with four d-limonene concentrations (60, 70, 80 and 90%). Repeat assessments made at days 1 and 3. Means and standard errors represented.

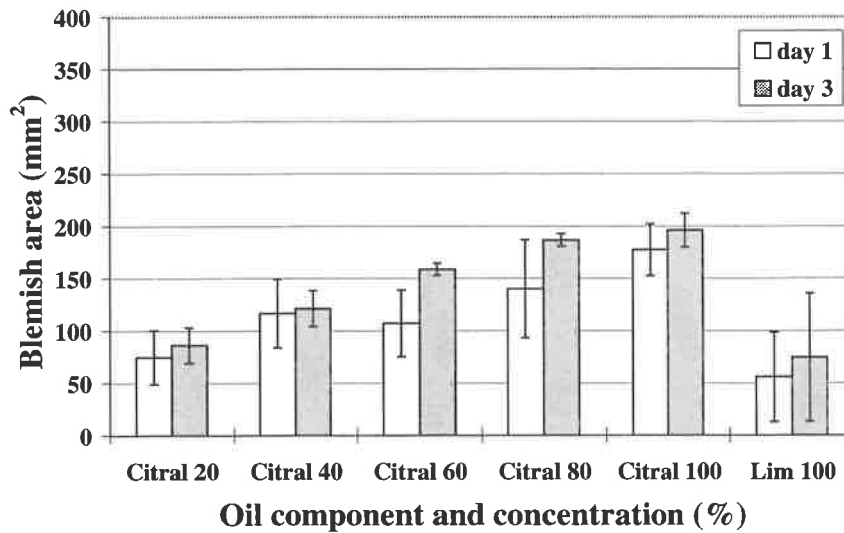


Figure 5.6. Oil method refinement. The effect of citral concentration and 100% d-limonene on blemish area at days 1 and 3. Experiment 3, Six fruit treated with six oil treatments (citral 20, 40, 60, 80, 100% and d-limonene 100%). Repeat assessments made at days 1 and 3. Means and standard errors represented.

5.3.3. Penetrometer method refinement

All penetrometer experiments showed similar blemish induction success; experiment 2 was chosen to be representative of oleocellosis induction with the penetrometer, and results from this experiment are outlined below.

5.3.3.1. Blemish severity

All induction times produced a mean severity score of less than 1 (or very slight) and little or no difference between days 1 and 3 (Fig. 5.7). High proportions of fruit showed no blemish development; 67% for 2 hour, 78% for 4 hour and 56% for 8 hour induction. The most severe blemish observed had a score of 4 (high) and resulted from the 2 hour induction.

5.3.3.2. Blemish area

In all penetrometer experiments, blemish area was difficult to measure because of the weak symptoms. At day 3, mean blemish area varied from 65 to 86 mm² (Fig. 5.8). High standard errors observed were attributed to fruit variation.

Plate 5.4 demonstrates the appearance of the oleocellosis blemish achieved with a penetrometer, three days after induction.

5.3.3.3. Rind oil release pressure (RORP)

Mean RORP at harvest varied from 526 kPa (5.1 kg) in experiment 3 to 588 kPa (5.7 kg) in experiment 2. For all experiments, mean RORP at delayed induction times was similar to that observed at 0 hour induction (data not shown). The most notable effect of fruit storage was observed in experiment 3, where RORP declined from 536 kPa (5.2 kg) to 433 kPa (4.2 kg) after five hours storage.

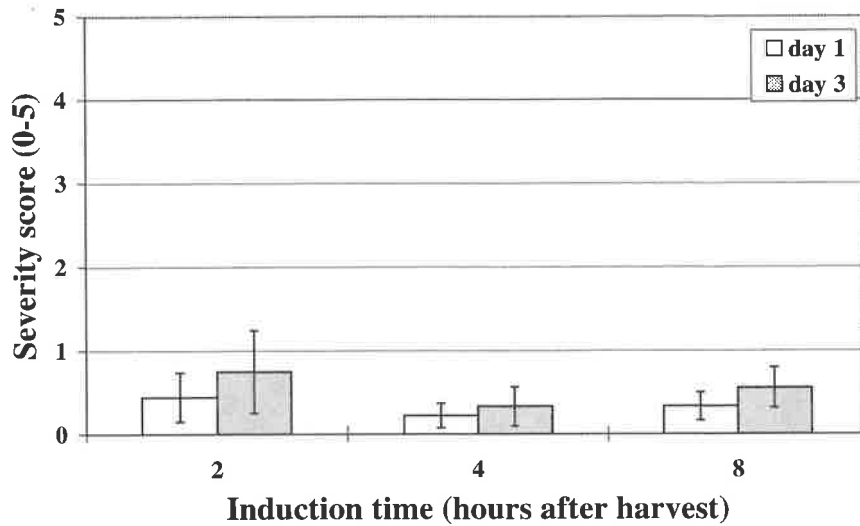


Figure 5.7. Penetrometer method refinement. The effect of induction time on blemish severity at days 1 and 3. Nine fruit, treated with three induction times (2, 4 and 8 hours). Repeat assessments made at days 1 and 3. Means and standard errors represented.

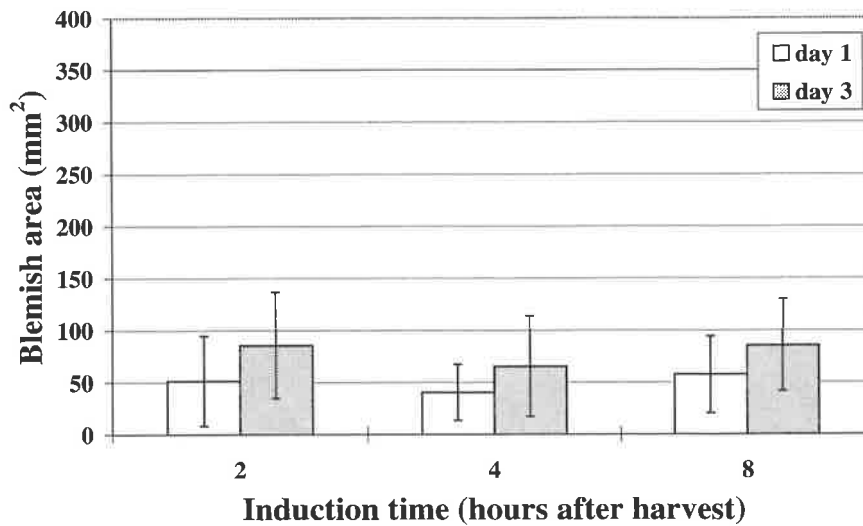
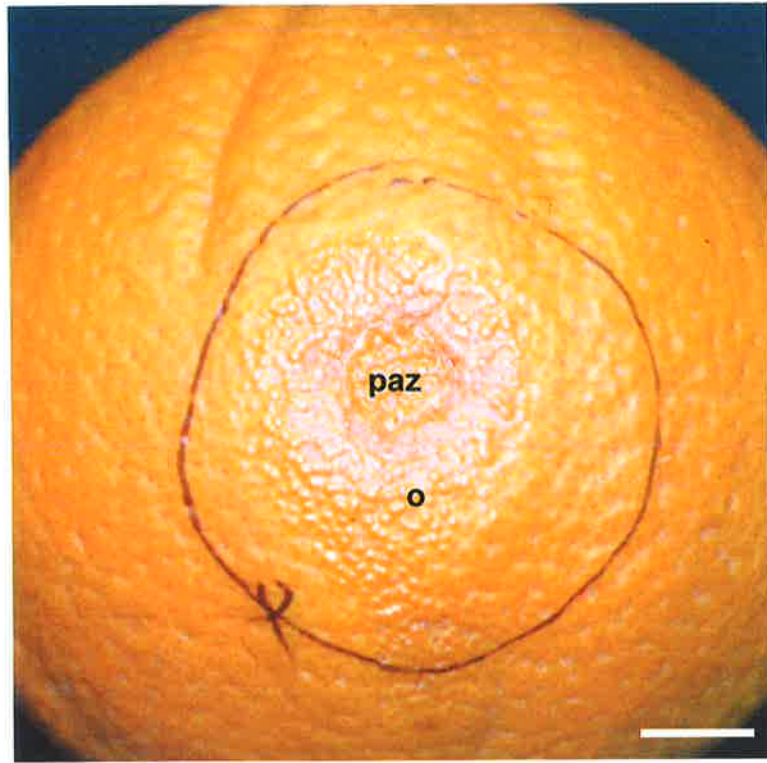


Figure 5.8. Penetrometer method refinement. The effect of induction time on blemish area at days 1 and 3. Nine fruit, treated with three induction times (2, 4 and 8 hours). Repeat assessments made at days 1 and 3. Means and standard errors represented.

Plate 5.4

Typical oleocellosis blemish resulting from penetrometer induction. Blemish arises in area of oil spread (o) away from the penetrometer application zone (paz). Bar = 1 cm.



5.4. Discussion

5.4.1. Mechanical induction

In the preliminary experiment, none of the mechanical methods used could be recommended for oleocellosis induction based on the selection criteria used. All methods failed to produce an adequate blemish area. The most severe blemishes produced were by the multiple pin prick treatment, but were classed as only slight. The inconsistent effect of induction time was attributed to variation due to tree or fruit effects. Unexpectedly, there was little change in blemish severity from day 1 to 3, but only a low level of blemish was found overall.

The single pin prick rarely produced blemish symptoms on Valencia orange fruit (*C. sinensis*). The pin prick was observed to release a small volume of oil, which showed little visible surface spread from the site of damage. These findings are in complete contrast to those of Sawamura *et al.* (1984), who induced rind injury in fruit of seven *Citrus* species using a single pin prick. In *C. sinensis*, severe rind injury, defined as spots ≥ 16 mm in diameter, was induced. In some species, the pin prick produced more severe injury than application of the fruit's own rind oils. This was explained to be due to the entry of the volatiles into the flavedo tissue, compared to the volatile loss of low-boiling point compounds associated with surface oil application. Discrepancies between studies may be partially explained by fruit storage conditions; enhanced volatile loss was more likely in the present study, in detached fruit under 20°C conditions, compared to fruit on the tree during winter months in Japan. However, Sawamura *et al.* (1984) did report less severe rind injury from the pin prick later in the season, which may explain the poor response of mature fruit in the present study. The effect of fruit age was not explored further, but it is unlikely that it is related to changes in oil yield or composition, as both have been shown to remain fairly stable at later stages of the season (Scora *et al.*, 1968).

For multiple pin prick and penetrometer methods, multiple glands were ruptured and a greater volume of oil released onto the fruit surface, but the degree

of oleocellosis blemish resulting remained similar to the single pin prick. Again, this observation may be explained at least partially by the loss of volatiles from the fruit surface. Previously, the penetrometer has been used to successfully induce oleocellosis in Shamouti orange fruit (Shomer and Erner, 1989; Erner, 1982). Fruit which had not yet obtained their full colour were used in these studies, compared to fully coloured fruit used in the present study, making symptom comparisons difficult. It is likely, however, that symptoms induced in previous studies were accentuated by the effect of fruit degreening after damage (Levy *et al.*, 1979). Similarly, the lack of oleocellosis blemish observed in this may be explained by the masking effect of enhanced rind colour (Levy *et al.*, 1979; Erner, 1982).

Despite the failure of all mechanical methods to successfully induce oleocellosis in the preliminary experiment, the penetrometer was favoured over pin prick methods. The penetrometer allowed more controlled damage; to achieve a standard damage level in all fruit, pressure was applied to each fruit until the oils were released (RORP). Based on blemish severity and area observations, it appears that standard damage was achieved, although it should be noted that the blemishes were generally weak. Of the methods tested, the penetrometer also simulated handling damage most closely, and avoided the excessive rind damage produced with pin pricking, which would lead to major misinterpretation of microscopy images.

The objective of penetrometer method refinement experiments was to improve the likelihood of oleocellosis development by increasing fruit turgor prior to harvest and potentially during fruit storage. Unfortunately, oleocellosis symptoms were less severe and occurrence of symptoms less frequent than in the preliminary experiment. Only in experiment 3 did fruit show lower RORP values at harvest compared to the preliminary experiment, most likely as a result of the rainfall on days preceding harvest. In experiment 2, the irrigation carried out the night before harvest was not successful in elevating fruit turgor at the time of harvest. The ineffectiveness of the irrigation was due to its timing; it is likely that a longer

irrigation, carried out further in advance of harvest would have been more effective. Information on the effect of irrigation timing on RORP is limited, but Cahoon *et al.* (1964) have shown that a 14 day interval between irrigations is preferred to 7 days in obtaining same-sized lemon fruit with a lower turgor, to reduce oleocellosis susceptibility at harvest.

Storing fruit in water saturated conditions following harvest has been shown to increase fruit turgor (Cahoon *et al.*, 1964). Cahoon *et al.* (1964) reported that lemon fruit stored for 16 hours under ambient temperature showed a slight decrease in weight and dramatic decrease in turgor, whilst fruit stored in a water saturation chamber at 28 °C with their stems in water, showed an increase in both fruit weight and turgor. In contrast, fruit stored under ambient conditions for up to 21 hours in the present study showed only a slight decrease in turgor (increase in RORP). In follow-up experiments, storing fruit under modified conditions for moisture retention showed little improvement to storing fruit at ambient temperature. The most notable effects were observed in experiment 3, where RORP was reduced from 536 kPa (5.2 kg) at harvest to 433 kPa (4.2 kg) after five hours storage, by wrapping fruit in moist paper towel and storing in a styrofoam box. A comparison of findings suggests that storage time was not a contributing factor, but that our storage conditions for moisture retention were inadequate compared to those of Cahoon *et al.* (1964).

Commercially, RORP is used as a predictive test for oleocellosis in the field (Cahoon *et al.*, 1964). Australian citrus growers use 3 kg RORP with an 8 mm diameter penetrometer tip (585 kPa) as a threshold value, above which oleocellosis is considered not likely to occur under normal handling conditions (Feutrill, 1997). In the present study, mean RORP at harvest was consistently close to or greater than this threshold value, varying from 526 to 588 kPa (5.1 to 5.7 kg). However, oleocellosis was observed to develop in fruit with RORP values as high as approximately 770 kPa (7.5 kg). Based on this observation, it appears likely that oleocellosis symptoms have the potential to develop as long as oil is released from the glands. If pressure applied to the fruit surface is greater than RORP, this can be achieved. An exception, however, is for fruit with exceedingly low turgor, in which

it is not possible to cause selective gland rupture without greater mechanical damage to the rind, as reported by Shomer and Erner (1989).

5.4.2. Oil induction

Studies into the phytotoxicity of different rind oil components to the rind of orange fruit have found that d-limonene and linalool are major contributors to oleocellosis (Sawamura *et al.*, 1984; Wild and Williams, 1992). In the preliminary experiment, 100% concentrations of d-limonene, linalool and orange oil all produced an adequate blemish severity for our experimental purposes. Linalool produced the most severe blemishes, often displaying a darkened border and in severe cases, collapsed glands. In comparison, d-limonene and orange oil produced less severe blemishes, with rind collapse localised between glands only, as is evident in naturally occurring oleocellosis. A comparison of identical (100%) concentrations of d-limonene and linalool in this study appears to support Wild and Williams (1992), who suggested that linalool is highly phytotoxic, more so than d-limonene. It was expected that 100% d-limonene would induce a blemish similar to that of natural oleocellosis, as it is the major component of orange oil, comprising between 83 and 97% of the total oil in the mature fruit of *C. sinensis* (Shaw, 1979). Linalool however, makes up a smaller proportion of the total oil, in the order of 0.3 to 5.3% (Shaw, 1979).

Induction time did not have a consistent effect on blemish severity, and differences observed were attributed to fruit variation, as separate fruit were used for each induction time. For all oil treatments, there was a considerable increase in blemish severity between days 1 and 3. This suggests that physiological changes in the rind due to oil action take place over a number of days. These changes were examined in detail in a time sequence study of oleocellosis development, outlined in Chapter 6.

The largest blemishes were produced by d-limonene. The inconsistent effect of induction time was again attributed to variation between fruit, and may have been avoided if repeat measurements had been made on single fruit. If induction time is not considered in the data assessment, mean blemish area due to d-limonene was

only slightly larger than linalool. In the study by Sawamura *et al.* (1984), a similar blemish size was also produced by d-limonene and linalool on *C. sinensis* fruit. In their study, blemish size was reported to be in excess of 16 mm diameter, which equates to approximately 200 mm², compared to 50 to 160 mm² observed in our study. The change in area between days 1 and 3 was slight for all oil treatments, suggesting the rapid spread of oil from the application site within one day. Indeed, at the time of induction, oil was observed to spread outwards from the oil disc almost immediately following its application. From the preliminary experiment, d-limonene was chosen to be the preferred oil treatment for use in further studies. d-limonene blemishes were of adequate severity and ample area by day 3, progressed in severity from day 1 to 3, and were most similar in appearance to naturally occurring oleocellosis of the treatments examined.

The objective of oil method refinement experiments was to test a broader range of d-limonene concentrations, and an additional oil component not tested in preliminary experiment, citral. In experiments 1 and 2, both blemish severity and area results showed consistency. In experiment 1, 100% d-limonene was greatly preferred to concentrations of 25 and 50%, which produced weak blemishes or no blemish at all. In experiment 2, 90% was the only d-limonene concentration in the range of 60 to 90% which gave a similar blemish to 100% d-limonene with respect to severity and area. In experiment 3, 100% d-limonene produced weaker blemishes, which may be partially explained by the masking effect of enhanced peel colour (Erner, 1982). In the same experiment, citral concentrations of 20 to 100% devastated the rind, giving larger and more severe blemishes than the 100% d-limonene treatment. Citral blemish appearance was uncharacteristic of naturally occurring oleocellosis, showing extreme tissue collapse and rind indentation, greater than that resulting from 100% linalool. Observations suggest that citral is an extremely phytotoxic component of Washington navel orange rind oil. Citral, which occurs naturally as a mixture of the two aldehydes neral and geranial, occurs at even lower levels than linalool, in the order of 0.05 to 0.2% (Shaw, 1979).

Valencia orange fruit were used in preliminary experiments due to availability, but for all method refinement experiments, were replaced with the variety of

interest, Washington navel orange. A comparison of identical induction treatments on the two varieties allowed speculation as to which variety may be considered more susceptible to oleocellosis. In penetrometer-treated fruit, both varieties showed very similar fruit turgor (measured as RORP) and similar low levels of resulting oleocellosis. In 100% d-limonene treated fruit, navel orange showed blemishes which were slightly less severe, but much larger than Valencia orange. Previous studies have shown different *Citrus* species to respond differently to identical oil treatments (Sawamura *et al.*, 1984; Williams and Wild, 1996), but reasons for these differences have not been explored. Factors influencing fruit susceptibility to oleocellosis will be discussed in more detail in Chapter 7.

5.5. Conclusion

Based on the selection criteria, pure d-limonene was chosen as the preferred oil treatment for inducing oleocellosis. Using the oil disc method, it is easy to apply and reproducible. It produces a localised blemish, but the large blemish size enables one to easily assess blemish severity and collect samples for microscopy. Symptoms appeared to develop gradually over time, which is preferable for a detailed time sequence study of oleocellosis development. Of the oil treatments tested, d-limonene also produced a blemish, which appeared most similar to naturally occurring oleocellosis. Of the mechanical methods, the penetrometer was chosen to be used in further experiments. The penetrometer has been used in previous studies, is easy to use, and simulates handling damage most accurately, and in a controlled manner. Reproduction of mechanical damage as it would occur in the field is important for microscopy interpretations. In conclusion, penetrometer damage and d-limonene treatment were chosen as the optimal methods for inducing oleocellosis under laboratory conditions based on our selection criteria.

Chapter 6

Oleocellosis: macroscopic and microscopic development

6.1. Introduction

6.1.1. Background

Our understanding of oleocellosis physiology is limited, and based largely on a small number of microscopy studies. The natural mode of oil release from the glands is not understood. Mechanical damage to the fruit has been observed to result in surface oil release (Fawcett, 1916; Cahoon *et al.*, 1964; Eaks, 1968), and based upon such observations, oleocellosis is considered to be caused by the effect of the oil released onto the fruit surface (Whiteside *et al.*, 1988). Surface oil release following mechanical damage to the fruit was confirmed by early light microscope (LM) studies, which reported epidermal rupture above glands (Labuschagne *et al.*, 1977; du Plessis, 1978). However, the possibility of oil release into the rind tissue has also been suggested, based on the presence of sub-surface rind damage (Shomer and Erner, 1989). Such a proposition is also supported by Loveys *et al.* (1998), who observed symptoms to develop in fruit despite the removal of surface oil, and also induced symptoms by injecting oil into the rind.

The nature of the reaction between the phytotoxic oils and the rind tissue is also ill-defined in the literature. Using LM, oleocellosis rind damage was first described as a band of flattened cells located six to eight cells deep from the surface and between glands (du Plessis, 1978). In later microscopy studies, tissue postfixation with osmium tetroxide enabled researchers to observe the dense contents of oil-damaged cells (Shomer and Erner, 1989; Williams and Wild, 1996). Using this improved tissue fixation method, oleocellosis has been examined in degreened Shamouti orange fruit (Shomer and Erner, 1989) and mature Valencia orange fruit (Williams and Wild, 1996). These studies show significant discrepancies based on both LM and transmission electron microscope (TEM)

observations. Using LM, Shomer and Erner (1989) reported oleocellosis rind damage to occur either sub-epidermally or in all rind layers, whereas Williams and Wild (1996) observed densely aggregated upper rind layers only. Using TEM, Shomer and Erner (1989) described a process of cell plasmolysis and collapse, however they also attributed the green colour of damaged tissue to the presence of 'giant chloroplasts'. Williams and Wild (1996) attributed flattened cell layers to abnormal cell division rather than cell collapse.

Previous microscopy studies of oleocellosis have been characterised by inconsistencies in their methods of tissue preparation, discrepancies in their interpretation of microscopy images, and none have produced a convincing picture of oleocellosis development. The sequence of events which leads to the appearance of the oleocellosis blemish has not been clearly established.

6.1.2. Aims

The aim of this study was to gain an improved understanding of the physiological development of oleocellosis in mature fruit, by following a time sequence of surface symptoms and examining changes in rind anatomy and ultrastructure. Oleocellosis was induced by both mechanical means and oil application, using methods developed in Chapter 5. The methods were used to simulate the two naturally occurring forms of oleocellosis; namely gland rupture and oil transfer between fruit. Comparisons of the two methods also helped to better elucidate physiological processes based on structural observations. In addition to the time sequence study, morphological features and oil localisation were examined in oleocellosis-damaged rind tissue, using methods developed in Chapter 4.

6.2. Materials and Methods

6.2.1. Symptom time course

6.2.1.1. Experiment 1

a. Plant material

Fruit were harvested from 40 year old Washington navel orange trees in an orchard located at Mypolonga, South Australia (35°58'S, 139°25'E). Fruit were harvested on July 9, 1998.

Fruit sampling was carried out as described in Section 5.2.1.1. Sampling was based on uniformity of fruit size and colour. Polar and equatorial diameter (mm) and fresh weight (g) values were recorded for each fruit.

To obtain fruit with a high turgor, fruit were picked at 9:00 am and from the SE tree aspect, which had not been exposed to the sun that day. In addition, rain had fallen for several days prior to harvest. At harvest, measurements of air temperature, relative humidity and wet bulb temperature were made. Rind oil release pressure (RORP) was measured on ten fruit from each tree in the orchard, and measured again in the lab to provide an estimate of fruit moisture loss during transport. After harvest, fruit were individually wrapped in wet paper towel, to retain water, and pattern-packed into plastic lined crates, with cushioning between fruit layers. Mechanical damage to harvested fruit was minimised by the use of secateurs and careful handling.

b. Induction methods

Oleocellosis was induced approximately one hour after harvest, using two methods; penetrometer damage and oil treatment. Penetrometer induction was carried out as described in Section 5.2.1.2. However, a modified penetrometer tip, 8 mm in diameter and made of acrylic, was used. Compared to the conventional brass tip, the transparent tip has been shown to increase the accuracy of RORP measurements by improving the visualisation of gland rupture (Loveys *et al.*, 1998). Oil induction, using 100% d-limonene was carried out according to the oil

disc method described in Section 5.2.1.2. Each method was replicated twice on each fruit, and replicate treatments referred to as 'samples'.

c. Symptom assessment

Following induction, symptoms were assessed at eight time intervals over three days: 30 mins, 1h, 2h, 6h, 12h, 24h, 48h, 72h. Nine fruit were assessed at each time interval (three from each tree).

Blemish area (in mm²) was measured as described in Section 5.2.1.3. Blemish severity was measured using a modified scoring system. Rind collapse and colour (discolouration) were assessed using two separate subjective scales (outlined below), rather than one (as in Section 5.2.1.3). This allowed assessment of the individual timing of collapse and discolouration events. Plate 6.1 shows the six standard blemish images used for assessment in Chapter 5, assigned with severity scores according to the modified system.

collapse

0 - nil
1 - very slight
2 - slight
3 - medium
4 - high

colour

0- nil
1 - very slight
2 - slight
3 - medium
4 - high
5 - extreme

d. Experimental design

Seventy-two mature fruit were harvested in total, from three trees. Treatments were randomly allocated to the twenty-four fruit from each tree: eight assessment times x three replicates.

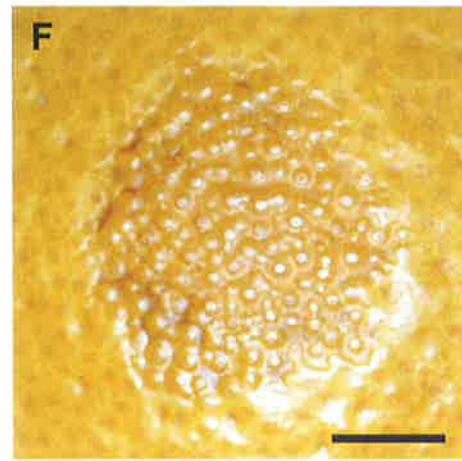
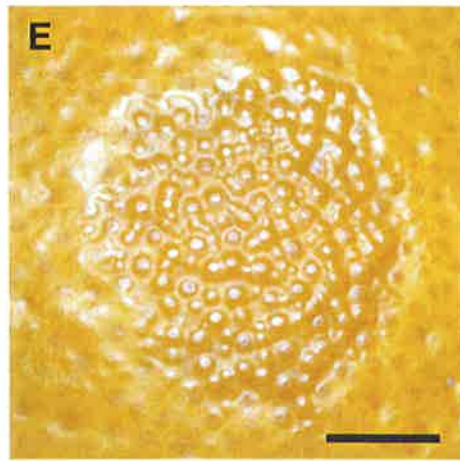
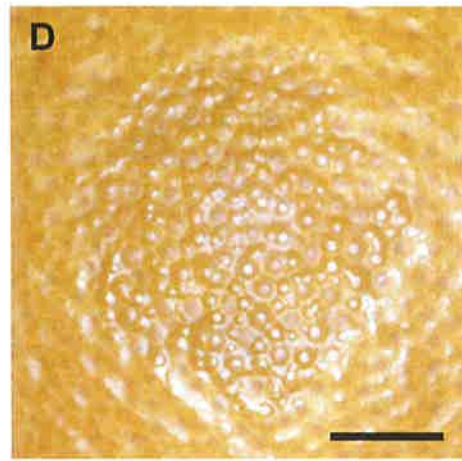
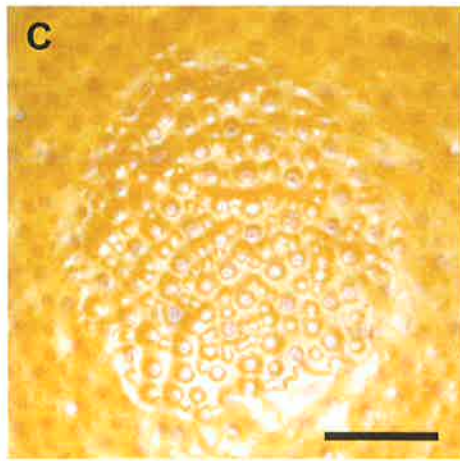
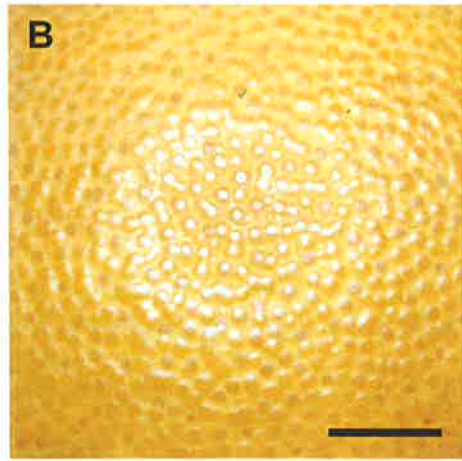
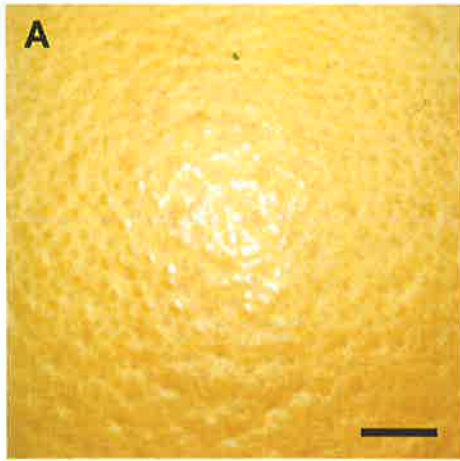
e. Statistical Analysis

Rind collapse, colour and blemish area data were analysed using the statistical package Genstat for Windows version 4.1 (Lawes Agricultural Trust, IACR Rothamsted). A split plot design was applied to the data and Analysis of Variance (ANOVA) tables used to test for statistical significance at the 95% confidence level. Variance components were also analysed at the 72 hour time interval.

Plate 6.1

Modified blemish severity scoring system. Bars = 1 cm.

- A. 0,0 (no collapse, no discolouration).
- B. 1,0 (very slight collapse, no discolouration).
- C. 2,1 (slight collapse, very slight discolouration).
- D. 3,2 (medium collapse, slight discolouration).
- E. 3,4 (medium collapse, high discolouration).
- F. 4,5 (high collapse, extreme discolouration).



6.2.1.2. Experiment 2

A modified time course assessment was carried out to reduce variation observed in experiment 1. To achieve this, 15 mature fruit were collected from one tree, and all fruit were assessed at each time interval. Fruit were harvested from a 23 year old Washington navel orange tree on *Poncirus trifoliata* rootstock located in the University of Adelaide, Waite Campus Alverstoke orchard (34°97'S, 138°63'E). Fruit were harvested on August 25, 1998. Data collected in experiment 2 were used for symptom assessment. No microscopy observations of this material were made.

6.2.2. Microscopy

6.2.2.1. Tissue sampling

In experiment 1, rind samples were collected at each of the eight time intervals, and prepared for LM and TEM examination. In penetrometer-damaged fruit, rind samples were taken from three areas: the area of penetrometer application, the area of oil spread outside the perimeter of penetrometer damage, and an unaffected area (healthy tissue control). In oil-treated fruit, similar samples were taken, from the area of oil disc application, the area of oil spread outside of the disc perimeter, and an unaffected area (healthy tissue control).

6.2.2.2. Light microscopy (LM)

a. Tissue preparation

Tissue preparation was carried out according to methods outlined in Section 3.2.3.2. Two tissue processing methods were employed: aldehyde fixation and aldehyde fixation plus osmium tetroxide postfixation.

In the first method, rind samples of 5 x 5 mm were fixed overnight in glutaraldehyde, dehydrated through an alcohol series and embedded in glycol-methacrylate (GMA). As microscopy samples were collected at staggered time intervals over three days, samples were stored after fixation in methoxy-ethanol to allow bulk processing. Sections (4 µm thickness) were cut with a Reichert-Jung 2050 Supercut Microtome using glass knives, placed on glass slides and stained

with periodic acid-Schiff's (PAS) and Toluidine Blue O (TBO) (O'Brien and McCully, 1981).

In the second method, rind samples of 1 x 1 mm were fixed overnight in a formaldehyde/glutaraldehyde solution, postfixed in osmium tetroxide, dehydrated through an acetone series and embedded in Procure-Araldite (PA) resin. Samples were stored after primary fixation in washing buffer, to allow bulk processing. Sections (1 μm thickness) were cut with a Reichert-Jung Ultracut E Microtome, placed on glass slides and stained with TBO (O'Brien and McCully, 1981).

Histochemical staining for lignin using Phloroglucinol-HCl (Jensen, 1962) and suberin using Sudan Black B (SBB) (O'Brien and McCully, 1981) was also employed. All material was observed with a Zeiss Axiophot Photomicroscope, using transmitted light.

b. Sample selection

For aldehyde fixed tissue, serial sections were collected from approximately 20 samples. For aldehyde plus osmium postfixed material, survey sections were collected from approximately 25 samples. Approximately 100 sections were collected from each sample. The latter material was preferred for rind damage observations. Fifteen samples were selected for TEM preparation, to achieve intact ultra-thin sections for six samples.

6.2.2.3. Transmission electron microscopy (TEM)

a. Tissue preparation

Ultra-thin sections (70 nm in thickness) were collected on a diamond knife, using a Reichert-Jung Ultracut E Microtome. Sections were transferred to collodion coated copper grids, 200 mesh thin bar. Sections were stained with uranyl acetate and lead citrate (O'Brien and McCully, 1981), and observed under an accelerating voltage of 80 kV with a Philips CM 100 TEM.

b. TEM assessment

Montage images of the rind profile were created with the analySIS program (Soft Imaging Systems, Muenster, Germany). Plate 6.2 shows the rind profile of a healthy, untreated tissue sample. Flavedo tissue was divided into three layers: epidermis, hypodermis and cortex. Within each layer, a minimum of three cells was examined. The cell wall, cytoplasm, nucleus and vacuoles of each cell were observed (Mauseth, 1988). The main components of the cytoplasm assessed for integrity included the plasmalemma, plastids and mitochondria. This method enabled a standard comparison of ultrastructural damage between samples. TEM was used to compare rind damage between induction methods, and to examine oleocellosis development in oil-treated fruit.

6.2.2.4. Scanning electron microscopy (SEM)

Healthy and oleocellosis-damaged tissue samples were prepared for cryofixation according to the method outlined in Section 4.2.2.2. In addition, cryofixed samples were examined in backscatter mode to enable elemental detection.

6.2.2.5. Confocal microscopy

Healthy and oleocellosis-damaged tissue samples were prepared for multi-photon microscopy according to Section 4.2.3.3.

Plate 6.2

Rind profile image of healthy rind tissue. Image merged from a sequence of TEM images. The rind profile was divided into three layers: epidermis, hypodermis and cortex. Bar = 5 μm .



Epidermis

Hypodermis

Cortex

6.3. Results

6.3.1. Symptoms

6.3.1.1. Time course assessment

a. Blemish severity

Rind collapse was first detected at 1 hour following induction in the penetrometer-damaged fruit and 6 hours in oil-treated fruit (Fig. 6.1). The period of most rapid collapse for penetrometer-damaged fruit was within the first 12 hours, with significant increases ($P < 0.05$) observed between 2 and 6, and again between 6 and 12 hours. Oil-treated fruit also showed a significant increase between 6 and 12 hours, and also at later stages, between 24 and 48, and 48 and 72 hours. By day 3, mean collapse scores were 2.3 for oil-treated fruit and 1.5 for penetrometer-damaged fruit.

Rind discolouration was first detected at 2 hours following induction in oil-treated fruit and 12 hours in penetrometer-damaged fruit (Fig. 6.2). Oil-treated fruit showed a mean score of 1 by 6 hours, compared to penetrometer-damaged fruit, which showed a maximum score of 0.3 at day 3. In oil-treated fruit, a significant increase ($P < 0.05$) was observed between 2 and 6 hours, and 24 and 48 hours, resulting in a mean colour score of 2.3 by day 3. The mean scores for both collapse and discolouration were considered to be low given the scoring scales of 0 to 4 and 0 to 5, respectively. This was attributed to the high proportion of samples which did not develop blemish.

b. Blemish area

For blemish area, a similar trend was observed for both induction methods (Fig. 6.3). A significant area increase ($P < 0.05$) was observed between 12 and 24 hours for both methods, as well as between 2 and 6 hours for oil-treated fruit. By day 3, oil-treated fruit showed a larger mean blemish area than penetrometer-damaged fruit, with mean scores of 229 mm² and 173 mm², respectively. However, there was little change in mean blemish area after day 1.

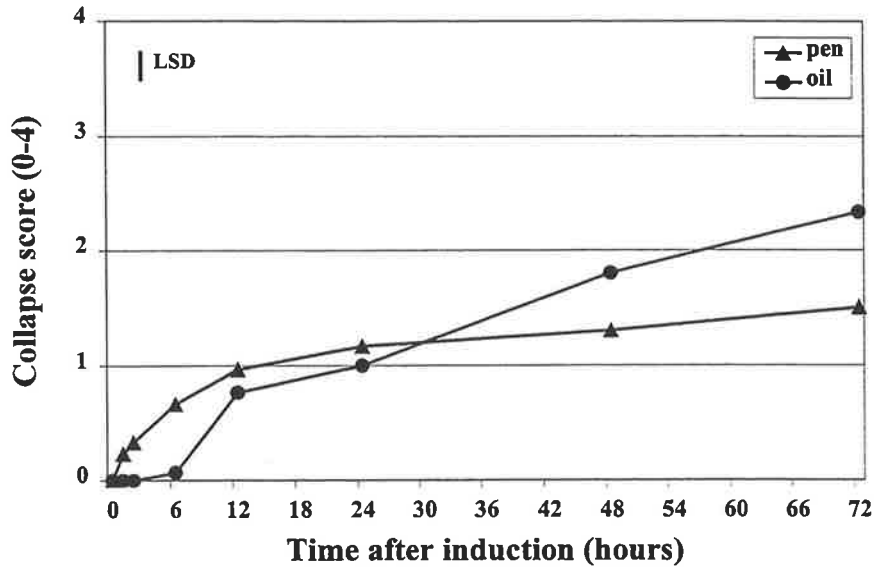


Figure 6.1. The relationship between time and rind collapse. Collapse score: 0 (nil), 1 (very slight), 2 (slight), 3 (medium), 4 (high). Pen = penetrometer induction, oil = oil induction. Fifteen fruit, assessed at each of eight time intervals from zero to three days. Means represented. LSD = 0.26.

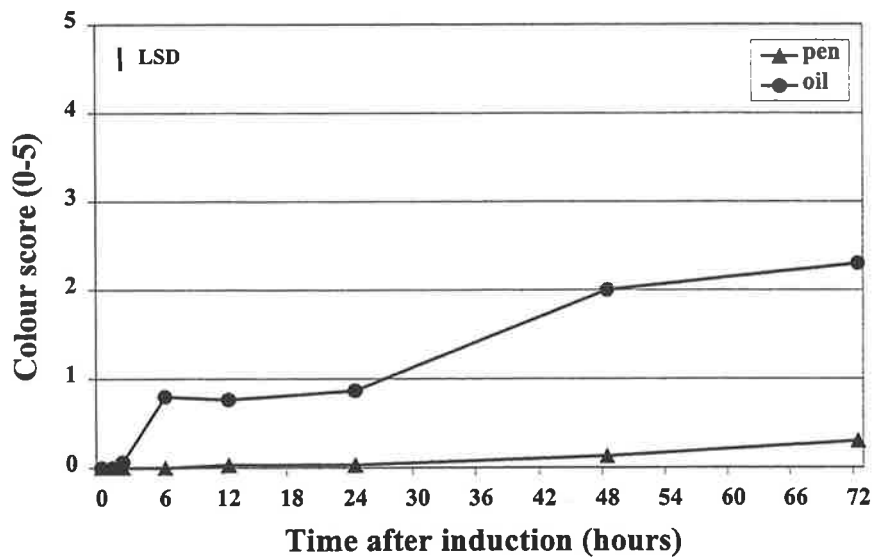


Figure 6.2. The relationship between time and rind discolouration. Colour score: 0 (nil), 1 (very slight), 2 (slight), 3 (medium), 4 (high), 5 (extreme). Pen = penetrometer induction, oil = oil induction. Fifteen fruit, assessed at each of eight time intervals from zero to three days. Means represented. LSD = 0.33.

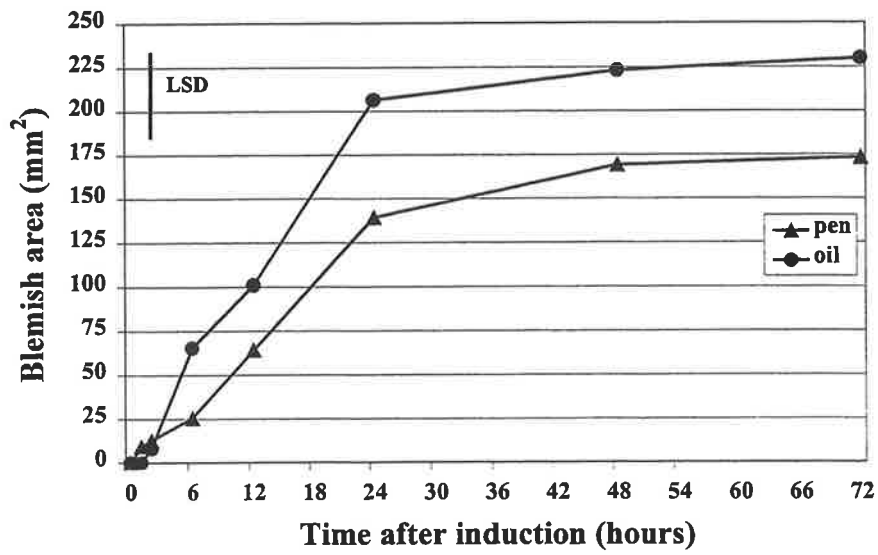


Figure 6.3. The relationship between time and blemish area. Pen = penetrometer induction, oil = oil induction. Fifteen fruit, assessed at each of eight time intervals from zero to three days. Means represented. LSD = 50 mm².

c. Symptom variation

Variance components were assessed at 72 hours, and compared between experiment 1 and experiment 2 (Table 6.1). In experiment 1, fruit effects were responsible for a high proportion of variation in area and collapse. The tree effect was nil or negligible for all responses. The method effect was notable for all responses, but particularly colour, where it accounted for 78% of variation. The variation between replicate samples was larger than expected for all responses. In experiment 2, a tree stratum was not present in the analysis, as fruit were picked from one tree only. The fruit effect was responsible for negligible variation, much reduced from experiment 1. The method effect showed a similar trend to experiment 1, and accounted for most of the variation in colour (85%). Replicate sample variation also showed a similar trend, and accounted for most of the variation in collapse (73%) and area (68%), but to a lesser extent colour change (15%).

Table 6.1. Variance strata for blemish collapse, colour and area at day 3, expressed as percentage of total variation. Experiment 1, fruit harvested from five trees and different fruit assessed at each time. Experiment 2, fruit harvested from one tree and same fruit assessed at each time. Sample refers to replicate treatments on the one fruit.

Stratum component	Variation of score (%)		
	Collapse	Colour	Area
Experiment 1			
Tree	0	0	1
Fruit	25	0	25
Method	14	78	37
Sample	60	23	37
Experiment 2			
Fruit	2	0	3
Method	25	85	29
Sample	73	15	68

d. Rind oil release pressure (RORP)

As observed in Chapter 5, RORP at induction showed very little variation between fruit, varying between 164 and 245 kPa (data not shown). In general, RORP values were lower than those observed in Chapter 5, suggesting a higher

fruit turgor at induction. As in Chapter 5, RORP did not appear to influence the resulting blemish severity or area (data not shown).

6.3.1.2. Additional observations

In penetrometer-damaged fruit, gland rupture was observed predominantly around the periphery of the penetrometer application zone (Plate 6.3A). Some interesting blemish characteristics were also observed. In a small proportion of oil-treated fruit, small black spots were evident on the fruit surface, associated with oleocellosis-damaged tissue (Plate 6.3B). In some fruit, larger necrotic areas on the fruit surface became associated with the damaged tissue after several days (Plate 6.3C). In oil-treated fruit, a reddish coloured blemish was evident in many samples after approximately one week (Plate 6.3D).

6.3.2. Rind surface damage

SEM was used to examine features of the fruit surface following penetrometer damage. A pool of oil was apparent above each ruptured gland (Plate 6.4A). Removal of the oil exposed a hole in the epidermis, where the gland had ruptured (Plate 6.4B). Stomata were also apparent over the entire fruit surface, in damaged and undamaged areas (Plate 6.4C). In damaged tissue, ruptured glands were distinguishable from stomata by their torn edges and lack of guard cells. Stomata were observed to be denser on the fruit surface than ruptured glands. Mechanical damage to the fruit surface was observed at the zone of penetrometer application and surface cracks and tears were often present (Plates 6.4D and 6.4E). It was not clear whether this damage was restricted to the cuticle or extended into the epidermis, but neither of these features were apparent on the surface of undamaged tissue.

Plate 6.3

Dissecting microscope images of fruit surface damage and oleocellosis symptoms.

A. Gland rupture and oil release (arrows) predominantly around the perimeter of the penetrometer application zone (paz). Bar = 2 mm.

B. Black spots evident on the surface of a small proportion of oil-treated fruit, possibly necrotic guard cells. Bar = 0.5 mm.

C. Necrotic areas (arrows) developed around the edges of the oleocellosis blemish in a small proportion of fruit, after several days. Bar = 5 mm.

D. Red pigmentation observed in some extreme blemishes after approximately one week. Bar = 5 mm.

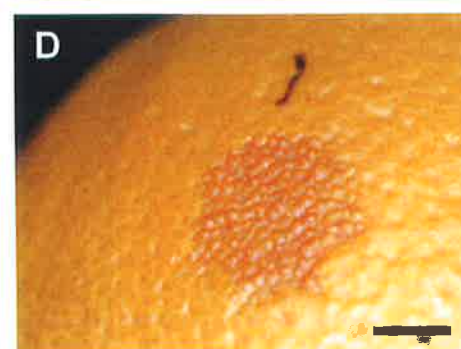
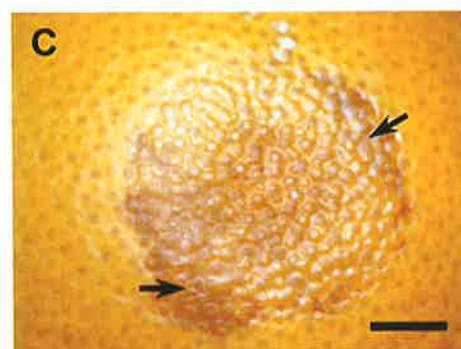
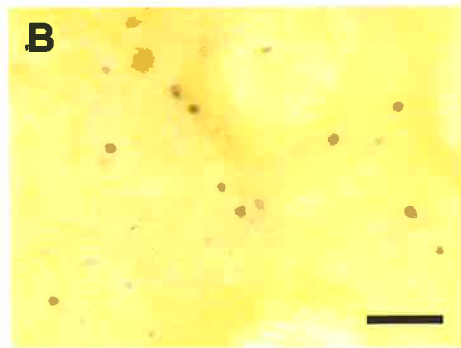
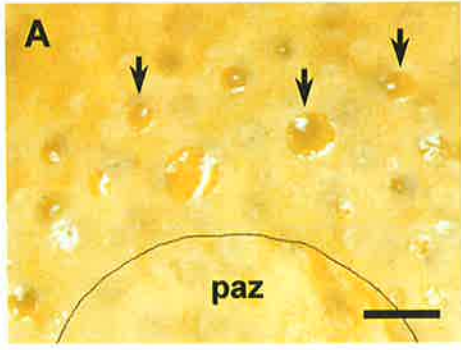
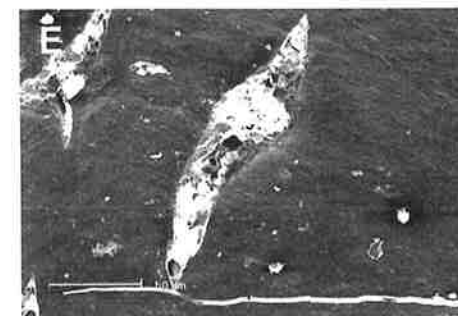
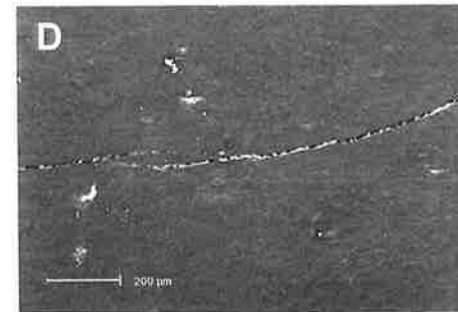
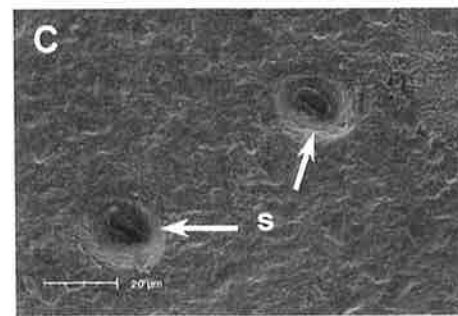
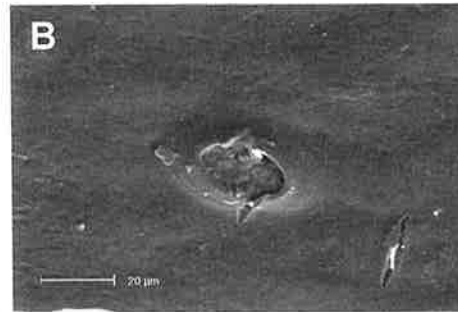
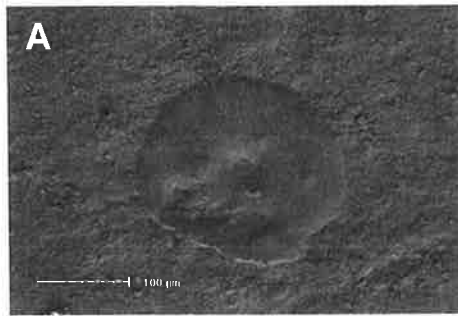


Plate 6.4

Scanning electron micrographs of the fruit surface following mechanical damage, with the penetrometer.

- A. Oil pool on the fruit surface, above a ruptured gland. Bar = 100 μm .
- B. Holes in the epidermis resulting from gland rupture showed non-uniform shape and rough edges. Bar = 20 μm .
- C. Stomata (s) were present over the entire fruit surface. Bar = 20 μm .
- D. Surface cracks resulted from penetrometer action upon the rind. Bar = 200 μm .
- E. Surface tears and cracks resulted from penetrometer action upon the rind. Bar = 50 μm .



6.3.3. Rind sub-surface damage

6.3.3.1. Rind anatomy

Untreated rind tissue showed no signs of cell collapse (Plate 6.5A). In penetrometer-damaged fruit, epidermal rupture above glands was observed (Plate 6.5B). In aldehyde fixed tissue, oil-damaged cells showed distortion or collapse (Plates 6.5C and 6.5D). In both penetrometer-damaged (Plate 6.5C) and oil-treated tissue (Plate 6.5D), oil-damaged cells were localised between glands and a number of layers below the epidermis. In osmicated tissue, oil-damaged cells were more clearly distinguishable from healthy cells by their degenerated cell contents (Plates 6.5E and 6.5F). Unlike aldehyde fixed tissue, a difference in the localisation of oil damage was observed between penetrometer-damaged and oil-treated fruit. In penetrometer-damaged tissue, the majority of samples showed damaged cells to be localised a number of cell layers below the epidermis (Plate 6.5E). However, in oil-treated fruit, damaged cells were located in all cell layers from the epidermis downwards (Plate 6.5F). Samples taken from the zone of oil application and the zone of oil spread appeared similar. Histochemical staining of aldehyde fixed tissue failed to show the presence of lignin and suberin in oleocellosis-damaged tissue. In cryofixed samples examined using SEM, oil-damaged cells appeared to be severely collapsed. In oil-treated fruit, a thick band of collapsed cells, incorporating all cell layers from the epidermis downwards was observed (Plate 6.6). X-ray micro-analysis of cryofixed samples showed no elemental difference between healthy tissue and oleocellosis-damaged tissue.

6.3.3.2. Oil localisation

Untreated rind tissue showed no sign of major oil deposits outside of the glands (Plate 6.7A). However, small, fluorescent bodies in the upper rind layers were most likely plastid or cytoplasm localised oil bodies. Tissue was examined 18 hours after penetrometer damage, but no oil was apparent in tissue between the glands. After three days however, the degenerated contents of oil-damaged cells observed in osmicated tissue sections were also detected in fresh tissue (Plate 6.7B). Degenerated cell contents that were stained by both cell wall (green) and lipid (red) stains, appeared yellow/orange in colour.

Plate 6.5

Light micrographs of the oleocellosis-damaged rind. Longitudinal, aldehyde fixed, PAS/TBO stained sections (A to D). Longitudinal, aldehyde plus osmium tetroxide postfixed, TBO stained sections (E and F).

A. Untreated fruit sample. Bar = 100 μm .

B. Ruptured epidermis (arrow) above a gland (g), resulting from penetrometer damage. Bar = 100 μm .

C. Penetrometer-damaged fruit sample, showing sub-epidermal cell collapse (arrows). Bar = 100 μm .

D. Oil-treated fruit sample, showing sub-epidermal cell collapse (arrows). Bar = 100 μm .

E. Penetrometer-damaged fruit sample, showing sub-epidermal cell content degeneration (arrows), below intact upper rind layers. Bar = 100 μm .

F. Oil-treated fruit sample, showing cell content degeneration in all layers, including the epidermis (arrows). Bar = 100 μm .

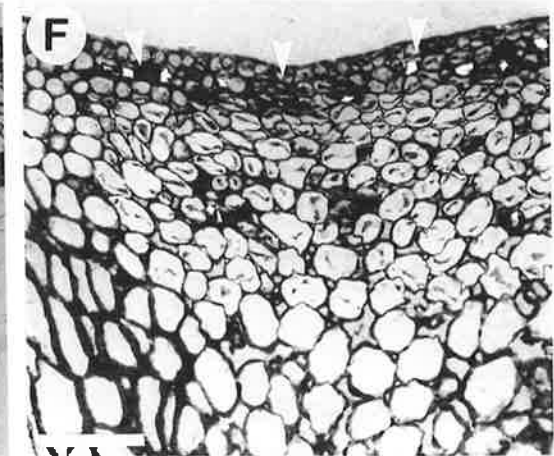
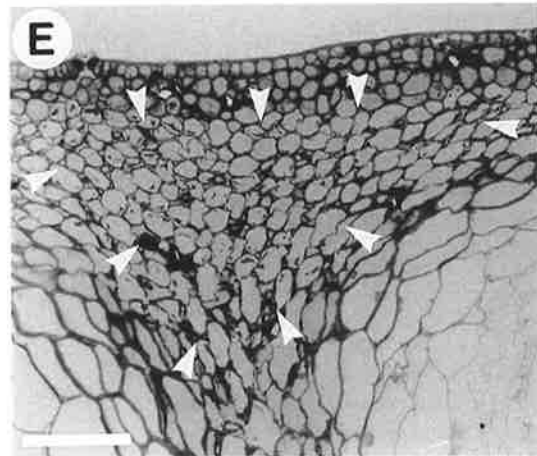
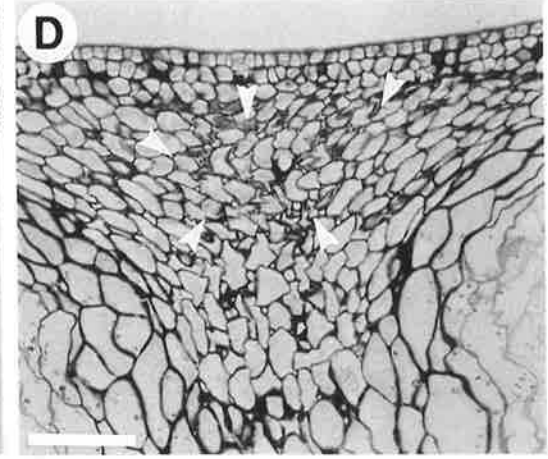
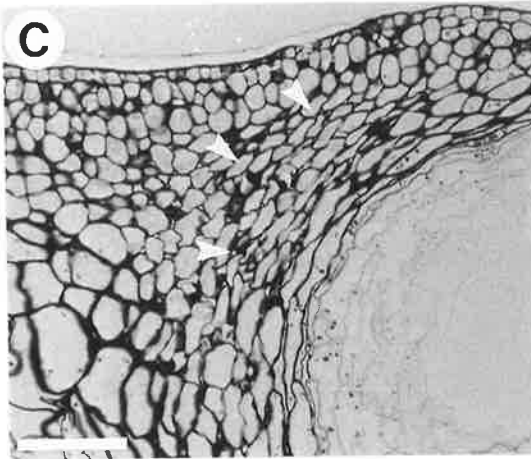
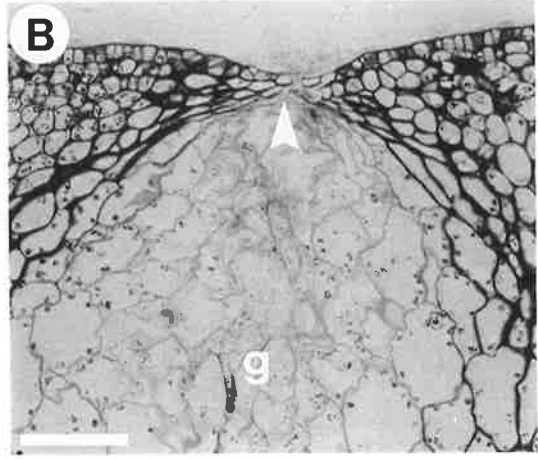
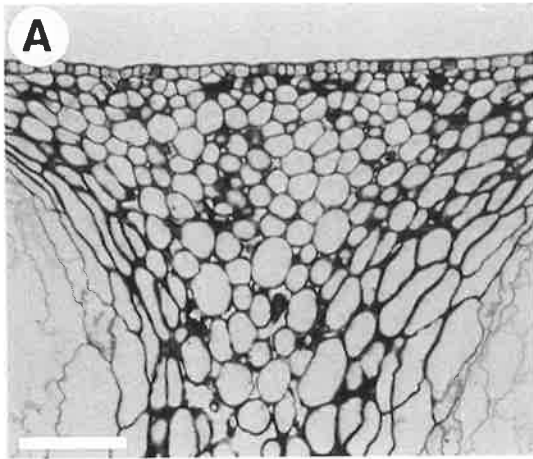


Plate 6.6

Scanning electron micrograph of the oleocellosis-damaged rind, resulting from oil treatment. Longitudinal rind cross-section showed a thick band of collapsed cells, incorporating all cell layers from the epidermis downwards.

Bar = 50 μm .

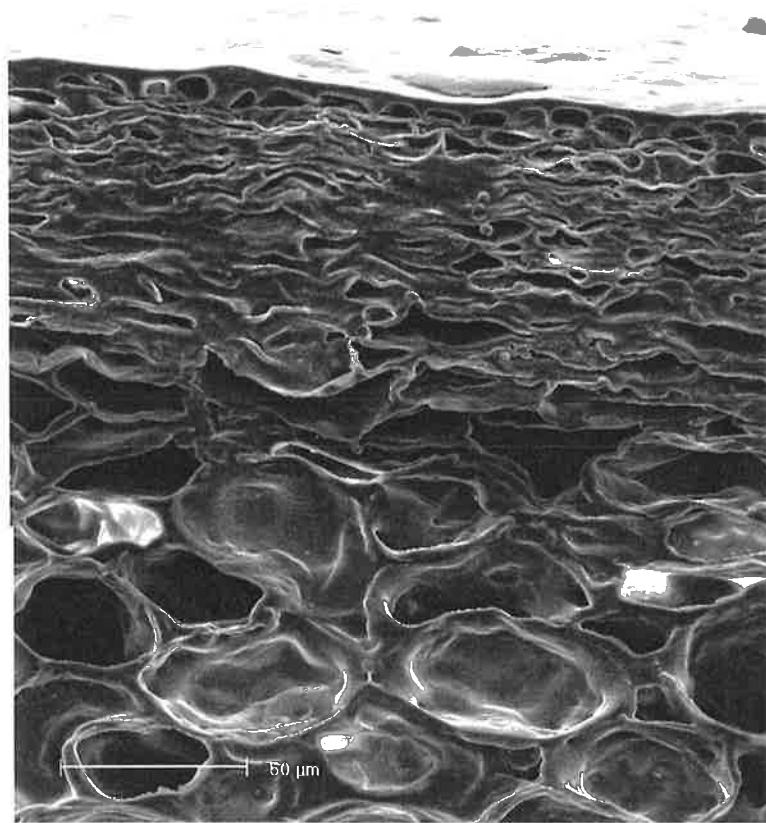
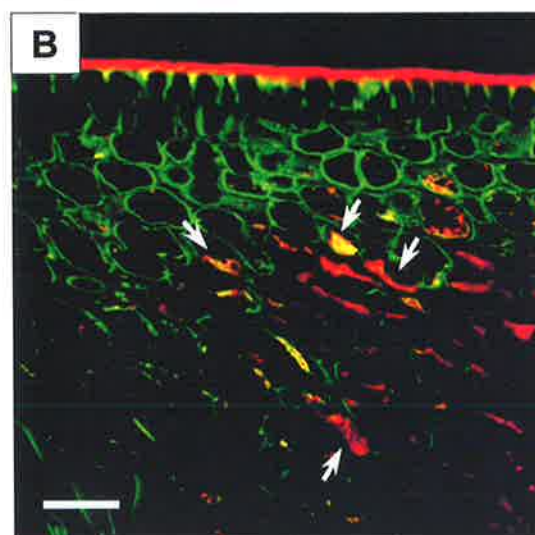
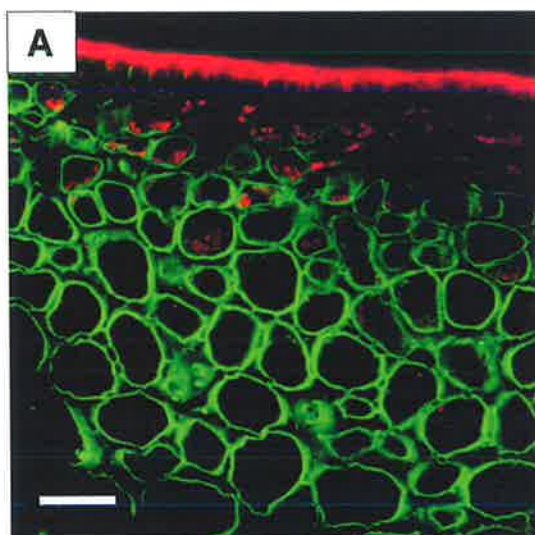


Plate 6.7

Multi-photon microscope images of healthy and oleocellosis-damaged rind. Two-colour merged optical sections of fresh tissue, stained with Calcofluor White for cell walls (green), and Nile Red for lipid (red).

A. Untreated tissue. Bar = 30 μm .

B. Penetrometer-damaged tissue after three days, showing degenerated contents of oil-damaged cells (arrows), stained by both stains and labelled a yellow/orange colour. Bar = 30 μm .



6.3.3.3. Rind ultrastructure

Rind samples from untreated fruit, penetrometer-damaged fruit and oil-treated fruit were examined using TEM. For each sample, the rind profile (Plate 6.8) and ultrastructural features of individual cells (Plates 6.9 to 6.14) were examined.

a. Untreated fruit

The cuticle appeared vesicular (Plate 6.9A). Epidermal cells contained one or two main vacuoles, often with smaller vacuoles also present (Plate 6.8A). The protoplast was located around the cell edge. The tonoplast and plasmalemma were intact and continuous in most cells. In some cells, the plasmalemma had vesicles associated with the walls (Plate 6.9B). The nuclei showed an intact nuclear envelope, often with very slight bulges between inner and outer envelopes (Plate 6.9C). Plastids, in the form of chromoplasts, were usually round to oval shaped and showed an intact outer membrane, and folded inner membrane (Plate 6.9D). Plastids contained plastoglobuli, which were generally lightly stained. Mitochondria showed an intact double membrane, including internal cristae (Plate 6.9E). Round to oval shaped oil bodies were present in epidermal cells, often closely associated with vacuole edges or in the cytoplasm. Oil movement was observed between the cytoplasm and vacuole (Plate 6.9F). Multivesicular bodies were present in some cells, often located between the plasmalemma and cell wall (Plate 6.9G). Hypodermal cells were similar in ultrastructural appearance to epidermal cells. Some contained a main vacuole, while others contained a few smaller sized vacuoles. Cortex cells also showed intact organelles and membrane systems. Plasmodesmata were observed between all cell types, on occasions causing constrictions in cell walls, particularly in hypodermal cells (Plate 6.9H).

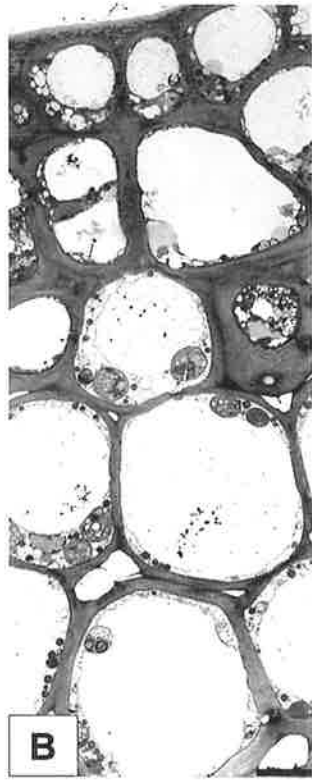
b. Oil-treated fruit, 30 minutes, no symptoms

The rind profile image of this sample (Plate 6.8B) appeared similar to that of the untreated sample (Plate 6.8A). The cuticle appeared similar to that in untreated fruit, as did the membranes in epidermal cells. Some cells showed intact tonoplast and plasmalemma, whereas in others the tonoplast was not continuous, and the plasmalemma appeared to be detached from the cell wall or was missing in

Plate 6.8

Rind profile images of healthy and oleocellosis-damaged rind. Each image merged from a sequence of TEM images. Bars = 5 μm . See over page.

- A. Untreated fruit sample.
- B. Oil-treated fruit sample, 30 minutes, no symptoms (0,0).
- C. Oil-treated fruit sample, six hours, very slight blemish (2,0).
- D. Oil-treated fruit sample, two days, medium level blemish (3,4).
- E. Oil-treated fruit sample, ten days, extreme blemish (4,5).
- F. Penetrometer-damaged fruit sample, three days, medium level blemish (3,2).



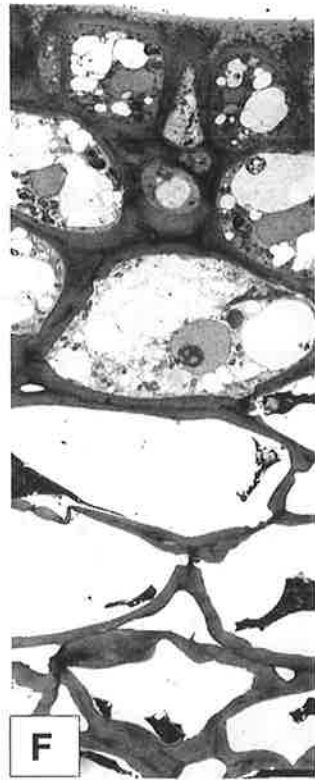
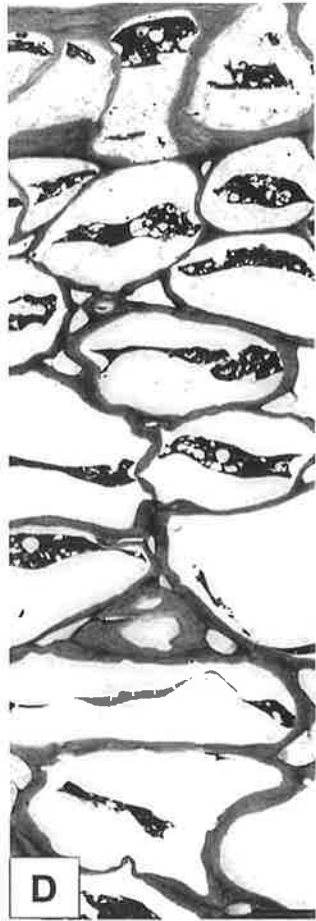


Plate 6.9

Transmission electron micrographs of rind ultrastructure in an untreated fruit sample.

A. The cuticle appeared vesicular. Bar = 1 μm .

B. Plasmalemma (arrows) with vesicles between it and the cell wall (cw). Bar = 0.5 μm .

C. Nucleus with an intact envelope and very slight swelling between inner and outer membranes (arrows). Bar = 1 μm .

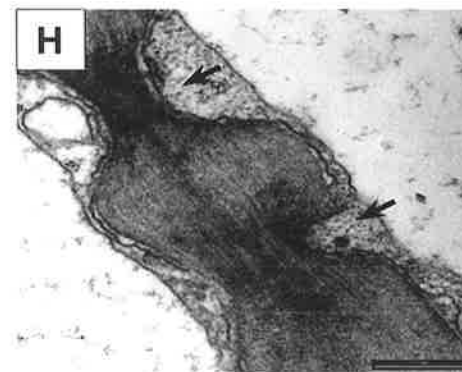
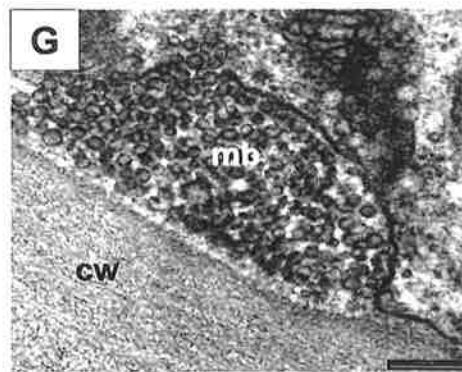
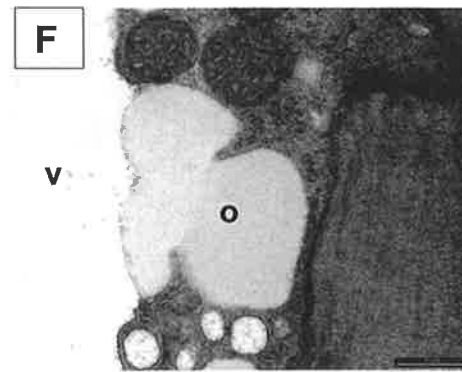
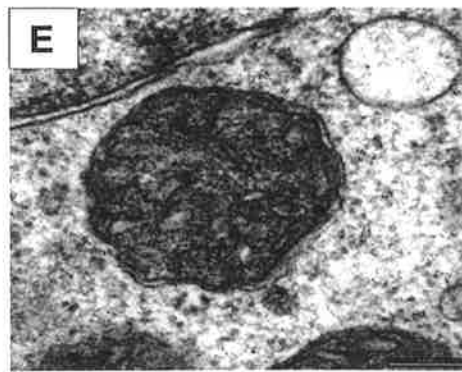
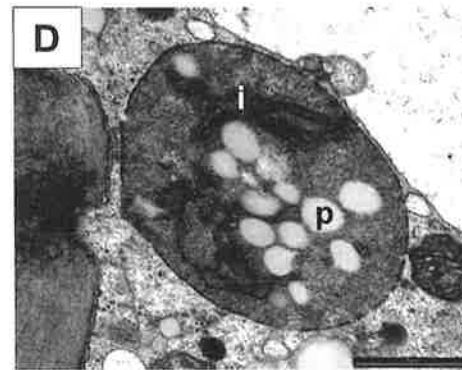
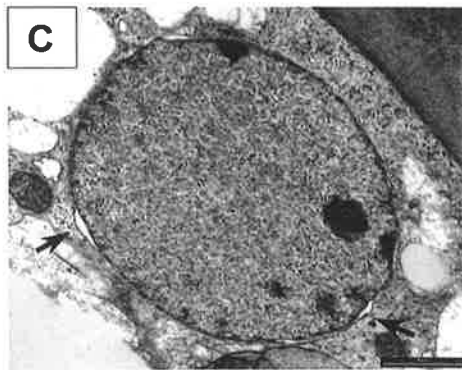
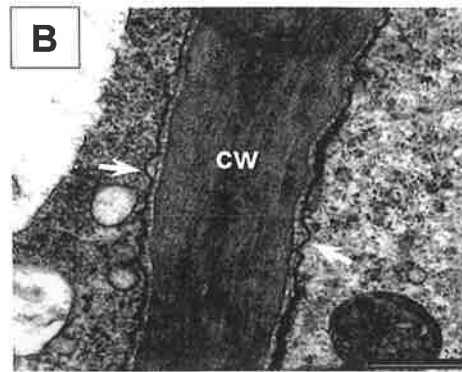
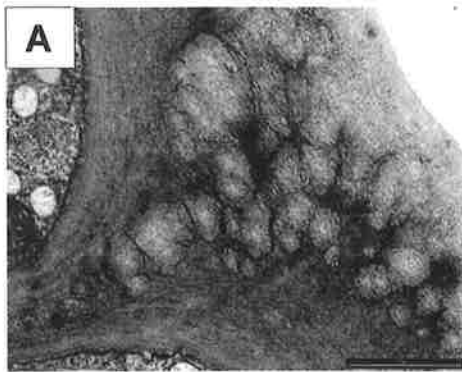
D. Plastid (chromoplast) with intact outer membrane, folded inner membrane (i) and lightly stained plastoglobuli (p). Bar = 1 μm .

E. Mitochondrion with intact double membrane and cristae. Bar = 0.2 μm .

F. Oil (o) in the cytoplasm adjacent to vacuole (v). Bar = 0.5 μm .

G. Multivesicular body (mb), located between the plasmalemma and cell wall (cw). Bar = 0.2 μm .

H. Constrictions in the cell wall at the site of plasmodesmata (arrows). Bar = 0.5 μm .



sections (Plate 6.10A). The majority of nuclei, mitochondria and plastids appeared similar to those in untreated tissue. Some nuclei showed bulging in their envelope, although on occasions more advanced stages of degeneration were observed (Plate 6.10B). Plastids contained intact double membranes, but some degeneration of membranes and internal structure was also observed (Plate 6.10C). Oil bodies were larger and more numerous than in untreated tissue, and were located in vacuoles and cytoplasm, or appeared to be moving between the two, as observed in untreated tissue. Oil bodies appeared to be more closely associated with organelles; for example, mitochondria (Plate 6.10D). The plasmalemma, tonoplast and nuclei of hypodermal cells appeared similar to those of epidermal cells. The double membrane of mitochondria appeared to be intact in some but slightly diffuse in others (Plate 6.10E). Plastids showed signs of membrane and internal degeneration (Plate 6.10F). Oil bodies were present in many hypodermal cells, again associated with the vacuole and organelles, and also present in intercellular spaces between hypodermal cells. The ultrastructural appearance of cortex cells varied at this stage. Some cells at layer seven appeared more damaged than those at layer four or five. In the least damaged cells, mitochondria, plastids and even tonoplast and plasmalemma appeared intact. In the most damaged cell observed, the vacuole was not intact and the cell contained debris, but some mitochondria remained intact. Oil bodies were less evident in cortex cells than epidermal and hypodermal cells, but were again closely associated with organelles, and were present in intercellular spaces between cortex cells, to a depth of approximately nine cell layers (Plate 6.10G). Small oil bodies were also observed in close association with plasmodesmata between adjoining cortex cells (Plate 6.10H).

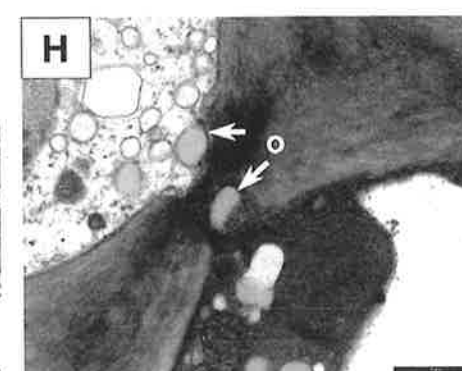
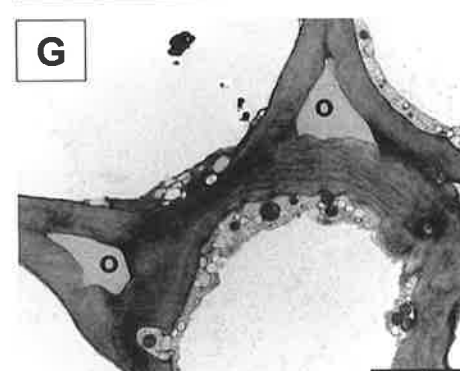
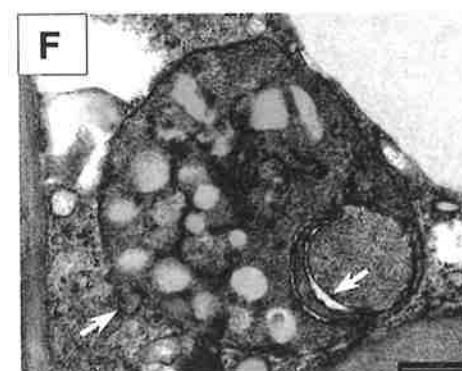
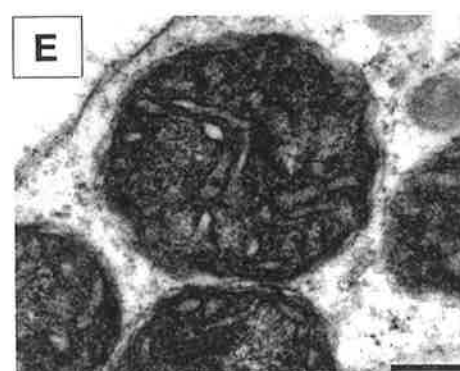
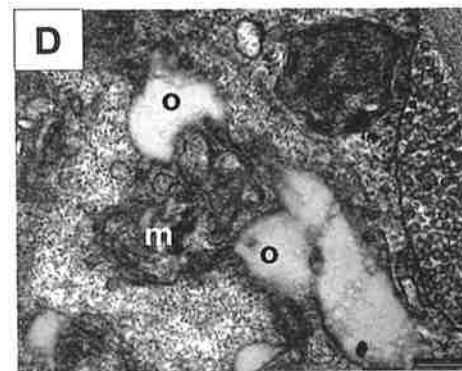
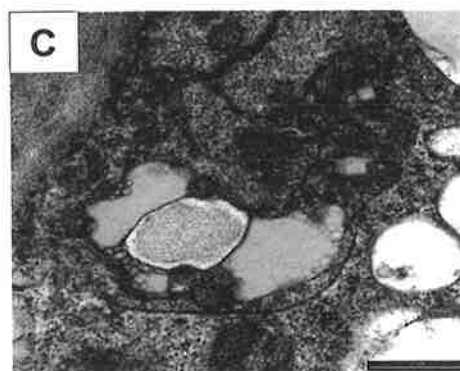
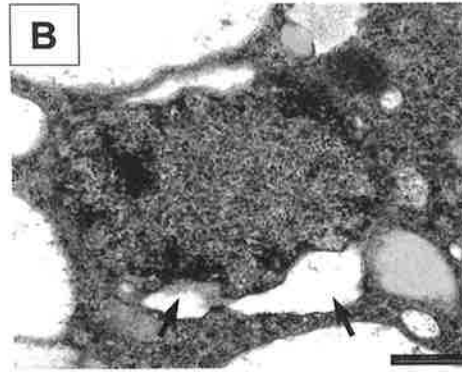
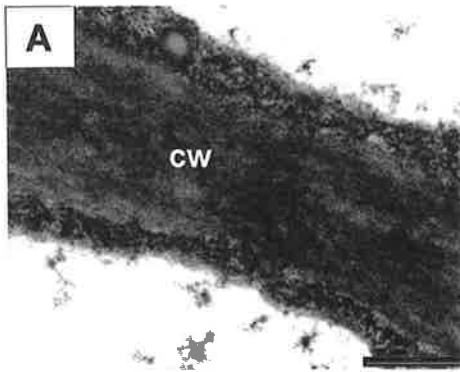
c. Oil-treated fruit, six hours, very slight blemish

Six hours after oil treatment, only very slight surface symptoms were observed in this fruit sample, with slight rind collapse but no discolouration. However, the rind profile image at 6 hours (Plate 6.8C) was dramatically different to 30 minutes (Plate 6.8B). Cells showed various stages of degeneration. The cuticle appeared similar to that in untreated fruit. Epidermal cells were at various stage of degeneration. In some cells, many vesicles were present and the cytoplasm had

Plate 6.10

Transmission electron micrographs of rind ultrastructure in an oil-treated fruit sample, after 30 minutes.

- A. Plasmalemma absent and cell wall (cw) edges diffuse. Bar = 0.5 μm .
- B. Nucleus with significant swelling of nuclear envelope (arrows). Bar = 0.5 μm .
- C. Degenerated plastid. Bar = 0.5 μm .
- D. Mitochondrion (m) with adjacent oil bodies (o). Bar = 0.2 μm .
- E. Mitochondrion with intact but slightly diffuse membrane. Bar = 0.2 μm .
- F. Plastid showing signs of outer membrane and internal degeneration (arrows). Bar = 0.5 μm .
- G. Intercellular spaces filled with oil (o). Bar = 5 μm .
- H. Oil bodies (o) in close association with a plasmodesma. Bar = 1 μm .



developed a granular appearance. At a more advanced stage of damage, the protoplast had fused to form one single dense mass, containing many vesicles; this was termed the 'fused protoplast' (Plate 6.11A). The plasmalemma was identifiable in some epidermal cells, but was not continuous. Portions of the plasmalemma (which were intact) were detached from the cell wall and appeared to be more closely associated with the edge of the fused protoplast (Plate 6.11B). The nucleus was distinct in some cells, but in others showed a diffuse membrane and was stained heavily (Plate 6.11C). Hypodermal cells also appeared to be at various stages of breakdown. Some cells contained a fused protoplast in which little structure could be identified, while others were highly vesiculated and contained discreet organelles. Mitochondria often showed remnants of their membrane, but loss of internal structure, and some showed complete loss of integrity. A darkened zone inside the stroma was often observed in damaged mitochondria (Plate 6.11D). Cortex cells appeared to be slightly more damaged than hypodermal cells. Membranes or organelles could not be readily identified, and a fused protoplast was commonly observed. A closer examination of the fused protoplast showed membrane remnants (Plate 6.11E). Walls of hypodermal and cortex cells showed a slight loss of integrity and intercellular spaces appeared to be greater in number and size (Plate 6.11F). Oil bodies were not observed in the intercellular spaces as they were at 30 minutes.

d. Oil-treated fruit, two days, medium level blemish

Two days after oil treatment, medium level rind collapse and discolouration were observed in this sample. The rind profile at two days (Plate 6.8D) showed more advanced cell content degeneration than that observed at six hours (Plate 6.8C), and a more uniform ultrastructural appearance between all cells layers. The cuticle appeared similar to that in untreated fruit. A fused protoplast was present in all epidermal cells, either close to the cell wall or centrally located (Plate 6.12A). The fused protoplast was highly vesiculated. The plasmalemma was not associated with the cell wall, and the cell wall and fused protoplast showed diffuse edges (Plate 6.12B). Organelles were not identifiable, however, what may have been remnants of the nucleus were apparent in a number of cells, as a darkened,

Plate 6.11

Transmission electron micrographs of rind ultrastructure in an oil-treated fruit sample, after six hours.

- A. Highly vesiculated fused protoplast. Bar = 1 μm .
- B. The plasmalemma (arrow), detached from the cell wall (cw) and surrounding the fused protoplast (fp). Bar = 0.2 μm .
- C. Nucleus, with diffuse envelope and densely osmiophilic appearance. Bar = 0.5 μm .
- D. Mitochondria (m) showing diffuse membranes and loss of internal structure. Bar = 0.2 μm .
- E. Membrane remnants trapped inside the fused protoplast. Bar = 0.2 μm .
- F. An expanded intercellular space (is). Bar = 2 μm .

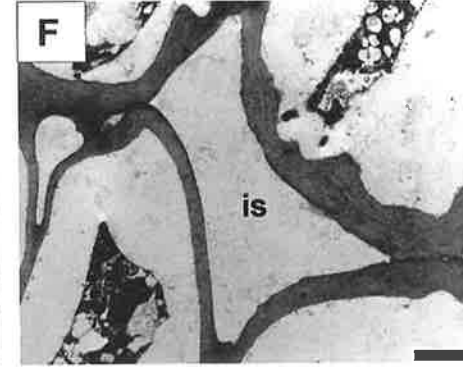
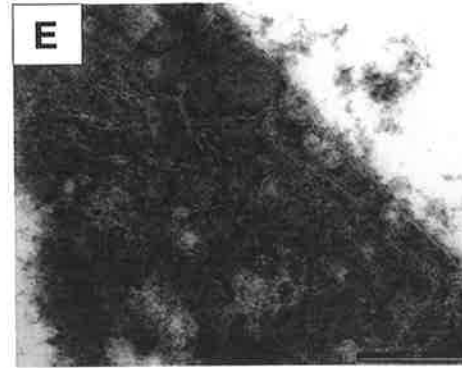
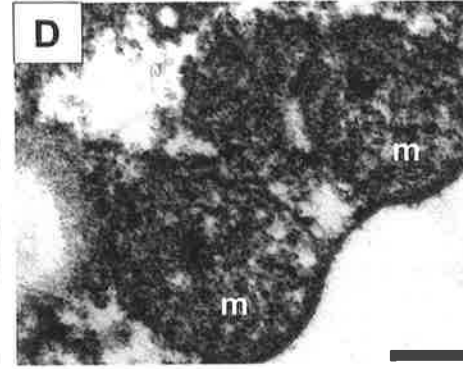
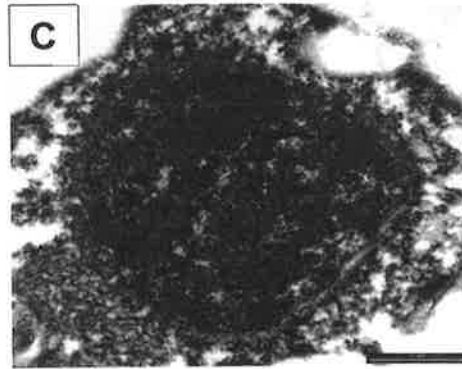
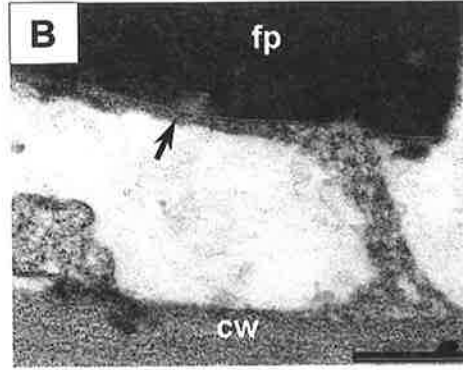
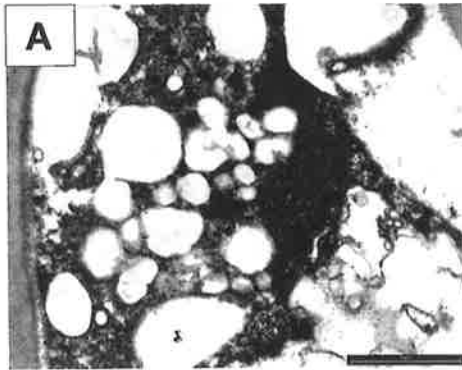
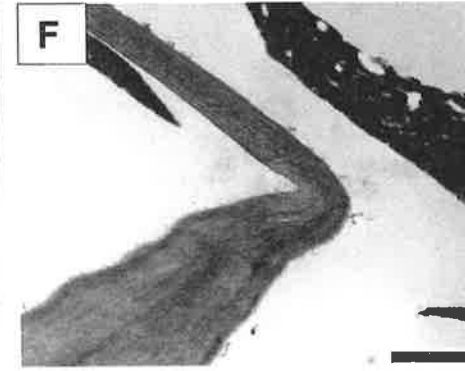
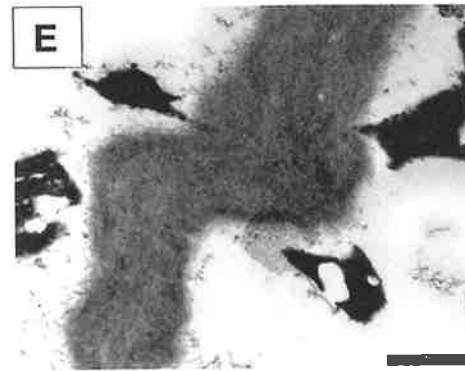
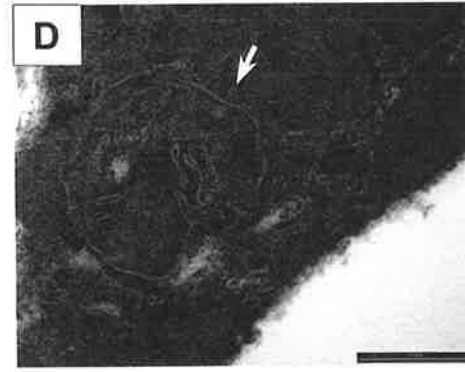
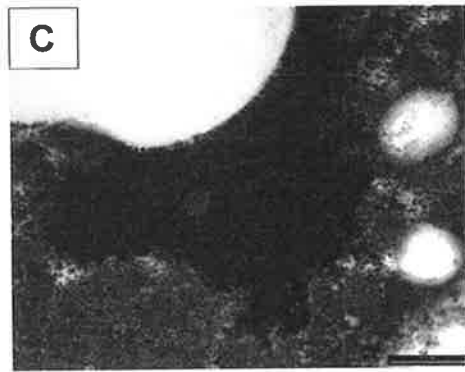
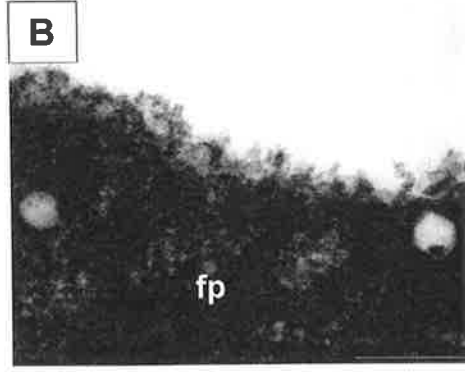
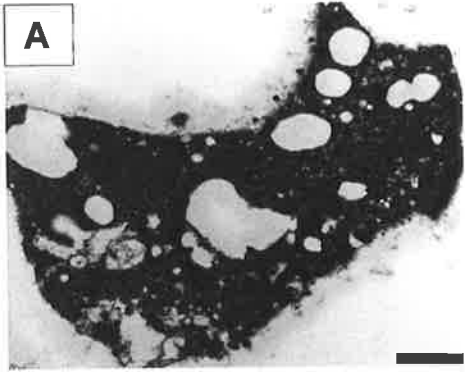


Plate 6.12

Transmission electron micrographs of rind ultrastructure in an oil-treated fruit sample, after two days.

- A. Highly vesiculated fused protoplast, located centrally in the cell. Bar = 1 μm .
- B. Diffuse edges of the fused protoplast (fp). Bar = 0.2 μm .
- C. Darkened region of the fused protoplast, possibly nucleus remains. Bar = 0.2 μm .
- D. Membrane remnants (arrow) trapped inside the fused protoplast. Bar = 0.2 μm .
- E. Cell wall thickening and slight folding in epidermal cells. Bar = 1 μm .
- F. Cell wall folding in cortex cells. Bar = 1 μm .



amorphous region in the fused protoplast (Plate 6.12C). Membrane remnants were apparent within the fused protoplast (Plate 6.12D). Epidermal cell walls showed signs of thickening and to a lesser extent, folding (Plate 6.12E). Hypodermal and cortex cells also contained a fused protoplast, appearing ribbon-like in lower cortex cell layers. Cell wall thickening and folding was also evident in hypodermal and cortex cells (Plate 6.12F). Intercellular spaces were present in hypodermal and cortex cell layers.

e. Oil-treated fruit, ten days, extreme blemish

Ten days after oil treatment, high level rind collapse and extreme discolouration were observed in this fruit sample. The rind profile at ten days (Plate 6.8E) showed more advanced cell content degeneration than that observed at two days (Plate 6.8D), and increased cell wall thickening and folding, particularly of hypodermal cells. The cutin appeared less vesicular and slightly more flattened than in earlier samples (Plate 6.13A). A fused protoplast was present in all epidermal cells, either close to the cell wall or centrally located, as at two days. Oil bodies were observed within the fused protoplast and external to the protoplast (Plate 6.13B), and being secreted from the fused protoplast (Plate 6.13C). Epidermal cell walls were thicker than those observed at two days. Hypodermal and cortex cells also contained a fused protoplast and oil bodies. Cells exhibiting these features were present to a depth of approximately seventeen layers in this sample. In addition, oil movement via plasmodesmata was also observed (Plate 6.13D). Hypodermal cells showed extreme folding (Plate 6.13E) and thickening, highlighted by constrictions at the site of plasmodesmata. Cortex cells also showed folding and to a lesser extent, thickening (Plate 6.13F).

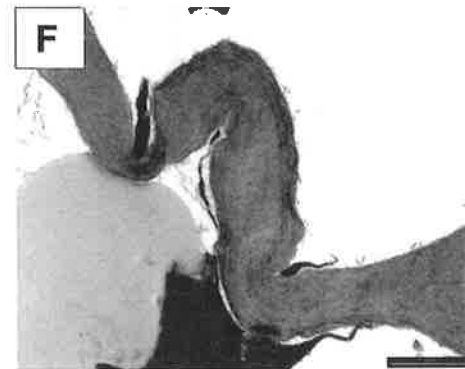
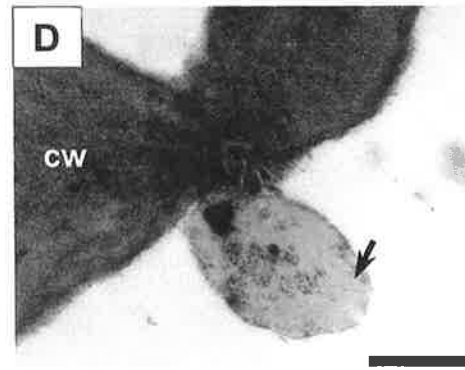
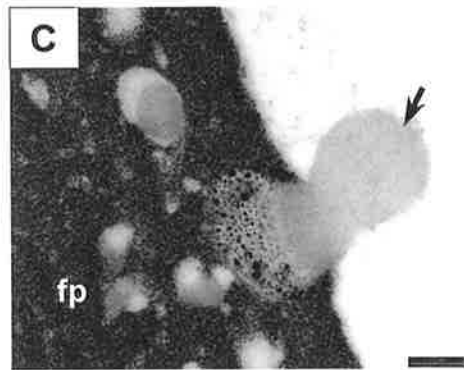
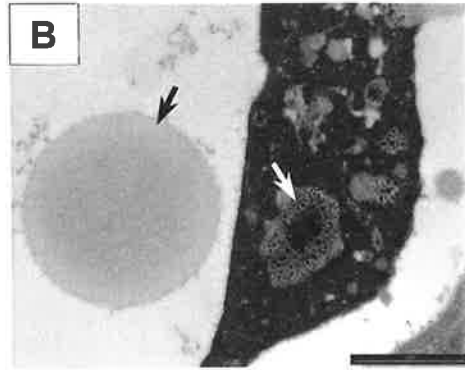
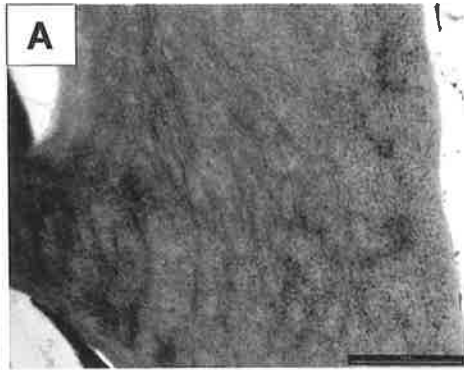
f. Penetrometer-damaged fruit, three days, medium level blemish

Three days after induction, surface symptoms in penetrometer-damaged fruit were less advanced than oil-treated fruit. In this sample, medium level rind collapse and only very slight discolouration were observed. The rind profile of penetrometer-damaged fruit showed oil-damaged cells localised to the cortex layer (Plate 6.8F). The cuticle appeared similar to that in untreated fruit. Epidermal cells

Plate 6.13

Transmission electron micrographs of rind ultrastructure in an oil-treated fruit sample, after ten days.

- A. The cuticle appeared less vesicular than earlier samples. Bar = 1 μm .
- B. Oil bodies located inside vesicles of the fused protoplast, and outside the protoplast (arrows). Bar = 1 μm .
- C. Oil (arrow) traversing vesicles and fused protoplast (fp). Bar = 0.2 μm .
- D. Oil (arrow) adjacent to cortex cell wall (cw) plasmodesma. Bar = 0.5 μm .
- E. Cell wall thickening and folding, in hypodermal cells. Bar = 1 μm .
- F. Cell wall thickening and folding, in cortex cells. Bar = 1 μm .



contained numerous vacuoles and a main vacuole, which often appeared to be compartmentalised. The plasmalemma and tonoplast were both present, but fragmented (Plate 6.14A). Similarly, the double envelope of nuclei was frequently discontinuous (Plate 6.14B). The double membrane of mitochondria appeared to be intact in some cells, while in others, small, osmiophilic bodies were associated with the mitochondria. Similar osmiophilic bodies were also present around the cell edge, between the plasmalemma and wall (Plate 6.14C). In more damaged cells, densely osmiophilic bodies were also present in the stroma of plastids, as distinct from lighter-staining plastoglobuli (Plate 6.14D). Hypodermal cells had a similar appearance to epidermal cells. Osmiophilic bodies were less evident, but again associated with mitochondria and plastids. Vesicles also appeared to be associated with some organelles. Both epidermal and hypodermal cells also showed abundant rough ER (Plate 6.14E). Cortex cells adjacent to hypodermal cells were dramatically different in ultrastructural appearance, resembling cortex cells at two days after oil treatment. All cortex cells appeared to be oil-damaged, containing a fused protoplast, and exhibiting thickened and folded cell walls (Plates 6.14F and 6.14G). The cell wall between hypodermal (intact) and cortex cells (damaged) appeared to be structurally sound, and plasmodesmata were observed between these cell layers (Plate 6.14H).

Plate 6.14

Transmission electron micrographs of rind ultrastructure in a penetrometer-damaged fruit sample, after three days.

A. Plasmalemma (arrow), intact in portions. Bar = 0.2 μm .

B. Nuclear envelope (arrows), intact in portions. Bar = 0.2 μm .

C. Osmiophilic bodies (arrows) located between the plasmalemma and cell wall (cw). Bar = 0.2 μm .

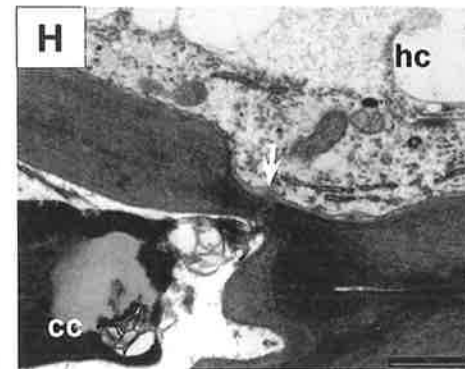
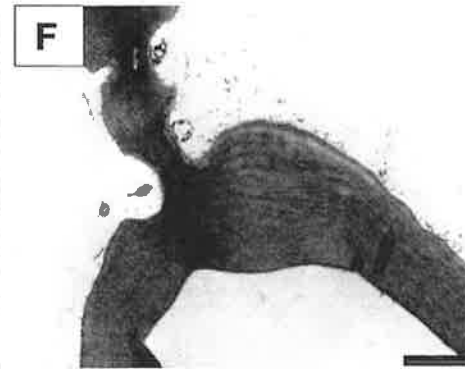
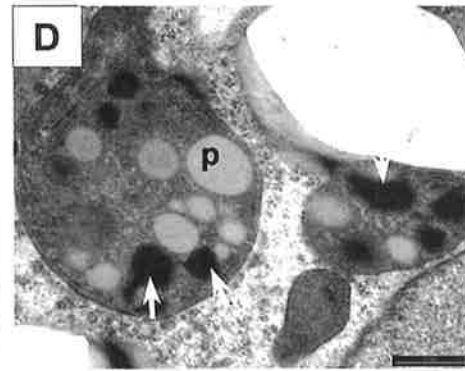
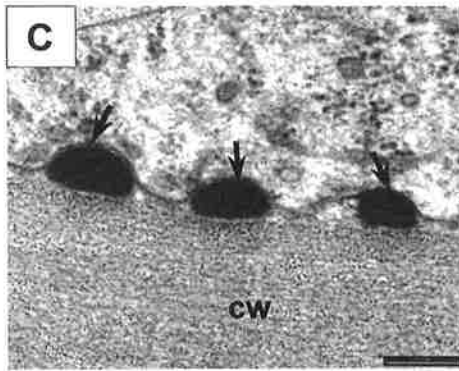
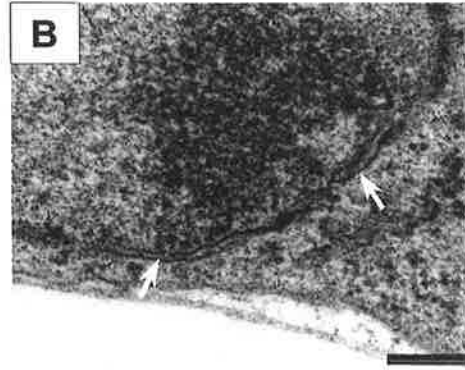
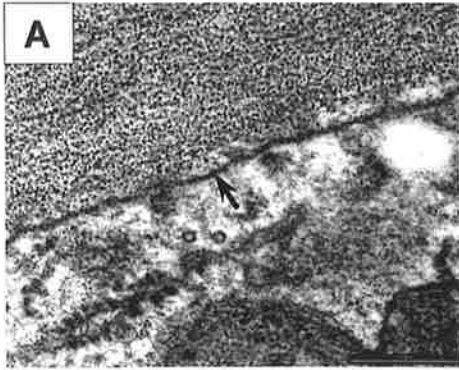
D. Osmiophilic bodies (arrows) located in the stroma of plastids, distinct from lighter-staining plastoglobuli (p). Bar = 0.5 μm .

E. Rough endoplasmic reticulum (arrows), abundant in hypodermal cells. Bar = 0.5 μm .

F. Cell wall thickening in cortex cells. Bar = 1 μm .

G. Cell wall folding in cortex cells. Bar = 1 μm .

H. A plasmodesma (arrow) located between an intact hypodermal cell (hc) and oil-damaged cortex cell (cc). Bar = 1 μm .



6.4. Discussion

6.4.1. Symptoms

In mature, coloured fruit, oleocellosis symptoms consist of both collapse and darkening of the fruit surface between the oil glands (Shomer and Erner, 1989). Symptoms have been reported to develop within a week of harvest in lime fruit (Eaks, 1955), and within two to three days in navel oranges (Wild, 1998). Observations of oleocellosis in Valencia orange and mandarin fruit have suggested that rind collapse precedes discolouration (Williams and Wild, 1996). However, until this study, oleocellosis symptom development has not been examined in detail. Measuring blemish severity using a scoring system enabled the quantitative assessment of blemish development. The timing of blemish development appeared to differ between physical and oil induced oleocellosis. Over a period of three days, penetrometer-damaged fruit primarily showed tissue collapse and only slight discolouration, compared to oil-treated fruit which showed a similar rate of collapse and discolouration. Observations suggested that physiological development may differ between mechanical and oil induced forms of oleocellosis. Microscopic examination proved this to be the case. Blemish area appeared to show a rapid increase up to 24 hours. However, area could not be accurately measured until symptoms had developed, at approximately 24 hours. Blemish area remained fairly constant after this time, suggesting rapid oil spread following induction.

Statistical analysis of the effects of time and method on blemish severity and area identified variability between trees, fruit and even different zones on the same fruit. In experiment 2, the tree effect was removed and repeat measures were made on each fruit, however variation between induction zones on the same fruit remained high. This variation may be explained by the effect of fruit orientation, which was not taken into account during sampling. Similar observations were made by Wild (1998), who showed the sun exposed face of navel orange fruit to be more sensitive to applied oil than the protected face. Future experiments should take this effect into account during experimental design.

6.4.2. Oleocellosis mechanism

The mode of oil release following gland rupture is unclear. Surface oil release has been observed (Fawcett, 1916; Cahoon *et al.*, 1964; Eaks, 1968), however, the likelihood of internal oil release has also been suggested (Shomer and Erner, 1989; Loveys *et al.*, 1998). Some doubt also exists over previous microscopy findings due to poor tissue preservation and misinterpretation of images. Using LM, epidermal rupture above glands has been observed in mechanically damaged rind tissue (Labuschagne *et al.*, 1977; du Plessis, 1978). However, tissue sections presented in these studies showed excessive damage, possibly artefactual, attributable to poor tissue preservation or sectioning damage. Improved tissue preservation was achieved in a study by Shomer and Erner (1989), who suggested that “oleocellosis-damaged cells were the result of either external or internal contamination by essential oil”. In their study, light micrographs depicted a ruptured gland, which appeared to open into the flavedo tissue above the gland. With our knowledge that all glands are attached to the fruit surface by a ‘stalk’ (see Chapter 3), it appears that misinterpretations were made, as medial sections of glands were not examined.

In the present study, fruit were mechanically damaged with a penetrometer; surface oil release was detected using multiple microscopy methods and no evidence of internal oil release was established. Confocal microscopy, while a useful tool for oil visualisation as it avoids tissue fixation (see Chapter 4), did not allow oil to be detected outside of the glands in damaged tissue. As a result, microstructural rind damage was used as the basis of our examination. Penetrometer-damaged tissue prepared for LM examination was well preserved. Tissue was serially sectioned and the medial sections of glands were examined. Gland rupture was only observed to occur at the junction of the apical region of the gland and the epidermis. These findings were supported by our prior knowledge that all glands were linked to the epidermis by a stalk (see Chapter 3). In mature fruit, the gland is positioned very close to the fruit surface, facilitating easy surface oil release. The gland stalk is not hollow and does not open to the fruit surface, which would explain the need for mechanical force to facilitate oil

release (Ting and Attaway, 1971). Serial sections of penetrometer-damaged tissue revealed no other structural disruption to the gland that may have facilitated oil release into the tissue. Internal oil release may be prevented by the layers of thickened boundary cells which enclose the gland. CryoSEM findings verified the damage observed in tissue sections, highlighting the presence of holes in the fruit epidermis at the site of gland ruptures, and pools of oil.

The proposition that surface oil is responsible for the oleocellosis blemish was supported by an additional experiment in which oil released to the fruit surface was removed immediately, with absorbent tissue, and symptoms failed to develop (data not shown). Similar results have been reported in fruit washed in water at 32°C within two minutes of oil release (Eckert and Eaks, 1989). These findings however are in direct contrast to those of Loveys *et al.* (1998). In their study, fruit were dropped onto a filter paper and liberated oil was absorbed, however some fruit were observed to develop symptoms. The most likely explanation for some fruit developing symptoms was that surface oil was not removed completely.

Microstructural rind damage was used to determine the route of oil movement following surface release. Past microscopy studies of oleocellosis have used aldehyde fixation for tissue preparation, and identified sub-surface cell deformation or flattening in physically damaged fruit (Labuschagne *et al.*, 1977; du Plessis, 1978). In the present study, similar observations were made in both physically damaged and oil-treated tissue fixed in aldehyde. In osmicated tissue, however, rind damage appeared more extensive in oil-treated fruit, with oil-damaged cells occurring in all rind layers from the epidermis downwards. Observations suggested that aldehyde fixation alone may lead to misinterpretation. Primary aldehyde fixation followed by osmium postfixation was preferred as it allowed observation of the protoplasm as well as cell walls.

Given that gland rupture results in surface oil release, it was expected that mechanically damaged fruit would show identical rind damage to surface oil-treated fruit, but this was not the case. In penetrometer-damaged fruit, only a very small proportion of samples showed cell content degeneration in all layers of the

rind, and the majority of these were collected at the edge of the penetrometer application zone, where surface oil release was observed to occur. The majority of samples showed cells with degenerated contents localised several layers below the epidermis. Closer inspection using TEM showed damage to be localised to cortex cells, whilst the cuticle, and epidermal and hypodermal cells appeared structurally intact. These findings expand on those of Shomer and Erner (1989), who reported identical rind damage from penetrometer and surface oil treatments, occurring either several layers under the epidermis or in all cell layers.

Previously, separate studies have reported surface oil release and sub-epidermal rind damage, but a link between the two phenomena had not been identified. Based on our LM and TEM observations, it appears that oil may filter into the rind tissue via the ruptured epidermis, move into the cortex layer alongside the outer gland walls, and spread laterally. This proposition is supported by the suggestion that gland boundary cell walls are less permeable to oil (Thomson *et al.*, 1976; Shomer, 1980). Oil movement in the cortex may also be aided by more numerous intercellular spaces. Oil localisation to the cortex, however, is difficult to explain. Plasmodesmatal connections were observed between intact hypodermal and oil-damaged cortex cells. Collenchymatic hypodermal cells had thicker walls than cortex cells, but did not possess suberised or lignified secondary walls which may have restricted oil movement between the two cell layers. Such depositions have been observed in the endodermis of citrus roots, separating hypodermal and cortex cells (Walker *et al.*, 1984). An alternative proposition is that surface oil enters lower rind layers through other openings in the fruit surface, such as the cracks and tears caused by mechanical damage. This would be similar to the mechanism of water spot described by Scott and Baker (1947), in which water enters the rind via stomata or microscopic cracks formed during tissue expansion.

Interestingly, sub-epidermal cell breakdown has also been associated with the citrus rind disorders 'preharvest peel pitting' (Medeira *et al.*, 1999) and 'rind-oil spot' (Chikaizumi, 2000). The rind oils were suggested as a possible cause for both disorders, but the underlying mechanisms could not be clearly established. The 'rind-oil spot' described by Chikaizumi (2000) showed similarities to oleocellosis

with respect to symptoms, ruptured glands and sub-epidermal damage, but differed in that it was consistently associated with high radiation exposure. Medeira *et al.* (1999) drew a correlation between the sub-surface damage associated with pitting and that observed in chilling injury of eggplant, which has been attributed to localised dehydration (Rhee and Iwata, 1982). In the present study, cell ultrastructural degeneration is not considered to result from dehydration, as it occurred as early as six hours following penetrometer damage, which paralleled timing in oil-treated fruit.

6.4.3. Oil effects

Prior to the examination of ultrastructural rind damage, the quality of tissue preservation was assessed in untreated tissue using TEM. Organelles appeared intact, and cell ultrastructure was similar to that of mature, deep orange coloured or 'after-ripe' navel orange fruit, described by Thomson and Platt-Aloia (1976). Plastids, in the form of chromoplasts, were identified by their abundant plastoglobuli and lack of grana (Mauseth, 1988). Nuclei were intact, with some showing slight expansion of the perinuclear space, thought to be a sign of nuclear activity, rather than degeneration (Thomson and Platt-Aloia, 1976). Intracellular oil bodies were observed in untreated tissue, located in the cytoplasm, vacuole and often observed moving between the two. Thomson and Platt-Aloia (1976) also observed lipid in the cytoplasm, generally associated with the tonoplast. Lipid associated with mitochondria and plastids was also reported at an earlier stage of ripening.

Details of oil localisation in the oleocellosis-damaged rind were provided to some extent by TEM. Following oil treatment, lipid bodies were clearly distinguished in all layers of the rind, in greater abundance than in untreated tissue. Oil appeared to move indiscriminantly through the rind tissue, with observations suggesting both apoplastic (oil within intercellular spaces) and symplastic movement (oil bodies associated with plasmodesmata). The presence of lipid bodies in intercellular spaces to a depth of approximately nine cell layers only 30 minutes after surface oil treatment also suggested rapid oil penetration into the rind. It appeared that indirect oil effects may include the restriction of gaseous

diffusion, by filling intercellular spaces and damaging stomata, potentially hastening senescence.

Oil-damaged cells appeared to undergo a loss of membrane integrity, followed by degeneration of cell contents. Ultrastructural changes were similar to those observed in oleocellosis of degreened Shamouti orange fruit (Shomer and Erner, 1989). In that study, concentration of the protoplast was observed three hours after oil treatment. Earlier signs of degeneration were detected in the present study, due to the time sequence sample collection. Degeneration of membranes was observed as early as 30 minutes after treatment. Oil bodies were also closely associated with deformed mitochondria and plastids at this time. This was not observed in untreated tissue, and may have indicated a direct targeting of organelles by the oil, not previously described. By six hours, the degeneration of membranes had induced the fusion of protoplasmic elements, although nuclei and mitochondria appeared to maintain their integrity for longer prior to protoplast collapse. In some cells, the fused protoplast at the cell centre was observed to remain attached to the cell wall and plasmodesmata by 'Hechtian strands' (Oparka *et al.*, 1994). Using confocal microscopy, the fused protoplast was observed to take up both lipid and cell wall stains. Disruption of the plasmalemma at early stages of oleocellosis development helps distinguish it from senescence processes, in which the plasmalemma remains intact until later stages to maintain homeostasis (Nooden and Leopold, 1988). The physiological development of oleocellosis may be more aptly described as necrosis, which is caused by poisons or other external factors (Nooden and Leopold, 1988).

Shomer and Erner (1989) misinterpreted the fused protoplast of oil-damaged cells to be a 'giant chloroplast', resulting from chloroplast fusion. In their study, the giant chloroplast was reported to contain more starch and denser grana than undamaged cells. In the present study, the large structures apparent in the fused protoplast did not show the refractory nature of starch bodies, and instead appeared to be vesicular. The presence of grana seems unlikely, considering that prior to damage cells contained chromoplasts, which do not contain a substantial grana system. In addition to their ultrastructural observations, Shomer and Erner

(1989) speculated that giant chloroplasts may produce larger amounts of chlorophyll than normal chloroplasts. Based on the degenerative state of cells described, the possibility of normal cellular metabolism, such as chlorophyll synthesis, is unlikely. Naturally occurring chloroplast fusion is extremely rare, but chloroplast aggregation has been correlated to reduced growth activity or cell death at low temperatures (Kimball and Salisbury, 1973).

Cell wall thickening and collapse was observed to take place in oil-damaged cells. Cell wall thickening is most likely attributable to swelling. Cell collapse, which appeared to result from folding of the cell walls, was not detected until protoplast fusion had occurred. However, the fact that parenchymatic cortex cells showed signs of collapse before the thicker-walled collenchymatic hypodermal cells, suggests that collapse resulted from loss of physical strength (Labuschagne *et al.*, 1977; du Plessis, 1978; Shomer and Erner, 1989). Rather than cell collapse, flattened cell layers have also been attributed to a change from radial to tangential division (Williams and Wild, 1996). Williams and Wild (1996) likened the process to that observed in wounding; however, inadequate evidence was provided to support their case. In the present study, TEM observations showed no evidence of dividing cells, by radial or tangential division. With respect to wounding, suberin and lignin, which are commonly formed at early stages of the wounding response (Larson, 1994), were not present in damaged tissues.

6.4.4. The link between microscopic damage and symptoms

6.4.4.1. Rind collapse

Rind collapse in oleocellosis-damaged tissue is localised between glands. This feature helps to distinguish it from disorders such as pitting (Labuschagne *et al.*, 1977; Petracek *et al.*, 1998) and chilling injury (Underhill *et al.*, 1995), which show collapsed glands. Dehydration is also known to produce collapsed glands (Williams and Wild, 1996). Rind collapse due to oleocellosis was originally attributed to the breakdown of surface cells by oil (Fawcett, 1916), but LM studies linked it to sub-surface cell collapse (du Plessis, 1978). Microscopy observations of this study support this proposition. Oil-damaged cells were localised between glands in all rind samples, which may be explained by the fact that gland boundary

cells are considered to be impermeable to oil (Thomson *et al.*, 1976; Shomer, 1980). TEM observations in the present suggested that outermost boundary cells may be penetrated by oil, but their mechanical strength prevents collapse from occurring. Walls of boundary cells are thicker than those of other gland cells, and surrounding parenchyma cells of the rind, however compositional differences are yet to be ascertained (see Chapter 3).

6.4.4.2. Rind discolouration

Past studies have attributed rind discolouration to changes in the fruit cuticle or epidermis (Labuschagne *et al.*, 1977; Sawamura *et al.*, 1984; Williams and Wild, 1996). Williams and Wild (1996) reported small necrotic spots on the surface of mandarin fruit 36 hours after oil treatment, which joined to form necrotic regions between the glands. Similar 'necrotic spots' were observed in a very small proportion of oil-treated fruit examined in the present study; however, blemish colour was observed to develop independently of these surface spots. The size and distribution of these structures on the fruit surface suggest that they were most likely oil-damaged stomata, or more specifically, necrotic guard cells. Similar spots, caused by darkening around the stomata have also been observed in citrus fruit as a result of non-phytotoxic spray oils (Veierov *et al.*, 1979).

Based on the time sequence examination of ultrastructural oleocellosis development, it seems likely that surface discolouration is a result of sub-surface damage, or more specifically, cell content degeneration and cell wall changes. No symptoms were observed in a rind sample showing early signs of degeneration and slight collapse of cortex cells. However, significant discolouration was evident in a rind sample showing cells with a fused protoplast and collapsed and thickened cell walls, in all rind layers. The much reduced rind discolouration observed in penetrometer-damaged fruit compared to oil-treated fruit may be explained by the fact that upper layers of the flavedo, the coloured portion of the rind, remained intact. Previously, similar sub-epidermal cell damage has been used to explain the chlorotic spots of peel pitting (Medeira *et al.*, 1999).

Given the rapid breakdown in cellular compartmentalisation, it is also possible that browning reactions involving enzymes such as polyphenol oxidase (PPO) and peroxidase are involved. PPO has been implicated in the tissue browning of various fruit disorders, including superficial scald in apples (Bain and Mercer, 1963) and pericarp browning in litchi (Joubert and Van Lelyveld, 1975). PPO catalyses the oxidation of phenols, which are sequestered in the vacuole (Mayer and Harel, 1979), but are released upon tonoplast breakdown, which was observed at early stages of oleocellosis development. The involvement of PPO is also supported by the fact that oleocellosis-damaged tissues have been reported to show reduced darkening under low oxygen storage conditions (Wild, 1998). The reddish colour observed in extreme oleocellosis samples is most likely due to oxidation products of pigments and other compounds. Similar reddish discolouration has been associated with zebra skin and other age-related disorders in senescent citrus fruit (Taverner *et al.*, 2001).

In immature fruit, oleocellosis-damaged tissues remain green after degreening, whilst healthy tissue colours normally (Fawcett, 1916; Cahoon *et al.*, 1964; Wardowski *et al.*, 1976; Shomer and Erner, 1989). Ultrastructural differences between oleocellosis in mature fruit and degreened fruit (Shomer and Erner, 1989) have not been established, and the explanation of 'giant chloroplasts' has been refuted in this study. Based on the evidence provided by Shomer and Erner (1989), it appears likely that damaged areas retain their green colour, due to the sub-epidermal localisation of damaged cells and the possible impairment of chloroplast differentiation in otherwise intact upper rind layers. However, another study has also demonstrated what appears to be wound periderm tissue in the immature fruit oleocellosis resulting from compression damage (Giudice and Catara, 1972). It is clear that further microscopy investigation of immature fruit oleocellosis is required.

6.5. Conclusion

This study provides a detailed time course of oleocellosis development using varied microscopy techniques. Surface oil, released following gland rupture, was confirmed to be the cause of oleocellosis. Surface oil infiltrated the rind tissue via the cuticle or the ruptured epidermis. In surface oil-treated fruit, all cell layers were damaged by the oils, whilst in mechanically damaged fruit, oil-damaged cells were localised sub-epidermally, below intact epidermal and hypodermal cell layers. Oil movement within the rind tissue and oil action upon the tissue were rapid. The oils produced tissue necrosis; damaged cells underwent cell content degeneration and collapse, but showed no signs of lignification or suberisation. Early signs of ultrastructural degeneration were detected within six hours of oil treatment. The resulting surface blemish developed substantially within three days. Rind collapse was attributed to sub-surface cell collapse, and rind darkening to the dense degenerated contents and thickened walls of these collapsed cells.

Chapter 7

General Discussion

The research presented in this thesis has contributed to an improved understanding of the physiological basis of oleocellosis. Findings have been based on a time sequence examination of oleocellosis development, combined with examinations of oil gland structure and development, and oil localisation, in healthy Washington navel orange fruit. The method of tissue preparation was found to be important in all microscopy studies, particularly for rind oil visualisation, but also for anatomical observation of the oil glands and oleocellosis-damaged rind. A range of microscopy techniques were used; the traditional techniques of light microscopy (LM) and transmission electron microscopy (TEM) were complemented by more recently developed methods such as cryofixation for scanning electron microscopy (SEM), and state-of-the-art methods such as confocal laser scanning microscopy (CLSM) and multi-photon microscopy.

7.1. Addressing limitations of current control practices

A sequence of events constituting oleocellosis development has been presented in this study. It is as follows:

1. Mechanical damage causes gland rupture.
2. Gland rupture leads to the release of oil onto the fruit surface.
3. Surface oil infiltrates the rind, causing tissue necrosis.
4. Tissue necrosis is responsible for the surface blemish.

This study was instigated as a result of concerns over the limitations of the current oleocellosis control practices, which target the identification of early stages of oleocellosis development only. The aim of current methods is to minimise gland rupture by handling fruit with care and picking fruit with low

turgor. Despite the need for careful fruit handling practices, it will always be impossible to rigidly enforce such practices at all stages of delivery between the field and the marketplace. To predict oleocellosis, fruit turgor is estimated using a combination of two measurements: pressure gradient and rind oil release pressure (RORP) (Feutrill, 1997). These tests have proved to be inconvenient and unreliable. Pressure gradient has been judged as a 'reasonable' indicator of fruit susceptibility to oleocellosis, however major delays in harvesting navel oranges have occurred when adhering to pressure gradient guidelines (Loveys *et al.*, 1998). RORP has been judged as a poor indicator of fruit susceptibility to oleocellosis (Gillespie and Tugwell, 1971; Erner, 1982; Loveys *et al.*, 1998).

Poor correlation between RORP and oleocellosis has been attributed to the fact that RORP only assesses oil glands "on the surface of the fruit" (Loveys *et al.*, 1998); however, findings from the present study question this proposition. In mature Washington navel orange fruit, all glands appeared to be positioned close to the fruit surface. In younger fruit, gland cavities were observed to occur at different depths in the rind, however, all glands were observed to join the epidermis by a 'stalk'. This attachment was later confirmed as the route of oil movement to the fruit surface.

The relationship between RORP and oleocellosis was not examined *per se* as a part of this study. Instead, RORP was applied to each fruit to achieve a standard level of damage. Oleocellosis symptoms were observed to develop in fruit with high RORP values (low turgor), close to or in excess of the 585 kPa RORP threshold used to predict oleocellosis prior to harvest. Observations suggest that oleocellosis is likely to develop as long as gland rupture and oil release occur. Hence, to avoid gland rupture completely, the RORP threshold value must be representative of the maximum impact pressure to which the fruit will be exposed. For the current RORP threshold of 585 kPa (or 3 kg) to be effective, careful fruit handling is therefore vital.

7.2. More factors influencing fruit susceptibility to oleocellosis

Limitations of using fruit turgor to determine fruit susceptibility to oleocellosis have been discussed. Previous studies have also reported oleocellosis to vary with fruit age, variety and position in the tree canopy. It is not likely that such differences are all attributable to fruit turgor. Findings from this study, combined with a detailed review of the literature, enable speculation as to which intrinsic fruit characteristics may influence fruit susceptibility to oleocellosis.

In previous studies, 'fruit susceptibility' to oleocellosis has been discussed in terms of differences in RORP values (Cahoon *et al.*, 1964) or differences in fruit response to applied oils (Wild, 1998). However, for an accurate evaluation of past findings, it is important to recognise exactly what these two parameters represent. RORP can be more accurately regarded as a measure of gland rupture susceptibility, whilst response to applied oils can be more accurately regarded as a measure of rind sensitivity to oil. These two measures take into consideration different aspects of oleocellosis development, but can provide valuable information when used together.

Gland rupture susceptibility has been reported to vary with fruit orientation and position in the tree canopy (Gillfillan, 1996; Loveys *et al.*, 1998) and fruit age (Pantastico *et al.*, 1966). The effect of fruit position and orientation has been suggested to be due to sun exposure effects (Gillfillan, 1996). The outer face of fruit, and fruit positioned on the north or west aspect of the tree are more exposed to the sun, and show higher RORP values (lower turgor). The effect of fruit age, however, is not so easily explained by turgor and is more likely attributed to structural changes in the rind tissue associated with fruit maturation. Mechanical properties of cells are determined not only by turgor pressure, but also by cell wall strength (Kays, 1991). The mechanical behaviour of tissues is determined by such factors as cell wall strength, intercellular bonding between neighbouring cells, and intercellular space between the cells (Kays, 1991).

In the present study, the examination of changes in gland size, age and numbers in developing fruit allowed a detailed correlation between fruit age and susceptibility to oleocellosis. Mature glands were present in floral ovary tissue, and increased in proportion as fruit developed, until all reached maturity in fruit size 30 to 50 mm. Mature glands are considered to contain oil, as rapid oil synthesis has been reported to take place as soon as the cavity forms (Bosabalidis and Tsekos, 1982). These findings imply that oil is present in the floral ovary, which suggests that oleocellosis has the potential to occur in all fruit from this stage of development onwards. Smaller fruit showed more densely packed glands in the rind, which suggests that more glands may be damaged upon impact. However, larger fruit had much larger glands, with gland volume increasing with fruit age, especially between fruit of 50 to 90 mm diameter. A larger gland volume implies a larger oil holding capacity. This is supported by the fact that rind oil yield has been shown to increase with the development of navel orange fruit (Scora *et al.*, 1968). A previous study has suggested that 2 μl represents eight to ten glands of oil. In this study, the mean gland volume in mature fruit was approximately 1.1 mm^3 , which suggests a much larger oil holding capacity. It has been shown that 0.01 cm^3 of oil applied to the fruit surface is sufficient to cause oleocellosis (Fawcett, 1916).

Rind sensitivity to oil has been shown to vary with fruit species (Sawamura *et al.*, 1984; Williams and Wild, 1996) and fruit orientation (Wild, 1998). Observations in the present study supported previous reports of the phytotoxicity of linalool and d-limonene (Wild and Williams, 1992), and also showed the minor oil component citral to be very damaging to the rind. Although d-limonene is the major oil component in most *Citrus* species, oil composition has been reported to vary with fruit species and variety (Scora and Torrasi, 1966; Attaway *et al.*, 1967), fruit orientation (Daito and Morinaga, 1984), and fruit age (Scora *et al.*, 1968). Oil compositional differences may help to explain rind sensitivity observations. The study by Sawamura *et al.* (1984), which investigated the response of seven fruit species to each of their rind oils, suggested that differences in response were likely attributable to differences in oil composition.

Rind sensitivity to oil may also be influenced by the epicuticular wax layer of the fruit. In their comparison of mandarin and Valencia orange fruit, Williams and Wild (1996) observed oleocellosis symptoms to be more severe and develop more rapidly in mandarin fruit, with a 'smoothed' waxy cuticle, compared to Valencia orange fruit with a 'more structured' cuticle. Based on the understanding of oleocellosis development gained from the present study, it is possible that a thickened cuticle may inhibit surface oil movement into the rind, and as a result reduce oleocellosis damage. Epicuticular wax thickness may also influence oleocellosis through its ability to impart protection against mechanical damage (El-Otmani and Coggins Jr., 1985b). Wax content, composition and morphology have been shown to change with fruit maturation (El-Otmani and Coggins Jr., 1985a; Sala, 2000). However, it has been suggested that shading of the fruit delays these changes (El-Otmani *et al.*, 1989). This may help to explain differences in rind sensitivity due to fruit orientation or position in the canopy.

With an improved knowledge of fruit characteristics that influence susceptibility to oleocellosis, there is potential to manipulate these characteristics to make fruit less susceptible. It may be possible to achieve this by the application of specific preharvest fruit treatments, or in time, by conventional breeding or molecular approaches. Such strategies would augment current preventative measures, which address fruit turgor only. Preliminary reports have suggested that preharvest gibberellic acid (GA) application may be effective in reducing oleocellosis occurrence (Loveys *et al.*, 1998). GA application is known to delay fruit senescence, and has been reported to reduce the occurrence of various senescence-related disorders such as albedo breakdown, puffing, water spot and rind staining, and also mould wastage. These observations are likely to be explained by the fact that the application of GA reduces rind softening (Coggins Jr. and Lewis, 1965), subsequently making the rind more resistant to puncture (Bevington, 1973). However, it is important to note that GA application also delays changes in rind oil composition (Scora *et al.*, 1968; Fuh, 1988) and epicuticular wax (El-Otmani and Coggins Jr., 1986; Zaragoza *et al.*, 1996) associated with fruit maturation. Studies into GA highlight the fact that fruit

treatments frequently produce a multi-faceted physiological response. Future studies into potential treatments for oleocellosis control need to assess treatment effects in terms of overall fruit quality.

7.3. Developing new strategies for oleocellosis control

The ability to avoid gland rupture remains the best prevention method for oleocellosis. Findings from this study suggest that control strategies may however be implemented at later stages of the disorder's development. Given that gland rupture causes surface oil release, removing oil from the fruit surface may prevent oleocellosis from developing. In lemon fruit, Fawcett (1916) showed that oil acting on the fruit surface for as little as eight seconds showed a "slight effect" within 24 hours. In their review of postharvest citrus disorders, Eckert and Eaks (1989) suggested that oleocellosis could be avoided by washing fruit in water at 32°C within two minutes of oil release. The proposition of washing fruit to remove oil contradicts current recommendations that fruit must not be picked or handled when wet. However, it is interesting to note recent observations by Israeli citrus growers, which suggest that oleocellosis incidence is reduced when fruit are picked in the rain, and handled carefully (Yair Erner, Senior Researcher, The Volcani Center, Israel; Pers. Comm., 2000). Since careful handling of fruit during picking has been aided by the use of cotton gloves, the ability of such gloves to absorb released oils may also be worth investigating. Further research is required to test the optimal methods for removing oil, and the timing of oil removal to avoid oleocellosis blemish development.

If not removed, surface oil infiltrates the rind. Ultrastructural examination of oil-treated fruit showed the epicuticular wax layer of the fruit to be no barrier to surface oil penetration. The ability to reduce oil entry into the rind is theoretically possible by application of a protective coating to the fruit prior to harvest. Previously, application of commercially available citrus waxes Briteseal and Zivdar has been shown to give some protection against surface applied oil (Wild, 1998). In contemplating the properties required for a substance to act as a barrier to oil, the mechanism by which the oil glands naturally sequester the oils from the

rest of the plant body may give some clues. Observations suggest that this mechanism is not facilitated by the presence of specialised cell walls. Histochemical tests were carried out to detect lignin and suberin, but neither were found to be present in the cavity walls enclosing the oil reservoir, or in any other cells of the oil gland for that matter. Future research into the formulation of fruit surface coatings and their effectiveness in reducing oleocellosis may be worthwhile, although it should be recognised that such a treatment may be less successful in mechanically damaged fruit compared to fruit exposed to surface oil. Observations of mechanically damaged tissue suggest that oil may not enter the rind directly via the cuticle and epidermis, but may infiltrate the tissue at the site of damage, the ruptured epidermis. The potential detrimental effects of fruit coatings also need to be considered; for example, fruit waxing is known to inhibit gaseous exchange, and has been linked to another rind disorder, postharvest pitting (Petracek *et al.*, 1998).

Once in the rind, the phytotoxic oils were observed to cause rapid and devastating damage. Previous studies suggest that little can be done to retard the reaction between the oils and the rind tissue. The 'inactivation' of rind oils has been shown to be largely unsuccessful, and also inapplicable to the commercial situation (Wild, 1998). Of the various compounds tested, including sodium hydroxide, chlorine dip, ethanol, and dilute hydrochloric acid, Wild (1998) found that only one treatment, a mixture of KOH and ethanol, reduced the ability of oil to produce oleocellosis symptoms. The same study also showed that low temperature and low oxygen storage, both unachievable in a commercial situation, provided only a transient inhibition of blemish development (Wild, 1998).

Knowledge of the effect of low oxygen on oleocellosis, combined with ultrastructural observations in this study, suggest the involvement of polyphenol oxidase (PPO). PPO catalyses the oxidation of phenols, located in the cell vacuole, and it has been implicated in the tissue browning associated with various fruit disorders. Enzymology work is required to confirm the assumption; with this information, the prevention of tissue browning by enzyme inhibition may be

possible in the future. Such a treatment would be more effective and commercially practical in controlling oleocellosis than the manipulation of fruit storage conditions. Inhibition of PPO activity has already been demonstrated in litchi pericarp, with sulphur dioxide fumigation and dilute hydrochloric acid dipping (Zauberman *et al.*, 1991). Similar inhibition mechanisms may occur naturally. Ascorbic acid, a naturally occurring anti-oxidant, has been suggested to inhibit tissue browning by reducing phenolic substances (Joubert and Van Lelyveld, 1975). As an alternative to the inhibition of tissue browning, studies have also shown that perception of the oleocellosis blemish may be manipulated. For example, the severity of 'green spotting' associated with immature fruit oleocellosis can be avoided by artificial rind colouration with preharvest ethylene (Levy *et al.*, 1979; Erner, 1982).

7.4. Oleocellosis diagnosis

The effective and dependable control of oleocellosis relies upon accurate diagnosis. On the basis of symptoms, in particular tissue browning, oleocellosis in mature fruit may be difficult to distinguish from many other prevalent rind disorders such as rind staining, pitting and chilling injury. As stated by Grierson (1986); "the association of particular symptoms with a variety of causes will continue to complicate diagnosis of the physiological disorders of citrus". Since this time, the increased application of microscopy to studies of rind disorders has aided the characterisation of disorders such as pitting (Petracek *et al.*, 1998; Medeira *et al.*, 1999) and chilling injury (Underhill *et al.*, 1995). Previous studies have predominantly used LM and TEM, and have based their findings largely upon the timing and localisation of structural damage to the rind. Oleocellosis shows similarities to previous descriptions of rind-oil spot (Chikaizumi, 2000) and preharvest pitting (Medeira *et al.*, 1999). Studies have also suggested that rind breakdown (Klotz and Fawcett, 1935), chilling injury (Underhill *et al.*, 1995), rind-oil spot (Chikaizumi, 2000) and preharvest pitting (Medeira *et al.*, 1999) may all be caused to some extent by the release of rind oils from the oil glands.

Differentiation between disorders is also hampered by the fact that terminology used to describe rind disorders is not uniform. Currently, terminology appears to be based upon a number of parameters, including the type of rind damage (pitting, breakdown), symptom form (zebra-skin, stem-end breakdown) or symptom cause (chilling injury, brush burn). The term 'oleocellosis' can literally be translated as "oil cell disease", but it appears that this description may be apt in referring to a number of rind disorders. Improved methods of characterisation are required to find the link between blemish symptoms and their cause. The approach taken and the range of microscopy techniques used to investigate oleocellosis in this study will provide a useful foundation for future studies in this field.

7.5. Summary

- A more complete picture of the sequence of events comprising oleocellosis development has been presented. The ability to avoid gland rupture remains the most reliable method for preventing oleocellosis, however, observations suggest that oleocellosis can be prevented as long as oil is removed from the fruit surface following injury.
- Our understanding of fruit susceptibility to oleocellosis has been improved. In future, the manipulation of fruit characteristics, such as rind structure, oil composition and epicuticular wax attributes, may enable growers to develop fruit less prone to oleocellosis.
- Evidence suggests that the microscopy methods used in this study will prove valuable for future investigations into the cause and control of this and other problematic rind disorders of citrus fruit.

Appendix 1: Video Pro programs

Setup program

```
program control open
program control enable      ' Set up the data
program control             "Wait.."
data close                  ' Close any open data files
program control             "Enter a new data file name."
data column clear
data column 1 identifier
data column 2 code
data column 3 area          ' Area of gland
data column 4 length        ' Length of gland
data column 5 breadth        ' Width of gland
program control disable
program control             "Enter a new data file name."
data units microns          ' Calibration units
data scale 1.0              ' Scale in the X direction
data aspect 1.0             ' Scale in the Y direction
data new
data column * record
program control enable
data code 0                  ' Begin coding the data at 0
program run tkmeas
end tkdata
```

Measurement program

```
program control disable
program control          "Select an image to analyse
image read
program control          "Wait..."
program control          "Enter the specimen ID
data identifier          ' imagename
data code
program control enable
edit draw cover
edit draw size 8        ' Larger pen in case the edges are drawn in
program control          "Loop around the entire gland
edit line
program control          "Wait..."
binary hole fill
binary erode
binary clean
binary dilate
data column * protect
data column 3 record    ' and record measurements of the gland features
data column 4 record    ' in columns 3, 4 and 5
data column 5 record
measure field           ' Measure gland area, length and width
data code increment 1   ' Assigns new number to gland in next measurement
program control disable
program control          "Answer the query.."
program query           "Open a new file?" ' run orangedata program or
program control enable
program control          "Click Run to continue or Quit to finish."
program pause
program run tkmeas
end tkmeas
```

Appendix 2: Publications

- Knight, T.G., Klieber, A. and Sedgley, M. (2001). The relationship between oil gland and fruit development in Washington navel orange (*Citrus sinensis* L. Osbeck). *Annals of Botany* 88: 1039-1047.

Submitted to *Annals of Botany*:

- Knight, T.G., Klieber, A. and Sedgley, M. Structural basis of the rind disorder oleocellosis in Washington navel orange (*Citrus sinensis* L. Osbeck).

In preparation for *International Journal of Plant Sciences*:

- Knight, T.G., Klieber, A. and Sedgley, M. Visualisation of citrus rind oils using light, electron and fluorescence microscopy techniques.

Knight, T. G., Klieber, A. & Sedgley, M. (2001). The relationship between oil gland and fruit development in Washington navel orange (*Citrus sinensis* L. Osbeck). *Annals of Botany*, 88(6), 1039-1047.

NOTE:

This publication is included in the print copy of the thesis held in the University of Adelaide Library.

It is also available online to authorised users at:

<http://dx.doi.org/10.1006/anbo.2001.1546>

Knight, T., Sedgley, M. & Klieber, A. (1999, March). The development of secretory cavities in the fruit of *Citrus sinensis* cv. Washington navel. In *Sixth International Botanical Microscopy Meeting*. Meeting conducted at the University of St Andrews, Scotland.

NOTE:

This publication is included in the print copy
of the thesis held in the University of Adelaide Library.

**International Society of Citriculture Congress 2000, 3-7 December 2000,
Orlando, Florida**

Featured Poster Award, Postharvest section.

Poster abstract:

Oleocellosis of Navel oranges under the microscope

T. Knight*, A. Klieber and M. Sedgley

* presenter

The citrus rind disorder oleocellosis appears as an unattractive surface blemish characterised by tissue collapse and discolouration. It is caused by the phytotoxicity of the essential oil released from the ruptured glands in the rind. Oleocellosis is responsible for major fresh fruit losses, and affects many *Citrus* species, but Navel oranges are particularly sensitive.

Current oleocellosis control strategies focus on minimising gland rupture. Methods of reducing physical damage to the fruit have been implemented throughout the handling chain, from field to market. Turgid fruit are considered to be prone to gland rupture. Harvest guidelines based on fruit turgor and field conditions affecting it have been developed, but these are often unreliable and impractical. Despite rind oils being the causal agent of oleocellosis, there are conflicting reports on the mechanism of oil release from the glands and our understanding of the nature of oil action on fruit rind tissues is limited.

This review will explore the physiological basis of oleocellosis in the fruit of the Washington Navel orange, by observations of symptom development and microscopic examination of oleocellosis-damaged tissues using various forms of microscopy.

**International Society of Citriculture Congress 2000, 3-7 December 2000,
Orlando, Florida**

Paper abstract:

The Involvement of the Oil Gland in Pathogen Resistance of Citrus Fruit

A. Klieber*, T. Knight and S. Ben-Yehoshua⁺

⁺The Volcani Centre, PO Box 6, Bet-Dagan 50250, Israel

* presenter

Citrus fruit have a unique skin that contains many oil glands. These glands and the oil contained within them plays an important role in defending fruit against pathogenic and pest attack. The oils also contribute to the natural aroma of citrus fruit and are indeed often recovered as perfume agents and aroma compounds for food and industrial applications. From a postharvest and distribution perspective the antifungal properties of the oil gland are of utmost importance. Knowledge and management of the fruit's own defence mechanism allows reduced use of synthetic fungicides which the consumer increasingly shuns and which the fungi are gradually becoming resistant to. It also allows the exploitation of natural mechanisms to minimise losses from spoilage. Natural mechanisms in themselves do not mean increased safety of consumers; however, a range of citrus oils including citral are considered to be GRAS compounds and are already widely used.

This review will explore oil gland formation and development as the citrus fruit develops, oil localisation, content and composition in the fruit, effect of oils on fungi, fungal invasion pathways of the citrus rind, and potential strategies to use oils as an antifungal mechanism in the postharvest phase.

Knight, T., Klieber, A. & Sedgley, M. (2001, September). Olecellosis of Navel oranges under the microscope. In *The Australasian Postharvest Conference (Poster Abstract)*. Conference conducted in Adelaide, South Australia.

NOTE:

This publication is included in the print copy
of the thesis held in the University of Adelaide Library.

**17th Australian Conference on Electron Microscopy, 4-8 February 2002,
Adelaide, South Australia**

In preparation. Poster abstract:

Application of microscopy tools to the examination of citrus rind blemish

T. Knight*, A. Klieber and M. Sedgley

* presenter

Oleocellosis is a physiological rind disorder of citrus fruit, which produces an unattractive surface blemish. Oleocellosis is caused by phytotoxic oils, released from oil glands located in the rind following mechanical damage. To improve our understanding of oleocellosis physiology, healthy and oleocellosis-damaged rind tissue collected from navel orange fruit have been examined using a range of microscopy techniques, including light, electron and confocal microscopy.

On the basis of light microscopy observations, the anatomy of the oil gland was found to be similar to that previously described for *Citrus*. Glands were composed of a central oil-accumulating cavity surrounded by a sheath of epithelial cells. Of particular interest was the attachment of all glands to the fruit epidermis, by a structure which has been termed the gland 'stalk'.

Conventional tissue fixation methods used to preserve rind structure were found to be limiting in their ability to retain the oil within the glands. As a result, various microscopy techniques were tested, with the aim of visualising the rind oils. Chemically fixed, cryofixed and fresh tissue samples were examined. Of the methods tested, cryofixation combined with scanning electron microscope observation and confocal microscopy were found to be promising techniques.

Microscopy techniques developed in previous studies were applied to the examination of oleocellosis. Oleocellosis development at the cellular level was examined over a time course of 0 to 3 days. Electron microscopy was a valuable tool in our assessment. CryoSEM was used to examine the damaged fruit surface, and showed the presence of oil pools, released from ruptured oil glands. Over subsequent days, TEM observation of cell ultrastructure allowed the assessment of early developmental stages of the disorder. In addition, TEM images were merged to create rind 'profile' images, which provided a broader picture of rind damage progression.

Appendix 4: Industry communication

Industry publications

- New work to solve citrus rind disorder. The Grower, July 1998, p. 25-26.

Citrus Board of South Australia annual review meetings

- September 1998
- July 2000
- July 2001

Regional 'Cittgroup' meetings

- April 1997
 - Waikerie and Berri, SA.
 - Mildura, Vic.
 - Griffith, NSW.
- November 2000
 - Berri and Loxton, SA.

Bibliography

- Abeles, F.B. (1973). Ethylene in Plant Biology. Academic Press, New York.
- Albrigo, L.G. (1978). Occurrence and identification of preharvest fruit blemishes in Florida citrus orchards. *Proceedings of the Florida State Horticultural Society* **91**: 78-81.
- Artés, F., Escriche, A.J. and Marín, J.G. (1993). Treating 'Primofori' Lemons in Cold Storage with Intermittent Warming and Carbon Dioxide. *HortScience* **28**: 819-821.
- Attaway, J.A., Pieringer, A.P. and Barabas, L.J. (1967). The origin of citrus flavor components - III. *Phytochemistry* **6**: 25-32.
- Bain, J.M. (1958). Morphological, anatomical and physiological changes in the developing fruit of the Valencia orange *Citrus sinensis* (L.) Osbeck. *Australian Journal of Botany* **6**: 1-24.
- Bain, J.M. and Mercer, F.J. (1963). The submicroscopic cytology of superficial scald, a physiological disease of apples. *Australian Journal of Biological Science* **16**: 442-449.
- Bakker, M.E. and Gerritsen, A.F. (1990). Ultrastructure and Development of Oil Idioblasts in *Annona muricata* L. *Annals of Botany* **66**: 673-686.
- Bartholomew, E.T. and Reed, H.S. (1943). General morphology, histology and physiology. In: The Citrus Industry. Volume I. History, Botany and Breeding, Vol. 1 (Eds. H.J. Webber and L.D. Batchelor) University of California Press, Los Angeles. pp. 669-717.
- Ben-Yehoshua, S., Rodov, V., Kim, J.J. and Carmeli, S. (1992). Preformed and induced antifungal materials of citrus fruit in relation to the enhancement of decay resistance by heat and ultraviolet light. *Journal of Agricultural and Food Chemistry* **40**: 1217-1221.
- Bevington, K. (1973). Effect of gibberellic acid on rind quality and storage of coastal navel oranges. *Australian Journal of Experimental Agriculture and Animal Husbandry* **13**: 196-199.
- Biermann, M. (1896). Beiträge zur Kenntnis der Entwicklungsgeschichte der Früchte von *Citrus vulgaris* Risso und anderer Citrusarten. J.C.C. Bruns, Berne, Switzerland.

- Bosabalidis, A. and Tsekos, I. (1982a). Ultrastructural studies on the secretory cavities of *Citrus deliciosa* Ten. I. Early stages of the gland cells differentiation. *Protoplasma* **112**: 55-62.
- Bosabalidis, A. and Tsekos, I. (1982b). Ultrastructural studies on the secretory cavities of *Citrus deliciosa* Ten. II. Development of the essential oil-accumulating central space of the gland and process of active secretion. *Protoplasma* **112**: 63-70.
- Bouma, D. (1959). The development of the fruit of the Washington Navel orange. *Australian Journal of Agricultural Research* **10**: 804-817.
- Brodrick, H.T. (1970). Investigations into blemishes on Citrus Fruits - Part III. The development of early and late injuries in relation to rind oils. *South African Citrus Journal* **441**: 19-26.
- Bronner, R. (1975). Simultaneous demonstration of lipids and starch in plant tissues. *Stain Technology* **50**: 1-4.
- Brundrett, M.C., Kendrick, B. and Peterson, C.A. (1991). Efficient Lipid Staining in Plant Material with Sudan Red 7B or Fluoral Yellow 088 in Polyethylene Glycol-Glycerol. *Biotechnic & Histochemistry* **66**: 111-116.
- Cahoon, G.A., Grover, B.L. and Eaks, I.L. (1964). Cause and Control of Oleocellosis on Lemons. *Proceedings of the American Society for Horticultural Science* **84**: 188-198.
- Calero, F.A., Guillén, M.C. and Escriche, A. (1981). Physiological disorders in the storage of lemon fruits. In: Proceedings of IV International Citrus Congress, Tokyo, Japan, Vol. 2 (Ed. K. Matsumoto) International Society of Citriculture. pp. 768-772.
- Carr, D.J. and Carr, S.G.M. (1970). Oil glands and ducts in *Eucalyptus* L'Herit. II. Development and structure of oil glands in the embryo. *Australian Journal of Botany* **18**: 191-212.
- Casas, A. and Rodrigo, M.I. (1981). Changes in the Limonin Monolactone Content During Development of Washington Navel Oranges. *Journal of the Science of Food and Agriculture* **32**: 252-256.
- Casselmann, B.W.G. (1959). Histochemical technique. Wiley, London.
- Chandler, B.V., Nicol, K.J. and von Biedermann, C. (1976). Factors Controlling the Accumulation of Limonin and Soluble Constituents Within Orange Fruits. *Journal of the Science of Food and Agriculture* **27**: 866-876.

- Chikaizumi, S. (2000). Mechanisms of Rind-Oil Spot Development in 'Encore' (*Citrus nobilis* Lour. X *C. deliciosa* Ten.) Fruit. *Journal of the Japanese Society for Horticultural Science* **69**: 149-155.
- Christ, A. (1967). The rind-tester, a new device to measure the pressure which is required to break the oil cells of citrus rind. *South African Journal of Agricultural Science* **10**: 741-746.
- Coggins Jr., C.W. and Lewis, L.N. (1965). Some Physical Properties of the Navel Orange Rind as Related to Ripening and to Gibberellic Acid Treatments. *American Society of Horticultural Science* **86**: 272-279.
- Daito, H. and Morinaga, K. (1984). Changes in the Volatile Flavor Components of Satsuma Mandarin Fruit during Maturation. *Journal of the Japanese Society for Horticultural Science* **53**: 141-149.
- Davies, F.S. and Albrigo, L.G. (1994). Citrus. CAB International, Wallingford.
- Don-Pedro, K.N. (1996). Fumigant Toxicity of Citruspeel Oils against Adult and Immature Stages of Storage Insect Pests. *Pesticide Science* **47**: 213-223.
- du Plessis, S.F. (1978). Skilprobleme by sitrus: oleoselloseen Gepokte skil. *The Citrus and Sub-tropical Fruit Journal* **534**: 12-16.
- Dykstra, M.J. (1992). Biological Electron Microscopy. Theory, Techniques and Troubleshooting. Plenum Press, New York.
- Eaks, I.L. (1955). The Physiological Breakdown of the Rind of Lime Fruits After Harvest. *Proceedings of the American Society for Horticultural Science* **66**: 141-145.
- Eaks, I.L. (1964). The effect of harvesting and packing house procedures on rind staining of central Californian 'Washington' navel oranges. *Proceedings of the American Society for Horticultural Science* **85**: 245-256.
- Eaks, I.L. (1968). Rind disorders of oranges and lemons in California. In: Proceedings of First International Citrus Symposium, Riverside, USA, Vol. 3 (Ed. H.D. Chapman) University of California. pp. 1343-1354.
- Eckert, J.W. and Eaks, I.L. (1989). Postharvest Disorders and Diseases of Citrus Fruits. In: The Citrus Industry. Volume V. Crop Protection, Postharvest Technology, and Early History of Citrus Research in California, Vol. 5 (Eds. W. Reuther, E.C. Calavan and G.E. Carman) The Regents of the University of California, Riverside. pp. 179-260.
- Edwards, M., Predebon, S., Dale, M. and Buchanan, G. (1994). The effect of cold disinfestation treatment on the quality of Washington Navel oranges in Sunraysia. *Australian Journal of Experimental Agriculture* **34**: 515-519.

- El-Otmami, M., Arpaia, M., Coggins Jr., C.W., Pehrson Jr., J.E. and O'Connell, N.V. (1989). Developmental Changes in 'Valencia' Orange Fruit Epicuticular Wax in Relation to Fruit Position on the Tree. *Scientia Horticulturae* 41: 69-81.
- El-Otmami, M. and Coggins Jr., C.W. (1985a). Fruit Age and Growth Regulator Effects on the Quantity and Structure of the Epicuticular Wax of 'Washington' Navel Orange Fruit. *Journal of the American Society for Horticultural Science* 110: 371-378.
- El-Otmami, M. and Coggins Jr., C.W. (1985b). Fruit Development and Growth Regulator Effects on Normal Alkanes of 'Washington' Navel Orange Fruit Epicuticular Wax. *Journal of Agricultural and Food Chemistry* 33: 656-663.
- El-Otmami, M. and Coggins Jr., C.W. (1986). Fruit Age and Gibberellic Acid Effect on Epicuticular Wax Accumulation, Respiration, and Internal Atmosphere of Navel Orange Fruit. *Journal of the American Society for Horticultural Science* 111: 228-232.
- El-Zeftawi, B.M. (1977). Factors affecting pigment levels during re-greening of Valencia orange. *Journal of Horticultural Science* 52: 127-134.
- Erner, Y. (1982). Reduction of oleocellosis damage in Shamouti orange peel with ethephon preharvest spray. *Journal of Horticultural Science* 57: 129-133.
- Fahn, A. (1979). *Secretory Tissues in Plants*, 1st ed. Academic Press, London.
- Fahn, A. (1990). *Plant Anatomy*, 4th ed. Pergamon Press, Oxford.
- Fawcett, H.S. (1916). A spotting of citrus fruits due to the action of oil liberated from the rind. California Agricultural Experiment Station Bulletin 266. pp. 259-270.
- Feder, N. and O'Brien, T.P. (1968). Plant microtechnique: some principles and new methods. *American Journal of Botany* 55: 123-142.
- Feutrill, C. (1997). National Citigroups Column. Australian Citrus News, June 1997, p. 7.
- Ford, E.S. (1942). Anatomy and histology of the Eureka lemon. *Botanical Gazette* 104: 288-305.
- Fuh, B.-S. (1988). Changes in the Lipid Composition in the Flavedo Tissues of Naruto (*Citrus medioglobosa*) during Storage, and the Effects of Growth Regulators and Storage Temperature. *Journal of the Japanese Society for Horticultural Science* 57: 529-537.

- Gillespie, K. and Tugwell, B.L. (1971). Predicting the development of oleocellosis by measuring the Rind Oil Rupture Pressure of citrus prior to harvest. Department of Agriculture, South Australia, Fruit Packaging Storage and Transport Report 6/71.
- Gillfillan, I. (1996). Studies on Reducing Oleocellosis Damage in the Palmer Navel Orange (*Citrus sinensis* [L.] Osbeck) During Harvest. In: Proceedings of VIII International Citrus Congress, Sun City, South Africa, Vol. 2 (Eds. B. Manicom, J. Robinson, S.F. du Plessis, P. Joubert, J.L. van Zyl and S. du Preez) International Society of Citriculture. pp. 1007-1012.
- Giudice, V.L. and Catara, A. (1972). Oleocellosi da contatto in frutti di agrumi. *Annali dell'Istituto Sperimentale per l'Agrumicoltura* 5: 339-343.
- Golding, J., Sarafis, V., McGlasson, B., Nailon, J. and Cribb, B. (1995). Ultrastructural cytology of superficial scald in Granny Smith apples. In: Proceedings of Australasian Postharvest Horticulture Conference, Melbourne, Australia (Eds. C. Frisina, K. Mason and J. Faragher) Institute for Horticultural Development, Department of Natural Resources and Environment. pp. 17-21.
- Grierson, W. (1958). Indicator Papers for Detecting Damage to Citrus Fruit. Agriculture Experiment Station, University of Florida, Report S-102.
- Grierson, W. (1981). Physiological disorders of citrus fruits. In: Proceedings of 1981 International Citrus Congress, Tokyo, Japan, Vol. 2 (Ed. K. Matsumoto) International Society of Citriculture. pp. 764-767.
- Grierson, W. (1986). Physiological Disorders. In: Fresh Citrus Fruits (Eds. W.F. Wardowski, S. Nagy and W. Grierson) Van Nostrand Reinhold Company, New York. pp. 361-378.
- Gurr, E. (1960). Encyclopedia of microscopic stains. Leonard Hill Books Ltd., London.
- Hasegawa, Y. and Iba, Y. (1981). Kohansho: A physiological disorder of the rind of citrus fruits during storage in Japan. In: Proceedings of IV International Citrus Congress, Tokyo, Japan, Vol. 2 (Ed. K. Matsumoto) International Society of Citriculture. pp. 774-776.
- Hasegawa, Y. and Yano, M. (1992). Kohansho (a physiological disorder of the rind) on the 'Kiyomi' tangor. In: Proceedings of VII International Citrus Congress, Acireale, Italy, Vol. 3 (Eds. E. Tribulato, A. Gentile and G. Reforgiato) International Society of Citriculture. pp. 1117-1120.
- Hayat, M.A. (1989). Principles and Techniques of Electron Microscopy, 3rd ed. CRC Press, Hong Kong.

- Heinrich, G. (1966). Licht- und elektronenmikroskopische Untersuchungen zur Genese der Exkrete in den lysigen Exkretäumen von *Citrus medica*. *Flora* **156**: 451-456.
- Heinrich, G. (1969). Elektronenmikroskopische Beobachtungen zur Entstehungsweise der Exkretbehälter von *Ruta graveolens*, *Citrus limon* and *Poncirus trifoliata*. *Österreichische Botanische Zeitschrift* **117**: 397-403.
- Hodgson, R.W. (1967). Horticultural Varieties of Citrus. In: The Citrus Industry. Volume I. History, World Distribution, Botany and Varieties, Vol. 1 (Eds. W. Reuther, H.J. Webber and L.D. Batchelor) University of California, Division of Agricultural Sciences, Riverside. pp. 431-591.
- Holtzhausen, L.C. (1969). Observations on the developing fruit of *Citrus sinensis* cultivar Washington Naval from anthesis to ripeness. Department of Agricultural Technical Services, Pretoria. Technical Communication No. 91.
- Hughes, J. and McCully, M.E. (1975). The use of an optical brightener in the study of plant structure. *Stain Technology* **50**: 319-321.
- Jensen, W.A. (1962). Botanical histochemistry. W.H. Freeman and Co., San Francisco.
- Joubert, A.J. and Van Lelyveld, L.J. (1975). An investigation of pre-harvest browning of litchi peel. *Phytophylactica* **7**: 9-14.
- Kaesler, W., Koyro, H.-W. and Moor, H. (1989). Cryofixation of plant tissues without pretreatment. *Journal of Microscopy* **154**: 279-288.
- Kanlayanarat, S., Oogaki, C. and Gemma, H. (1988a). Biochemical and Physiological Characteristics as Related to the Occurrence of Rind Oil Spot in *Citrus hassaku*. *Journal of the Japanese Society for Horticultural Science* **57**: 521-528.
- Kanlayanarat, S., Oogaki, C. and Gemma, H. (1988b). Occurrence of Rind-Oil Spot of Hassaku (*Citrus hassaku* Hort. ex Tanaka) Fruits Stored under Different Temperatures and Relative Humidities. *Journal of the Japanese Society for Horticultural Science* **57**: 513-520.
- Kays, S.J. (1991). Postharvest Physiology of Perishable Plant Products (Ed. S.J. Kays) Van Nostrand Reinhold Company Inc., New York.
- Kesterson, J.W. and Hendrickson, R. (1962). The composition of valencia orange oil as related to fruit maturity. *American Perfumer and Cosmetics* **77**: 21-24.
- Kimball, S.L. and Salisbury, F.B. (1973). Ultrastructural changes of plants exposed to low temperatures. *American Journal of Botany* **60**: 1028-1033.

- Klotz, L.J. and Fawcett, H.S. (1935). Rind Breakdown of Navel Orange. *Californian Citrography* **20**: 124.
- Kurosaki, T. and Kawakami, I.K. (1974). Histochemical and Biochemical Studies on Satsuma Mandarins I. Seasonal Fluctuations in the Distribution and Concentration of Ascorbic Acid within Pulp and Peel Tissues during Growth of Satsuma Mandarin Fruit. *Journal of the Japanese Society for Horticultural Science* **43**: 189-193.
- Labuschagne, J.L., Holtzhausen, L.C. and du Plessis, S.F. (1977). 'N Anatomiese ondersoek na die voorkoms van oleocellosis en gepokte skil by *Citrus sinensis* (L.) Osbeck. *The Citrus and Sub-tropical Fruit Journal* **527**: 7-14.
- Larson, P.R. (1994). *The Vascular Cambium: Development and Structure*, 1st ed. (Ed. P.R. Larson) Springer-Verlag, Berlin.
- Levy, Y., Greenberg, J. and Ben-Anat, S. (1979). Effect of Ethylene-Releasing Compounds on Oleocellosis in 'Washington' Navel Oranges. *Scientia Horticulturae* **11**: 61-68.
- Lewinsohn, E., Dudai, N., Tadmor, Y., Katzir, I., Ravid, U., Putievsky, E. and Joel, D.M. (1998). Histochemical Localization of Citral Accumulation in Lemongrass Leaves (*Cymbopogon citratus* (DC.) Stapf., Poaceae). *Annals of Botany* **81**: 35-39.
- Loveys, B., Tugwell, B.L., Bevington, K. and Wild, B.L. (1998). *New Approaches to Combating Oleocellosis*. Horticultural Research and Development Corporation (HRDC) Final Report, Project CT 403.
- Magness, J.R. and Taylor, G.F. (1925). An improved type of pressure tester for the determination of fruit maturity. USDA Circular 350. p. 8.
- Manago, M. (1988). Studies on 'Kohansho': a physiological disorder of fruit rind in Hassaku (*Citrus hassaku* Hort. ex Tanaka). *Journal of the Japanese Society for Horticultural Science* **57**: 295-303.
- Mauseth, J.D. (1988). *Plant Anatomy*, 1st ed. Benjamin/Cummings Pub. Co., California.
- Mayer, A.M. and Harel, E. (1979). Polyphenol oxidases in plants. *Phytochemistry* **18**: 193-215.
- Medeira, M.C., Maia, M.I. and Vitor, R.F. (1999). The First Stages of Pre-harvest 'Peel Pitting' Development in 'Encore' Mandarin. An Histological and Ultrastructural Study. *Annals of Botany* **83**: 667-673.
- Mersey, B. and McCully, M.E. (1978). Monitoring of the course of fixation of plant cells. *Journal of Microscopy* **114**: 49-76.

- Miller, E.V. and Winston, J.R. (1943). Green spotting in relation to time of day that early oranges are picked. *Citrus Industry* **24**: 14-15.
- Mollenhauer, H.H. (1964). Plastic embedding mixtures for use in electron microscopy. *Stain Technology* **39**: 111-114.
- Monaghan, P. and Robertson, D. (1990). Freeze-substitution without aldehyde or osmium fixatives: ultrastructure and implications for immunocytochemistry. *Journal of Microscopy* **158**: 355-363.
- Monselise, S.P. (1979). The use of growth regulators in citriculture; a review. *Scientia Horticulturae* **11**: 151-162.
- Monselise, S.P., Weiser, M., Shafir, N., Goren, R. and Goldschmidt, E.E. (1976). Creasing of orange peel - physiology and control. *Journal of Horticultural Science* **51**: 341-351.
- Mustard, M.J. (1954). Oleocellosis or rind-oil spot on Persian limes. *Proceedings of the Florida State Horticultural Society* **67**: 224-226.
- Nooden, L.D. and Leopold, A.C. (1988). Senescence and Aging in Plants. Academic Press, San Diego.
- Obenland, D.M., Margosan, D.A., Houck, L.G. and Aung, L.H. (1997). Essential Oils and Chilling Injury in Lemon. *HortScience* **32**: 108-111.
- Oberbacher, M.F. (1965). A method to predict the post-harvest incidence of oleocellosis on lemons. *Proceedings of the Florida State Horticultural Society* **78**: 237-240.
- O'Brien, T.P. and McCully, M.E. (1981). The study of plant structure. Principles and selected methods. Termarcarphi Pty Ltd, Melbourne.
- Oparka, K.L., Prior, D.A.M. and Crawford, J.W. (1994). Behaviour of plasma membrane, cortical ER and plasmodesmata during plasmolysis of onion epidermal cells. *Plant Cell Environment* **17**: 163-171.
- Pantastico, E.B., Grierson, W. and Soule, J. (1966). Peel injury and rind colour of 'Persian' limes as affected by harvesting and handling methods. *Proceedings of the Florida State Horticultural Society* **79**: 338-343.
- Pawley, J.B. (1995). Handbook of biological confocal microscopy, 2nd ed. Plenum Press, New York.
- Petracek, P.D., Montalvo, L., Dou, H. and Davis, C. (1998). Postharvest Pitting of 'Fallglo' Tangerine. *Journal of the American Society for Horticultural Science* **123**: 130-135.

- Petracek, P.D., Wardowski, W.F. and Brown, G.E. (1995). Pitting of Grapefruit that Resembles Chilling Injury. *HortScience* **30**: 1422-1426.
- Platt, K.A. and Thomson, W.W. (1992). Idioblast oil cells of avocado: distribution, isolation, ultrastructure, histochemistry, and biochemistry. *International Journal of Plant Sciences* **153**: 301-310.
- Predebon, S. and Edwards, M. (1992). Curing to prevent chilling injury during cold disinfestation and to improve the external and internal quality of lemons. *Australian Journal of Experimental Agriculture* **32**: 233-236.
- Rhee, J.K. and Iwata, M. (1982). Histological Observations on the Chilling Injury of Eggplant Fruit during Cold Storage. *Journal of the Japanese Society for Horticultural Science* **51**: 237-243.
- Roland, J.C. and Vian, B. (1991). General Preparation and Staining of Thin Sections. In: *Electron Microscopy of Plant Cells* (Eds. J.L. Hall and C. Hawes) Academic Press, London. pp. 1-66.
- Ruberto, G., Biondi, D., Rapisarda, P., Renda, A. and Starrantino, A. (1997). Essential Oil of Cami, a New Citrus Hybrid. *Journal of Agricultural and Food Chemistry* **45**: 3206-3210.
- Safran, H. (1980). Improved methods for demonstration of the isolated epidermis of citrus fruit, for use in development and disorder studies of the peel. *Scientia Horticulturae* **12**: 347-350.
- Sala, J.M. (2000). Content, chemical composition and morphology of epicuticular wax of Fortune mandarin fruits in relation to peel pitting. *Journal of the Science of Food and Agriculture* **80**: 1887-1894.
- Sawamura, M., Kuriyama, T. and Li, Z. (1988). Rind spot, antioxidative activity and tocopherols in the flavedo of citrus fruits. *Journal of Horticultural Science* **63**: 717-721.
- Sawamura, M., Manabe, T., Kuriyama, T. and Kusunose, H. (1987). Rind spot and ascorbic acid in the flavedo of citrus fruits. *Journal of Horticultural Science* **62**: 263-267.
- Sawamura, M., Manabe, T., Oonishi, S., Yasuoka, K. and Kusunose, H. (1984). Effects of rind oils and their components on the induction of rind spot in citrus species. *Journal of Horticultural Science* **59**: 575-579.
- Schneider, H. (1955). Ontogeny of lemon tree bark. *American Journal of Botany* **42**: 893-905.

- Schneider, H. (1968). The Anatomy of Citrus. In: The Citrus Industry. Volume II. Anatomy, Physiology, Genetics and Reproduction, Vol. 2 (Eds. W. Reuther, H.J. Webber and L.D. Batchelor) University of California, Division of Agricultural Sciences, Riverside. pp. 1-85.
- Scora, R.W. and Adams, C. (1973). Effect of oleocellosis, dessication, and fungal infection upon the terpenes of individual oil glands in *Citrus latipes*. *Phytochemistry* 12: 2347-2350.
- Scora, R.W., Coggins Jr., C.W. and Knapp, J.C.F. (1968). Influence of Maturation upon the Essential Rind Oil Components in *Citrus sinensis*. In: Proceedings of First International Citrus Symposium, Riverside, USA, Vol. 3 (Ed. H.D. Chapman) University of California. pp. 1171-1176.
- Scora, R.W. and Torrasi, S. (1966). Relation of Taxonomic, Climatic and Tissue Maturity Factors to the Essential Oil Constituents in Leaves and Fruits in the Aurantioideae. *American Society for Horticultural Science* 88: 262-271.
- Scott, F.M. and Baker, K.C. (1947). Anatomy of Washington Navel orange rind in relation to water spot. *Botanical Gazette* 108: 459-475.
- Scott, F.M., Bystrom, B.G. and Bowler, E. (1963). *Persea americana*, mesocarp cell structure, light and electron microscope study. *Botanical Gazette* 124: 423-428.
- Shaw, P.E. (1979). Review of Quantitative Analyses of Citrus Essential Oils. *Journal of Agricultural and Food Chemistry* 27: 246-257.
- Shomer, I. (1980). Sites of production and accumulation of essential oils in citrus fruits. In: Proceedings of Seventh European Congress on Electron Microscopy, The Hague, The Netherlands, Vol. 2. pp. 256-257.
- Shomer, I. and Erner, Y. (1989). The Nature of Oleocellosis in Citrus Fruits. *Botanical Gazette* 150: 281-288.
- Sieck, W. (1895). Die schizolysigenen Sekretbehälter. *Jahrbucher fur wissenschaftliche Botanik* 27: 197-242.
- Soule, J. and Grierson, W. (1986). Anatomy and Physiology. In: Fresh Citrus Fruit (Eds. W.F. Wardowski, S. Nagy and W. Grierson) Van Nostrand Reinhold Company Inc., New York. pp. 379-395.
- Spurr, A.R. (1969). A Low-Viscosity Epoxy Resin Embedding Medium for Electron Microscopy. *Journal of Ultrastructure Research* 26: 31-43.
- Sun, D. and Petracek, P.D. (1999). Grapefruit Gland Oil Composition Is Affected by Wax Application, Storage Temperature, and Storage Time. *Journal of Agricultural and Food Chemistry* 47: 2067-2069.

- Swingle, W.T. (1943). The Botany of Citrus and Its Wild Relatives of the Orange Subfamily. In: The Citrus Industry. Volume I. History, Botany and Breeding, Vol. 1 (Eds. H.J. Webber and L.D. Batchelor) University of California Press, Los Angeles. pp. 129-474.
- Taiz, L. and Zeiger, E. (1998). Plant Physiology, 2nd ed. Sinauer Associates, Sunderland.
- Tanaka, T. (1961). Citrologia. Citrologia Supporting Foundation, Osaka.
- Taverner, P., Tugwell, B.L. and Wild, B. (2001). A Guide to the Common Postharvest Diseases and Disorders of Navel oranges and mandarins grown in Inland Australia. South Australian Research and Development Institute (SARDI), Adelaide.
- Thomson, W.W. and Platt-Aloia, K. (1976). Ultrastructure of the Epidermis of Developing, Ripening, and Senescing Navel Oranges. *Hilgardia* 44: 61-82.
- Thomson, W.W., Platt-Aloia, K.A. and Endress, A.G. (1976). Ultrastructure of oil gland development in the leaf of *Citrus sinensis* L. *Botanical Gazette* 137: 330-340.
- Ting, S.V. and Attaway, J.A. (1971). Citrus Fruits. In: The Biochemistry of Fruits and their Products, Vol. 2 (Ed. A.C. Hulme) Academic Press, London. pp. 107-169.
- Tugwell, B.L. and Chvyl, W.L. (1995). The effect of storage temperature on development of rind blemish on Washington Navel oranges. In: Proceedings of Australasian Postharvest Horticulture Conference, Melbourne, Australia (Eds. C. Frisina, K. Mason and J. Faragher) Institute for Horticultural Development, Department of Natural Resources and Environment. pp. 105-108.
- Turner, G.W. (1999). A brief history of the lysigenous gland hypothesis. *The Botanical Review* 65: 76-88.
- Turner, G.W., Berry, A.M. and Gifford, E.M. (1998). Schizogenous secretory cavities of *Citrus limon* (L.) Burm. F. and a reevaluation of the lysigenous gland concept. *International Journal of Plant Sciences* 159: 75-88.
- Turrell, F.M. (1946). Tables of Surfaces and Volumes of Spheres and of Prolate and Oblate Spheroids, and Spheroidal Coefficients, 1st ed. University of California Press, Los Angeles.
- Turrell, F.M. and Klotz, L.J. (1940). Density of stomata and oil glands and incidence of water spot in the rind of Washington navel orange. *Botanical Gazette* 101: 862-871.

- Underhill, S.J.R., McLauchlan, R.L. and Eaks, I.L. (1995). 'Eureka' Lemon Chilling Injury. *HortScience* **30**: 309-312.
- Weierov, D., Erner, Y., Shomer, I. and Aharonson, N. (1979). Early evaluation of orange peel blotches caused by spray oils. *Phytoparasitica* **7**: 79-88.
- Walker, R.R., Sedgley, M., Blesing, M.A. and Douglas, T.J. (1984). Anatomy, Ultrastructure and Assimilate Concentrations of Roots of Citrus Genotypes Differing in Ability for Salt Exclusion. *Journal of Experimental Botany* **35**: 1481-1494.
- Wanner, G., Formanek, H. and Theimer, R.R. (1981). The Ontogeny of Lipid Bodies (Sphaerosomes) in Plant Cells. *Planta* **151**: 109-123.
- Wardowski, W.F., McCornack, A.A. and Grierson, W. (1976). Oil spotting (Oleocellosis) of Citrus Fruit. Institute of Food and Agricultural Sciences, University of Florida, Florida Cooperative Extension Service, Circular 410.
- Webber, H.J. (1943). Cultivated Varieties of Citrus. In: The Citrus Industry. Volume I. History, Botany and Breeding, Vol. 1 (Eds. H.J. Webber and L.D. Batchelor) University of California Press, Los Angeles. pp. 475-668.
- Webber, H.J. and Fawcett, H.S. (1935). Comparative histology of healthy and psorosis-affected tissues of *Citrus sinensis*. *Hilgardia* **9**: 71-93.
- Whiteside, J.O., Garnsey, S.M. and Timmer, L.W. (1988). Compendium of Citrus Diseases. APS Press, St. Paul.
- Wild, B.L. (1998). New method for quantitatively assessing susceptibility of citrus fruit to oleocellosis development and some factors that affect its expression. *Australian Journal of Experimental Agriculture* **38**: 279-285.
- Wild, B.L. and Williams, M.H. (1992). Oils Ain't Oils in Citrus Rinds. Australian Citrus News, June 1992, pp. 9-11.
- Williams, M.H. and Wild, B.L. (1996). Development of oleocellosis in 'Valencia' oranges and mandarins. Unpublished.
- Wood, P.J., Fulcher, R.G. and Stone, B.A. (1983). Studies on the Specificity of Interaction of Cereal Cell Wall Components with Congo Red and Calcofluor. Specific Detection and Histochemistry of (1-3), (1-4), - β -D-Glucan. *Journal of Cereal Science* **1**: 95-110.
- Yano, T., Ninomiya, Y. and Shimizu, Y. (1997). Anatomical Observation on Ulcerous Kohansho and Similar Disorders on the Peel Surface of Yuzu (*Citrus junos* Sieb. ex Tanaka) Fruit. *Journal of the Japanese Society for Horticultural Science* **66**: 489-493.

Zaragoza, S., Almela, V., Tadeo, F.R., Primo-Millo, E. and Agusti, M. (1996). Effectiveness of calcium nitrate and GA, on the control of peel-pitting of 'Fortune' mandarin. *Journal of Horticultural Science* 71: 321-326.

Zauberman, G., Ronen, R., Akerman, M., Weksler, A., Rot, I. and Fuchs, Y. (1991). Post-harvest retention of the red colour of litchi fruit pericarp. *Scientia Horticulturae* 47: 89-97.

Personal Communications

Carpenter, Ms. J.
FEI Australia
Account Manager, Australasia
Fitroy North, Victoria 3068
Formerly: Electron Microscopist
The University of Melbourne, School of Botany

Erner, Dr. Y.
Senior Researcher
The Volcani Center, Dept. of Horticulture
Bet Dagan 50250
Israel

Green, Mr. A.
Technical Officer
Citrus Board of South Australia (CBSA)
Adelaide, South Australia 5001

Hill, Mr. J.
Consultant
Primary Industries and Resources South Australia (PIRSA),
Rural Solutions
Loxton, South Australia 5333

Johnson, Mrs. S.
Technical Officer
Commonwealth Scientific and Industrial Research Organisation (CSIRO),
Plant Industry, Horticulture Unit
Glen Osmond, South Australia 5064

Loveys, Dr. B.
Affiliate Professor
Commonwealth Scientific and Industrial Research Organisation (CSIRO),
Plant Industry, Horticulture Unit
Glen Osmond, South Australia 5064

Tugwell, Mr. B.L.
Chief Scientist
South Australian Research and Development Institute (SARDI),
Postharvest Horticulture
Glen Osmond, South Australia 5064